ALCATEL

SPACE

HERSCHEL / PLANCK

PLANCK PLM Mechanical and Thermoelastic Analyses
H-P-3-ASP-AN-0329
Product Code:220000

	Function Name	Date	Signature
Rédigé par/ ***Written by***	**Mechanical Analyses** **D. REBUFFAT**	09/04/04	
Vérifié par/ ***Verified by***	**Sciences/Obs. Satellite Group Manager** **R. VIALE**	09/04/04	
Vérifié par/ ***Verified by***	**AMT responsible Manager** **T. LASIC**	09/04/04	
Vérifié par/ ***Verified by***	**System Engineering Manager** **JB. RITI**	09.04.2004	
Vérifié par/ ***Verified by***	**PPLM PA Manager** **E. POURRIER**	09/04/2004	
Vérifié par/ ***Verified by***	**PPLM Project Manager** **T. BANOS**	9/04/04	
Vérifié par/ ***Verified by***	**PA Manager** **C. MASSE**	09/04/04	
Approbation/ ***Approved by***	**Project Manager** **J.J. JUILLET**	09/04/04	

Entité Emettrice : Alcatel Space - Cannes
(détentrice de l'original) :

ENREGISTREMENT DES EVOLUTIONS / *CHANGE RECORDS*

ISSUE	DATE	§ : DESCRIPTION DES EVOLUTIONS *§ : CHANGE RECORD*	REDACTEUR *AUTHOR*
2	09/04/2004	Analyses updated for PPLM CDR	

TABLE OF CONTENTS

LIST OF TABLES

LIST OF FIGURES

1. INTRODUCTION

PLANCK PLM Mechanical analyses presented in this document have been performed using CDR PPLM and PLANCK FE Model in order to verify mechanical environment and mechanical specifications for Planck Payload module, substructures and equipment of PLANCK PLM.

The aim of this document is to present the main results extracted from these mechanical analyses, which concern the following mechanical characteristics and requirements:

- Quasi static loads
- Sine and acoustic environments
- Thermo-elastic distortion

For static, sine and thermo-elastic analyses, NASTRAN V70.0 software is used.

For acoustic analyses, ASTRYD software is used.

For the sine and acoustic analyses, Ariane 5 qualification levels [AD 01] are injected.
A supplementary coefficient of 1.2 is added on results to cover analyses uncertainties.

2. REFERENCE AND APPLICABLE DOCUMENTS

Ref.	***No.***	***Issue/date***	***Title***
AD 1		Iss. 3 Rev. 0	ARIANE 5 User's Manual
RD 1	H-P-3-CSAG-AN-0005	Issue 2, rev. 1 03/10/2003	Planck telescope and cryo-structure FEM description
RD 2	H-P-3-ASPI-AN-0178	21/01/02	PLANCK FPU simplified Finite Element Model
RD 3	H-P-3-ASPI-AN-0180	21/01/02	PLANCK J-FET simplified Finite Element model
RD 4	H-P-3-ASPI-AN-0179	21/01/02	PLANCK Primary and Secondary Reflector Finite Element models
RD 5	Doc. by LABEN sent by email on 19/11/2003	19/11/03	Reduced FEM description
RD 6	mail from ASED, 06/11/2003	06/11/2003	Reflector interface
RD 7	PLA-ASED-TN-064	iss. 2	Interface measurement on the Planck SR QM
RD 8	mail from ESA, 04/12/2003	04/12/2003	Planck PR QM mass properties
RD 9	IIDB HFI iss. 3.0	Iss. 3.0 03/10/2003	
RD 10	email from CESR (R. Pons)	04/11/2003	
RD 11	ICD PHCA-GAF-ICD-001	31/06/2003 Iss. 3	
RD 12	PL-LFI-PST-MM/03-001	24/09/2003	Minutes of meeting IASF « LFI progress meeting »
RD 13	10203014-X17		Interface drawing 10203014-X17
RD 14	IIDB Sorption iss. 2.1	iss. 2.1	
RD 15	Unreferenced doc. by IAS sent by email on 19/11/2003	19/11/2003	HFI Masses, centre of gravity and inertia
RD 16	H-P-3-ASP-RP-0313	Iss. 2	Planck PLM design report
RD 18	HP-1-ASPI-SP-0014	Iss. 1 07/06/2001	MECHANICAL MATHEMATICAL MODEL SPECIFICATION
RD 19	H-P-3-ASPI-SP-0021	Iss. 1 Rev. 3 17/01/2003	Planck cryo-structure and telescope baffle specification

Ref.	*No.*	*Issue/date*	*Title*
RD 20	H-P-3-ASPI-SP-0004	Iss. 1 Rev. 3 17/01/2003	Planck telescope specification
RD 21	H-P-3-CSAG-DD-0001	Iss. 2 06/08/2003	Planck telescope and cryo-structure Design and Definition Report
RD 22	H-P-3-CSAG-AN-0001	Iss. 3 Rev. 0 07/05/2003	Planck telescope and Cryo-structure FE Analysis Report
RD 23	H-P-3-CSAG-TN-0154	06/10/2003	FEM evolution since CDR model freeze
RD 24	Email H-P-CSAG-EM-1019	30/10/03	Planck FE clarifications
RD 25	H-P-22100-CSAG-RD-0011	Iss. 1	Minimum stiffness of telescope not achieved
RD 26	H-P-3-ASP-TN-0739	Issue 1.0 29/03/2004	CDR PLANCK FINITE ELEMENT MODEL DESCRIPTION
RD 27	SCI-PT-IIDA-04624	Iss. 3 Rev. 2	Instrument Interface Document
RD 28	H-P-3-CSAG-AN-0002	Iss. 2 Rev. 1 17/10/2003	Planck Telescope and Cryo-Structure Detail Stress Report
RD 29	H-P-ASP-LT-3387	Issue 2.0 15/07/03	CSAG and ASP sine analyses comparison
RD 30	H-P-ASPI-LT-2424	10/12/2002	Answer to action 2204/4 from PM11 about reflectors
RD 31	H-P-3-CSAG-AN-0005	Iss 2, rev 0 21/05/2003	Planck telescope and cryo-structure FEM description
RD 32	H-P-CSAG-EM-0813	03/07/2003	Acceleration PUNCH Output delivery
RD 34	H-P-3-ASPI-AN-0353	Iss. 1 14/02/2003	PLANCK Vibroacoustic Analyses
RD 35	H-P-ASP-LT-2717	18/02/2003	Synthesis of acoustic coupled analysis of 20K pipes mounted on V-grooves
RD 36	IM 352D:0407:WBT	10/02/2004	Summary of PACE Sine Survey, PF Sine Vibration and Acoustic Tests of PACE V-grooves Simulator Compared to Acoustic Analysis
RD 37	PLA-ASED-ML-301/04	09/03/2004	Features of Planck Reflector Finite Element Models
RD 38	Email H-P-ASPI-LT1592	03/05/2002	Temperatures for thermo-elastic

Ref.	*No.*	*Issue/date*	*Title*
RD 39	Un-referenced doc deliverd by LABEN	16/06/04	Finite element model description
RD 40	PLA-ASED-RP-013	28/05/2002	FEM of Planck reflectors
RD 41	Un-referenced doc delivered by LABEN	18/07/2003	FEM description
RD 42	H-P-ASP-LT-4337	30/01/04	Planck subplatform : BEU and lower structure IF loads definition version 2
RD 43	AN-PHEC-400296-AIRL (0)	19/02/2004	DCP/PPLM SUBSYSTEM STRUCTURAL ANALYSIS REPORT
RD 44	TN-PHD-030301	Iss. 1 R. 1	Tech note on the mechanical analysis of the 4K cooler connecting pipework - revised analysis
RD 45	PHCA-GAF-AN-001	Iss. 2 24/11/2003	Structural analysis for Planck HFI JFET box
RD 46	Email from JPL	05/06/2003	Response to AI 3, 4, 5 and 6 from the May 20 meeting
RD 47	Draft by HFI sent by email on 16/01/2004	Issue: 01 Revision: 00 08/12/2003	Mechanical coupled study On HFI and LFI FPU
RD 48	Draft by HFI sent by email on 16/01/2004	Iss. 1 rev. 0 15/12/2003	HFI FPU Mechanical Study And Vibration Test philosophy
RD 49	Draft by IAS	03/06/2003	PAU-JFET harness interface with the cryo-strut
RD 50	H-P-ASP-LT-4623	18/03/2004	Specification update for the DCP
RD 51	Email from JPL	07/03/2003	Response to AI 1 and 4
RD 52	H-P-3-ASP-TN-0582		PLANCK CSL supporting device micro vibration analysis
RD 53	352G :02 :024 :PDM	Sept. 2002	PACE FEM description
RD 54	H-P-3-ASP-AN-0330	2/1	PPLM thermal analyses

3. PLANCK PLM MODEL DESCRIPTION

3.1 P-PLM FEM general description

CDR Planck PLM model is issued from the CDR CSAG model RD1, delivered the 08/10/2003, on which some modifications described here-after have been implemented.

The CSAG CDR model includes the following equipment FEM :
- ✓ FPU (RD2)
- ✓ JFET (RD3)
- ✓ The 2 reflectors (RD4)

In order to be in line with last equipment design characteristics, the ALCATEL CDR model includes updated FEM for following equipment :
- ✓ FPU, described in § 3.2 (RD5), updated dynamic FEM delivered by LABEN (mass 51.2kg with HFI – see § 3.3)
- ✓ The 2 reflectors, described in § 3.3
- ✓ The JFET box, that is modelled by a rigid mass, with updated MCI and I/F points location.

Also, MCI has been updated as described in § 3.4

PPLM CDR FEM is in line with CDR design [RD 16].

ALCATEL CDR PPLM FEM is presented through next figures.

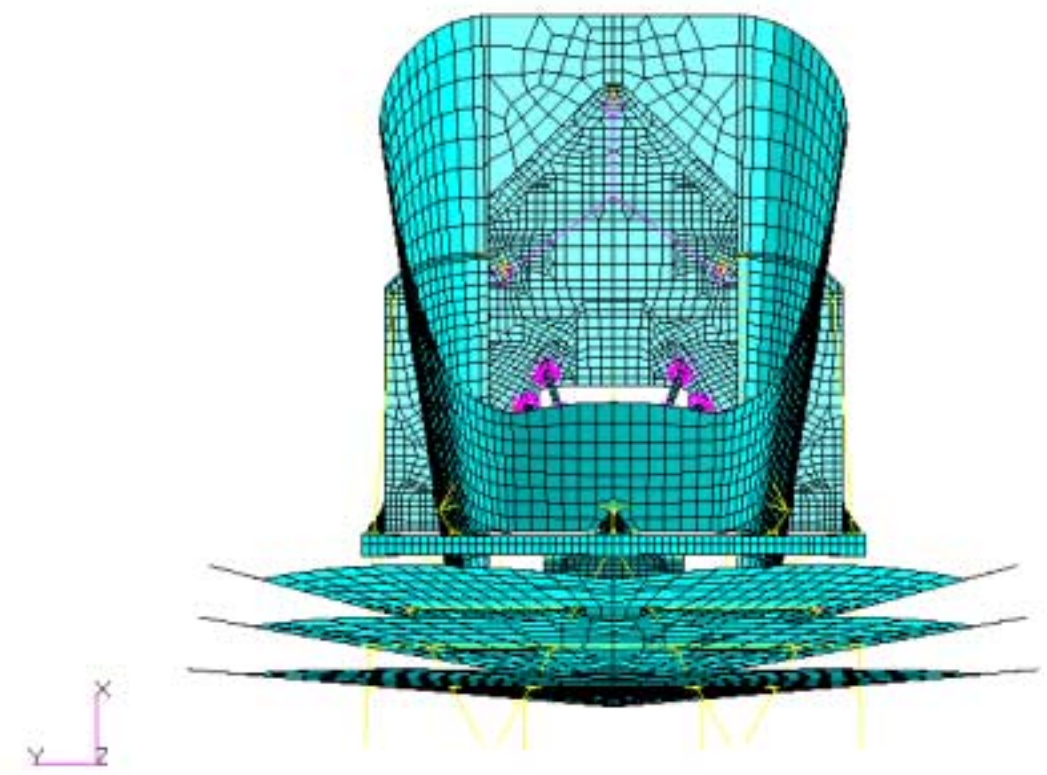

Figure 1: PPLM XY view

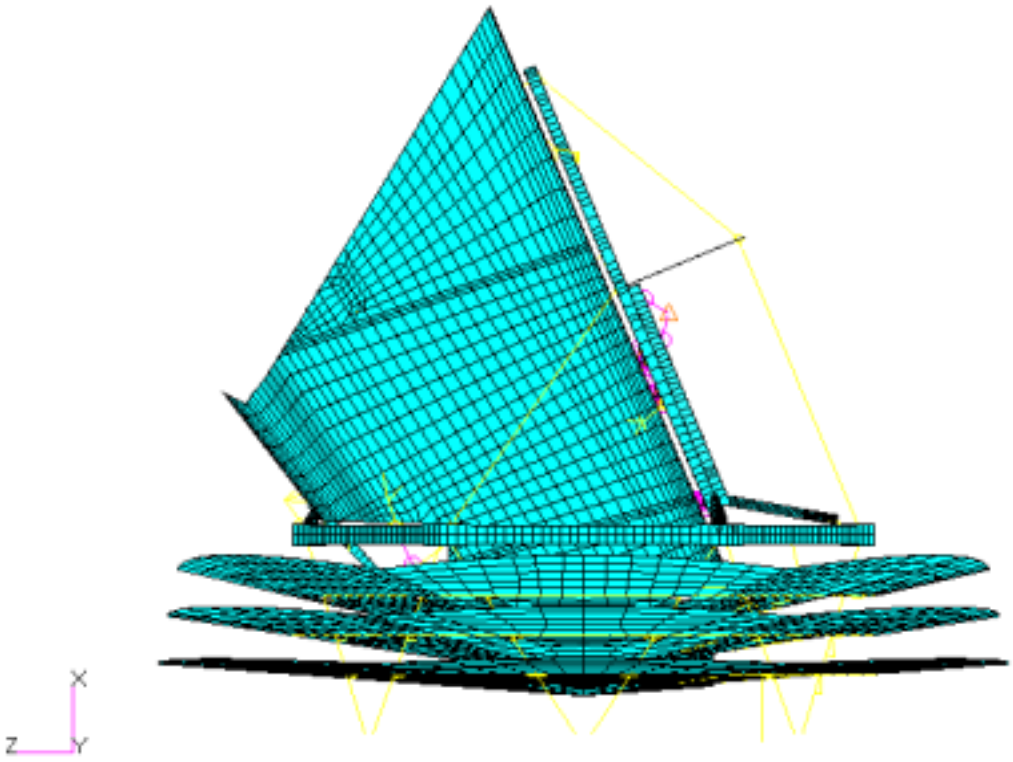

Figure 2: PPLM XZ view

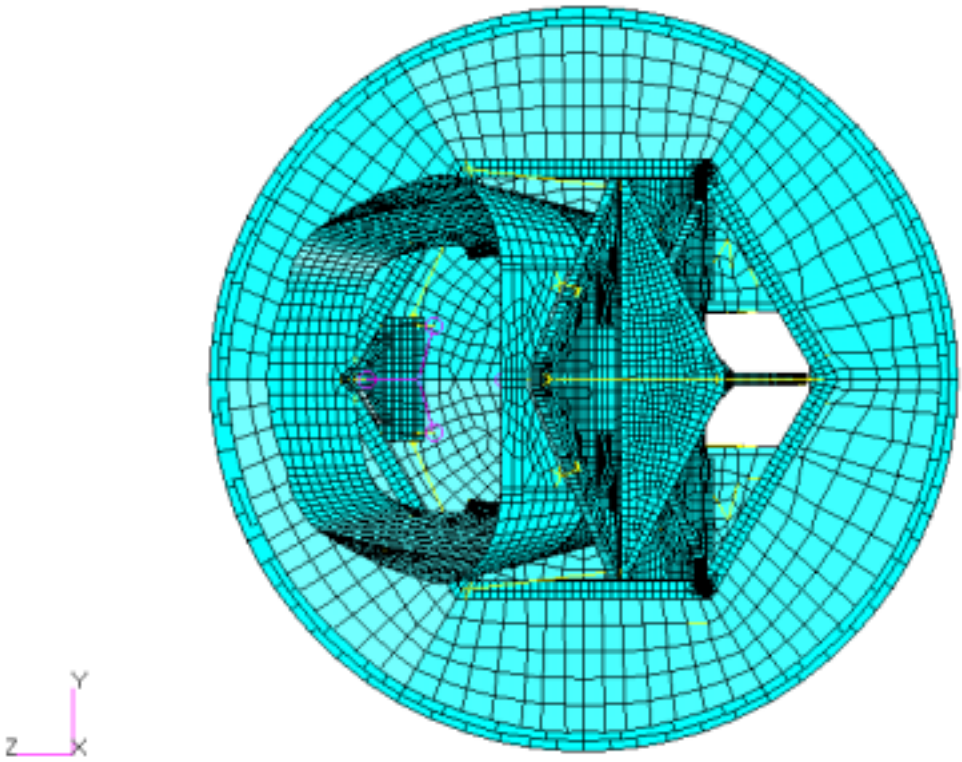

Figure 3: PPLM YZ view

PLANCK Payload module is defined from the 2 following main substructures :

- PPLM telescope
- PPLM cryo-structure + baffle

These substructures are shown hereafter :

- **PLANCK telescope**

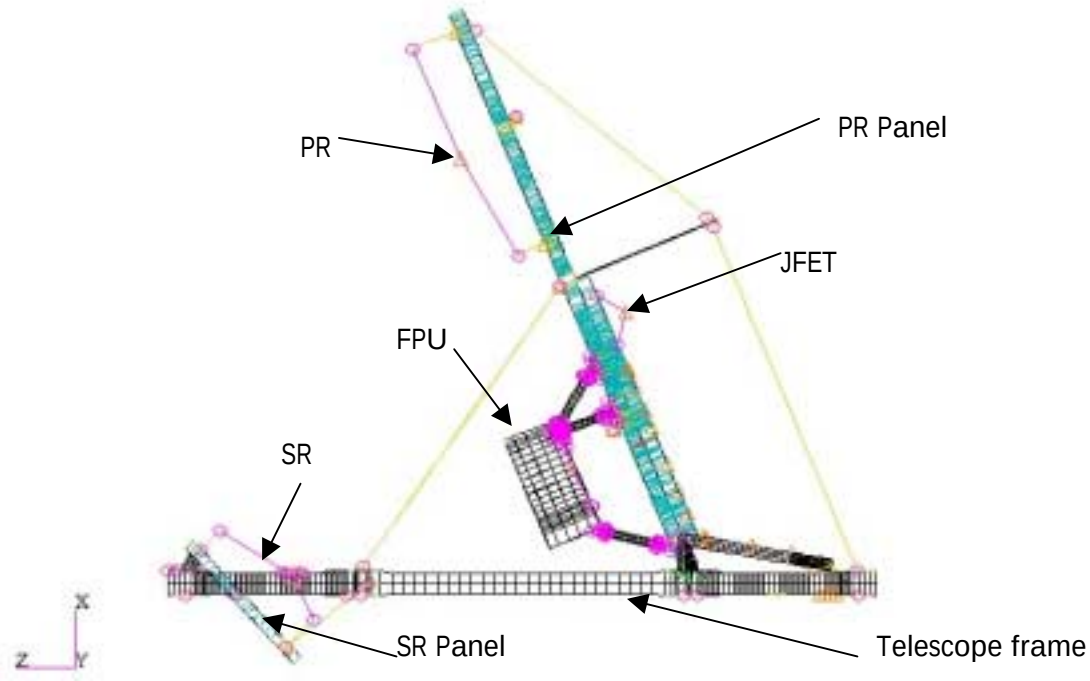

Figure 4 : PLANCK Telescope

The mechanical properties of PPLM telescope are up to date and described in [RD 1] and [RD 21].

- **PLANCK Cryo substructure + baffle**

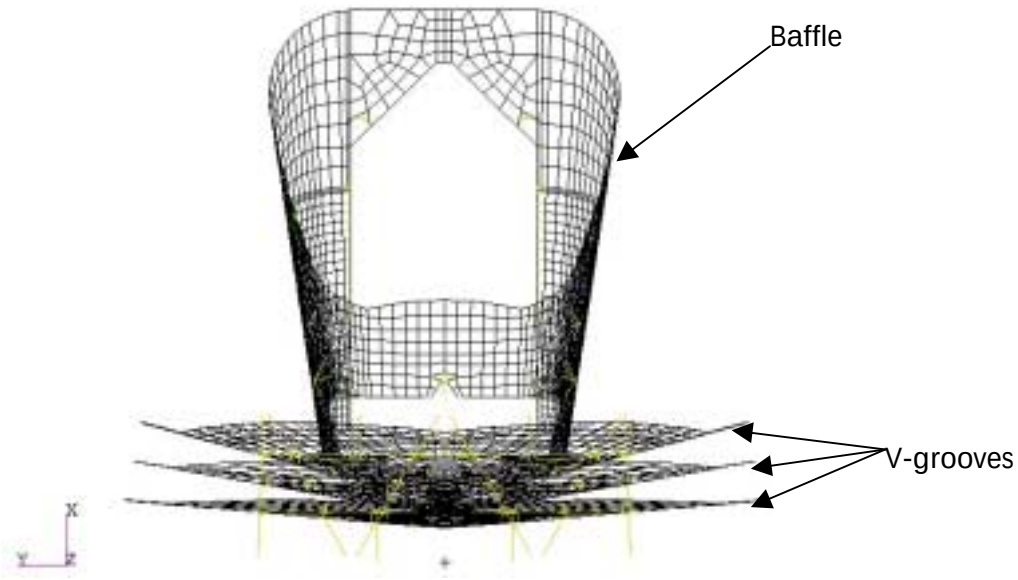

Figure 5 : PLANCK Cryo-structure + baffle

The mechanical properties of PPLM cryo structure are up to date and described in [RD 1] and [RD 21].

3.2 FPU FEM update

The FPU FEM used for CDR analyses has been updated with respect to CSAG FEM, and is compliant with LABEN current design.
The FPU FEM is based on a simplified dynamic FEM (RD5) delivered by LABEN (LFI part only), on which the HFI part is mounted as a rigid mass representative in term of MCI (see § 3.4 for details). This rigid mass is interfaced with representative I/F points on LFI part.
The total mass of the FPU is 51.2Kg.
The modal properties, expressed in the RDP local coordinate frame are the following :

MODE	FREQUENCY	EFFECTIVE MASSES (KG,KGM2)					
N	(HZ)	MX	MY	MZ	IX	IY	IZ
1	112.403	40.703	0.018	0.826	0.00	2.95	0.00
2	114.894	0.021	42.407	0.001	1.76	0.00	7.14
3	210.792	0.001	1.500	0.105	0.00	0.02	0.45
4	219.217	0.387	0.001	47.232	0.00	6.44	0.00
5	259.141	0.002	5.299	0.013	0.25	0.00	1.74
RESIDUAL MASS		10.091	1.982	3.029	0.32	1.27	0.68
TOTAL MASS		51.206	51.206	51.206	2.34	10.68	10.01

Table 1: FPU first modes

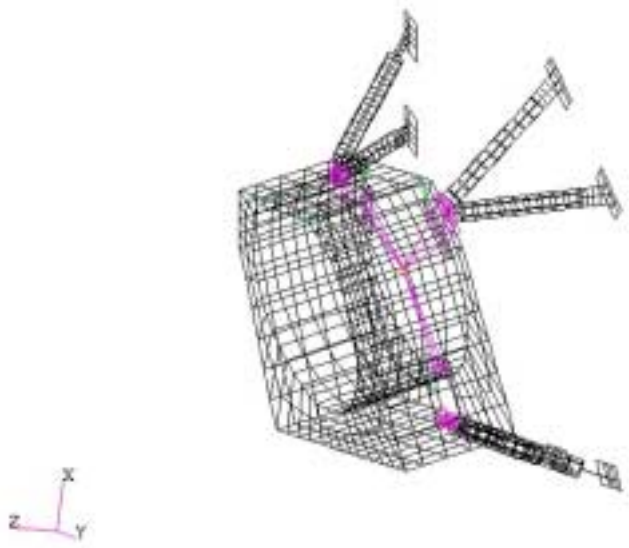

Figure 6 : FPU FEM

3.3 PR and SR FEMs update

Based on up to date ASED information concerning ISMs stiffness and reflectors measured MCI, simplified PR and SR FEMs have been meshed in order to obtain a more representative dynamic behaviour.

ISMs have been meshed with BAR and CELAS elements.
In order to take into account the interaction between the different stiffness directions, and obtain a representative ISM stiffness matrix, iterations have been performed following this method :

- adjustment of ISM mechanical properties
- computation of compliance matrix (or displacement matrix), ie displacements versus unitary loads

- inversion of the compliance matrix in order to obtain the stiffness matrix
- comparison of the stiffness matrix with ASED stiffness matrix
- re-do iteration

The following stiffness matrices are obtained :

long ISM	Fr (N)	Ft (N)	Fz (N)	Mr (Nm)	Mt (Nm)	Mz (Nm)
r=1m	3.34E+05	0	0	0	1.27E+04	0
t=1m	0	1.25E+07	0	-1.22E+04	0	0
z=1m	0	0	3.76E+07	0	0	0
rr=1rad	0	-1.22E+04	0	6.16E+02	0	0
tt=1rad	1.27E+04	0	0	0	8.89E+02	0
zz=1rad	0	0	0	0	0	3.80E+02

short ISM	Fr (N)	Ft (N)	Fz (N)	Mr (Nm)	Mt (Nm)	Mz (Nm)
r=1m	1.04E+06	0	0	0	2.66E+04	0
t=1m	0	1.70E+07	0	-2.17E+04	0	0
z=1m	0	0	3.93E+07	0	0	0
rr=1rad	0	-2.17E+04	0	7.40E+02	0	0
tt=1rad	2.66E+04	0	0	0	1.81E+03	0
zz=1rad	0	0	0	0	0	7.47E+02

Table 2: ALCATEL ISMs stiffness matrices

These matrices are to be compared to ASED ISMs stiffness matrices RD 6 :

Applied displacement	Calculated force					
	Fr [N]	Ft [N]	Fz [N]	Mr [Nm]	Mt [Nm]	Mz [Nm]
r = 1m	3.31E+05	3.34E+02	-3.35E+02	-1.64E+00	1.62E+04	1.50E+01
t = 1m	3.34E+02	1.25E+07	9.92E+03	-6.84E+04	7.04E+00	3.29E+00
z = 1m	-3.35E+02	9.92E+03	3.73E+07	-2.22E+00	-1.08E+01	-3.76E+00
rr = 1rad	-1.64E+00	-6.84E+04	-2.22E+00	6.15E+02	-3.29E-02	-2.00E-02
tt = 1rad	1.62E+04	7.04E+00	-1.08E+01	-3.29E-02	8.92E+02	9.99E-01
zz = 1rad	1.50E+01	3.29E+00	-3.76E+00	-2.00E-02	9.99E-01	3.82E+02

Tab. 3 Stiffness matrix of long ISM

Applied displacement	Calculated force					
	Fr [N]	Ft [N]	Fz [N]	Mr [Nm]	Mt [Nm]	Mz [Nm]
r = 1m	1.03E+06	1.27E+03	-3.25E+02	-6.59E+00	4.18E+04	-1.63E+01
t = 1m	1.27E+03	1.70E+07	-6.74E+03	-9.20E+04	5.01E+01	1.19E+00
z = 1m	-3.25E+02	-6.74E+03	3.88E+07	4.70E+01	-3.58E+00	-2.34E+01
rr = 1rad	-6.59E+00	-9.20E+04	4.70E+01	7.39E+02	-2.60E-01	-8.66E-03
tt = 1rad	4.18E+04	5.01E+01	-3.58E+00	-2.60E-01	1.85E+03	-8.54E-01
zz = 1rad	-1.63E+01	1.19E+00	-2.34E+01	-8.66E-03	-8.54E-01	7.49E+02

Tab. 4 Stiffness matrix of long ISM

Table 3: ASED ISMs stiffness matrices

It is seen that diagonal terms match well. Non diagonal terms are very unlikely to match with such simplified FEM, and are considered as second order.

Reflector mass properties are represented by a rigid mass (CONM2 element) including mass and inertia about CoG, at the CoG location (see [RD 7] and [RD 8]). It is linked to the ISMs top by a rigid element RBE2.

The PR and SR simplified FEMs modal properties are given below :

MODE	FREQUENCY	EFFECTIVE MASSES (KG,KGM2)					
N	(HZ)	MX	MY	MZ	IX	IY	IZ
1	115.032	21.579	0.000	6.317	0.00	25.15	0.00
2	145.488	0.000	26.272	0.000	0.59	0.00	135.07
3	155.182	0.000	1.611	0.000	3.42	0.00	34.40
4	238.239	1.221	0.000	4.649	0.00	60.40	0.00
RESIDUAL MASS		5.100	0.017	16.934	3.44	84.52	1.92
TOTAL MASS		27.900	27.900	27.900	7.46	170.07	171.38

Table 4: PR effective masses

MODE	FREQUENCY	EFFECTIVE MASSES (KG,KGM2)					
N	(HZ)	MX	MY	MZ	IX	IY	IZ
1	188.711	7.221	0.000	6.263	0.00	0.05	0.00
2	198.564	0.000	7.555	0.000	2.28	0.00	3.53
3	219.241	0.000	5.772	0.000	6.79	0.00	9.75
RESIDUAL MASS		6.381	0.274	7.339	1.48	21.79	0.04
TOTAL MASS		13.601	13.601	13.601	10.55	21.85	13.33

Table 5: SR effective masses

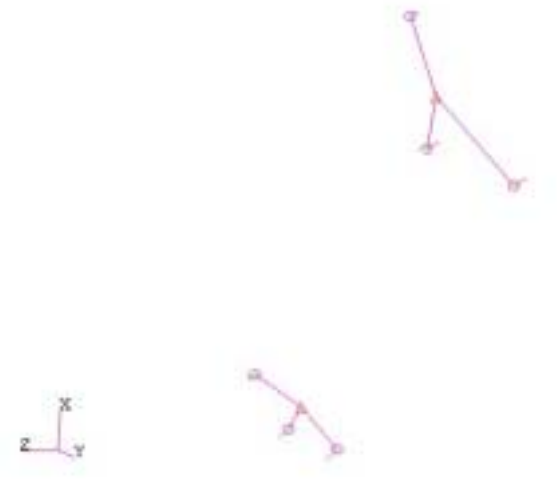

Figure 7 : PR and SR simplified FEMs

3.4 PPLM FEM MCI update

The mass budget of CSAG model has been updated in order to match the nominal CDR mass budget (see § 3.5 for the comparison).
Mass under CSAG responsibility (PPLM structure) has not been changed, since the most up to date information is contained in their CDR FEM RD1. However, it must be stated that CSAG FEM mass is with contingencies, which is close but slightly higher than the nominal mass. This has to be considered for the slight difference between CDR mass budget and CDR PPLM FEM mass evidenced in §3.5.

The following changes have been made, based on the last instrument information available (date : 17/11/2003).

3.4.1 HFI

- HFI instrument (punctual mass) : 17.8kg [RD 9] ; CoG : see [RD 15]
- JFET (punctual mass) : 2.4kg [RD 9] ; CoG at 70mm out of PR panel I/F plane [RD 11]
- PAU (punctual mass) : 13.2kg [RD 10] ; CoG at 80mm out of subplatform plane
- 4K pipe, including pre-coolers : 2.3kg [RD 9], spread this way : 700g on FPU (punctual mass), 400g on V-groove 3 (bar element), 150g on V-groove 2 (punctual mass), 150g on V-groove 1 (punctual mass), 300g on lower beam (punctual masses at each I/F point), 600g at bracket location on subplatform (punctual mass)
- Harness between FPU and JFET : 2kg [RD 9] spread this way : 1 kg on JFET (punctual mass), 0.5kg on PR panel (punctual mass), 0.5kg on FPU (punctual mass)

- Bellow : 5.6kg [RD 9] spread this way : 2.8kg on PR panel (punctual masses at each I/F point), 2.8kg on cryo-strut (punctual masses at each I/F point)

- 0.1K pipe, including pre-coolers : 2.5kg [RD 9] spread this way : 350g at bracket location on subplatform (punctual mass), 700g on V-groove 3 (bar element), 500g on frame and lower beam (punctual mass at each I/F point), 350g on V-groove 2 (punctual mass), 350g on V-groove 1 (punctual mass), 250g on FPU (punctual mass)

- 4K load : 650g [RD 9] on FPU (punctual mass)

3.4.2 LFI

- FEU : 22.9kg [RD 12], included in LABEN FEM [RD 5]

- FEU harness [RD 12] : 600g, included in LABEN FEM [RD 5]

- Wave Guides Assembly : wave guides (6.5kg – [RD 12]) + support structures (4.6kg upper, 7.4kg lower – [RD 12]) + harness (1kg – [RD 12]), spread this way :
  - 5.8kg on BEU (punctual mass) for in plane (lateral) directions
  - 11.6kg on BEU (punctual mass) for out of plane (longitudinal) direction
  - 5.8kg on frame (punctual masses at lower structure I/F blades locations) for lateral directions
  - 0 kg on frame for longitudinal direction
  - 2*100g per V-groove at the heat exchanger I/F
  - 5.9kg on PR panel (punctual masses at upper structure I/F points locations)
  - 1.4kg on FPU (non structural mass)

The mass difference between lateral and longitudinal directions for BEU and frame is due to the fact that the lower structure is attached to the frame via 2 blades flexible along longitudinal direction. It means that the BEU carries the mass of all the lower structure along longitudinal direction, whereas the frame takes approximately half the mass for the lateral directions.

- BEU 23.9kg [RD 12] + 2.5kg for harness [RD 12] (punctual mass) ; CoG at 100mm out of subplatform plane

3.4.3 Sorption

- SCCE : 2*3.2kg [RD 13] (non structural mass on LABEN FPU FEM)

- Pipe including pre-coolers (2*5.7kg) + harness (2*1kg) [RD 14], spread as follows : 2*3.7kg on V-groove 3 (bar element), 2*1.5kg on V-groove 2 (bar element), 2*1.5kg on V-groove 1 (bar element)

3.4.4 PR and SR

- 27.9kg for PR and 13.6 kg for SR [RD 7] and [RD 8]on punctual mass located at CoG location.

3.5 PPLM FEM properties

3.5.1 Storage

The FEM used for our CDR analyses, including modifications described previously, is stored in the following directory :

Cantore : /data/planck_struc/ARCHIVE_CDR/ANALYSES_CDR/MODELES/PPLM_CDR

Files to be used are CSAG original files, with the extension _asp if any, which means that the file has been changed for the Alcatel CDR configuration.
Thermo-elastic FEM is stored in the same directory and is the original CSAG CDR FEM.

3.5.2 FEM size

PPLM FEM (Alcatel CDR configuration) has	21232 Elements
	17914 Nodes

3.5.3 FEM MCI

PLANCK PLM FEM mass is 388.0 Kg (without BEU and PAU)

The inertia and CoG properties of the FEM model are listed hereafter from a NASTRAN computation.
The CoG coordinates and the inertia are expressed in the Planck satellite coordinate system (origin at the base of the SVM – see figure 8). The PPLM coordinate system has the same axes orientation, with its origin at the location (0.9665m, 0m, 0m) in the satellite coordinate system.

```
      O U T P U T   F R O M   G R I D   P O I N T   W E I G H T   G E N E R A T O R
                                REFERENCE POINT =       0
                                      M O
*  3.880366E+02  4.163336E-17 -1.776357E-15  6.661338E-16 -6.084741E+00  3.255476E+00 *
*  4.163336E-17  3.880366E+02 -3.108624E-15  6.084741E+00  4.163336E-16  7.925876E+02 *
* -1.776357E-15 -3.108624E-15  3.880366E+02 -3.255476E+00 -7.925876E+02  1.221245E-14 *
*  6.661338E-16  6.084741E+00 -3.255476E+00  3.689635E+02  5.963484E+00 -3.246481E+00 *
* -6.084741E+00  4.163336E-16 -7.925876E+02  5.963484E+00  1.993938E+03 -2.096583E+00 *
*  3.255476E+00  7.925876E+02  1.221245E-14 -3.246481E+00 -2.096583E+00  1.987936E+03 *
                                      S
                          *  1.000000E+00  0.000000E+00  0.000000E+00 *
                          *  0.000000E+00  1.000000E+00  0.000000E+00 *
                          *  0.000000E+00  0.000000E+00  1.000000E+00 *
          DIRECTION
     MASS AXIS SYSTEM (S)     MASS              X-C.G.       Y-C.G.       Z-C.G.
            X              3.880366E+02      1.716678E-18 -8.389609E-03 -1.568084E-02
            Y              3.880366E+02      2.042559E+00  1.072924E-18 -1.568084E-02
            Z              3.880366E+02      2.042559E+00 -8.389609E-03  3.147242E-17
                                     I(S)
                          *  3.688408E+02  6.860161E-01  1.567492E+01 *
                          *  6.860161E-01  3.749357E+02  2.045534E+00 *
                          *  1.567492E+01  2.045534E+00  3.690022E+02 *
                                     I(Q)
                          *  3.750093E+02                            *
                          *                3.530759E+02              *
                          *                            3.846935E+02 *
                                       Q
                          *  1.327335E-01 -7.042679E-01  6.974156E-01 *
                          * -9.911122E-01 -8.802141E-02  9.974416E-02 *
                          * -8.859106E-03 -7.044565E-01 -7.096919E-01 *
```

Table 6: PPLM FEM mass budget

In order to compare the FEM mass with the CDR PPLM nominal mass budget, masses concentrated at PAU and BEU, and corresponding location on SVM FEM must be added. We obtain the following MCI :

```
      O U T P U T   F R O M   G R I D   P O I N T   W E I G H T   G E N E R A T O R
                                REFERENCE POINT =       0
                                      M O
*  4.339660E+02 -5.551115E-16 -1.776357E-15  1.776357E-15 -3.834564E+01  1.108057E+01 *
* -5.551115E-16  4.339660E+02  3.552714E-15  3.834564E+01 -6.661338E-15  8.408449E+02 *
* -1.776357E-15  3.552714E-15  4.339660E+02 -1.108057E+01 -8.408449E+02 -1.776357E-15 *
*  1.776357E-15  3.834564E+01 -1.108057E+01  3.966811E+02  1.427441E+01  3.060960E+01 *
* -3.834564E+01 -6.661338E-15 -8.408449E+02  1.427441E+01  2.067511E+03 -6.652808E+00 *
*  1.108057E+01  8.408449E+02 -1.776357E-15  3.060960E+01 -6.652808E+00  2.043411E+03 *
                                      S
                          *  1.000000E+00  0.000000E+00  0.000000E+00 *
                          *  0.000000E+00  1.000000E+00  0.000000E+00 *
                          *  0.000000E+00  0.000000E+00  1.000000E+00 *
          DIRECTION
     MASS AXIS SYSTEM (S)     MASS              X-C.G.       Y-C.G.       Z-C.G.
            X              4.339660E+02      4.093309E-18 -2.553327E-02 -8.836094E-02
            Y              4.339660E+02      1.937582E+00 -1.534991E-17 -8.836094E-02
            Z              4.339660E+02      1.937582E+00 -2.553327E-02 -4.093309E-18
                                     I(S)
                          *  3.930099E+02  7.195106E+00  4.368824E+01 *
                          *  7.195106E+00  4.349161E+02  5.673718E+00 *
                          *  4.368824E+01  5.673718E+00  4.139219E+02 *
                                     I(Q)
                          *  4.483879E+02                            *
                          *                4.360001E+02              *
                          *                            3.574599E+02 *
                                       Q
                          *  6.193712E-01 -9.223321E-02  7.796617E-01 *
                          *  0.000000E+00  9.930753E-01  1.174798E-01 *
                          * -7.850983E-01 -7.276362E-02  6.150822E-01 *
```

Table 7: PPLM FEM + BEU and PAU mass budget

This is to be compared with PPLM CDR MCI :

29-MAR-04 / ESABASE / 5.2 MASS / PROPERTY PAGE: 1

MCI CDR (au 29/03/04)

MASS PROPERTY REPORT OF CONFIGURATION: (1)PLANCK

BASIC MASS AND CENTRE OF MASS

MASS =	429.930	KG
XCG =	0.9471	M
YCG =	-0.0207	M
ZCG =	-0.1129	M

INERTIA W.R.T. SYSTEM FRAME

IXX0 =	380.602	KGM2
IYY0 =	836.228	KGM2
IZZ0 =	799.157	KGM2
IXY0 =	-2.635	KGM2
IYZ0 =	7.333	KGM2
IZX0 =	3.096	KGM2

INERTIA W.R.T. MASS CENTRE

IXXCG =	374.934	KGM2
IYYCG =	445.061	KGM2
IZZCG =	413.289	KGM2
IXYCG =	5.794	KGM2
IYZCG =	6.328	KGM2
IZXCG =	49.086	KGM2

PRINCIPAL INERTIA W.R.T. MASS CENTRE

IP1 =	340.743	KGM2
IP2 =	444.245	KGM2
IP3 =	448.295	KGM2

DIRECTION COSINES OF PRINCIPAL AXES WITH THE SYSTEM FRAME

AXIS IP1 WITH (X,Y,Z) :	0.822336	0.079850	0.563371
AXIS IP2 WITH (X,Y,Z) :	-0.394626	0.793323	0.463582
AXIS IP3 WITH (X,Y,Z) :	-0.409918	-0.603541	0.683889

UNBALANCE ABOUT THE X-AXIS

STATIC UNBALANCE =	49.365	KGM
DYNAMIC UNBALANCE =	49.427	KGM2
CONING ANGLE =	34.681	DEGR

INERTIA RATIO

IP1/IP2 =	0.767
IP1/IP3 =	0.760
LAMBDA =	0.236 SQRT((IP1/IP2-1)*(IP1/IP3-1)

Table 8: PPLM CDR mass budget

Note : above mass budget is expressed in the PPLM reference frame, so 0.9665m must be added to X coordinates in order to obtain values in satellite reference frame. Satellite reference frame is shown in figure 8.

	Mass	Ixx CoG	Iyy CoG	Izz CoG	X CoG	Y CoG	Z CoG
FEM	434.0 Kg	393 Kg.m2	435 Kg.m2	414 Kg.m2	1.9376 m	-0.0255 m	-0.0884 m
Mass budget	430 Kg	375 Kg.m2	442 Kg.m2	410 Kg.m2	1.9136 m	-0.0206 m	-0.1130 m

Table 9: PPLM FEM MCI and mass budget comparison

The highest discrepancy is for Z CoG coordinate. This is mainly due to the fact that the RAA is represented by rigid masses on PR panel in PPLM FEM, thus the RAA CoG is not offset towards –Z as it is in reality. However, the impact of this simplified representation is very low with respect to the PPLM global dynamic behaviour, as shown in § 9.2.

Higher mass (+4Kg), and higher X CoG coordinate (+24mm) in PPLM FEM, are considered as conservative with respect to PPLM loading under sine environment.

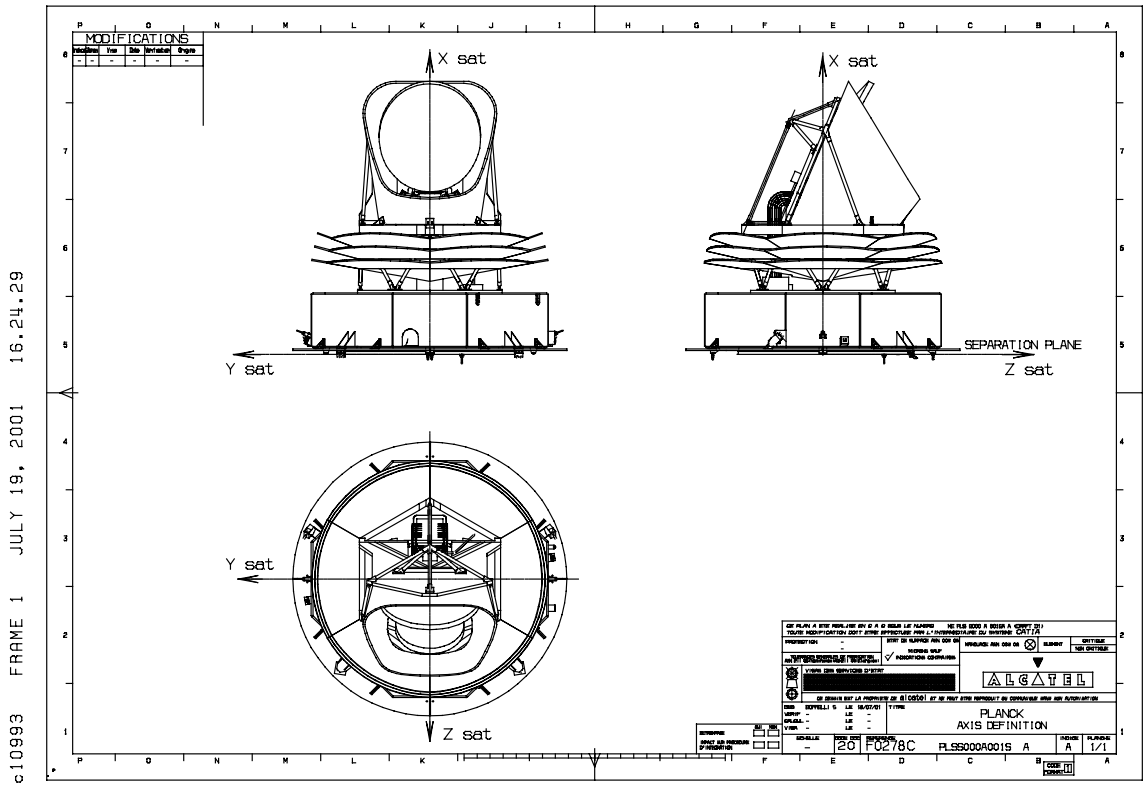

Figure 8: PLANCK Spacecraft Axes

3.5.4 FEM checks

3.5.4.1 Strain energy check

The numerical verification of the PLANCK PLM FEM is performed from computing conditioning matrix KRBG , KRBN and KRBF which are representative of the residual strain energy inside the model.

According to the ALCATEL specification [RD 18] (diagonal factors < E-3), the numerical verification test results presented hereafter are compliant.

MATRIX KRBG

```
0      MATRIX KRBF     (GINO NAME 101 ) IS A DB  PREC           6 COLUMN X           6 ROW SQUARE   MATRIX,
0COLUMN      1       ROWS       1 THRU       6
 ROW
      1)   -1,8375D-04  2,7738D-05 -1,4811D-05  1,0620D-05  9,9294D-05  2,7420D-05
0COLUMN      2       ROWS       1 THRU       6
 ROW
      1)    3,0692D-06 -1,4471D-04 -3,6000D-05 -1,8071D-04 -2,1191D-06 -5,8222D-05
0COLUMN      3       ROWS       1 THRU       6
 ROW
      1)   -8,2673D-05  9,7987D-05  3,3345D-05 -1,7058D-04  2,5355D-06  7,2068D-05
0COLUMN      4       ROWS       1 THRU       6
 ROW
      1)   -1,1676D-05 -1,2067D-04 -1,9258D-04  1,9908D-04  1,5417D-04 -6,6440D-05
0COLUMN      5       ROWS       1 THRU       6
 ROW
      1)    5,0289D-05 -3,0354D-06 -2,4191D-04 -2,3787D-05  2,5178D-04  9,9878D-07
0COLUMN      6       ROWS       1 THRU       6
 ROW
      1)    5,6951D-05 -6,0406D-05  2,1656D-05  1,1312D-04 -1,3285D-05 -1,4026D-04
```

MATRIX KRBN

```
0      MATRIX KRBG     (GINO NAME 101 ) IS A DB  PREC           6 COLUMN X           6 ROW SQUARE   MATRIX,
0COLUMN      1       ROWS       1 THRU       6
 ROW
      1)   -1,9909D-04  2,6252D-05 -1,9926D-05  1,3613D-05  1,1599D-04  1,1954D-05
0COLUMN      2       ROWS       1 THRU       6
 ROW
      1)   -2,0952D-06 -1,5943D-04 -3,6675D-05 -1,8117D-04 -2,5830D-06 -7,8020D-05
0COLUMN      3       ROWS       1 THRU       6
 ROW
      1)   -8,2250D-05  9,5792D-05  2,4940D-05 -1,6733D-04  1,7527D-05  6,5370D-05
0COLUMN      4       ROWS       1 THRU       6
 ROW
      1)   -1,3262D-05 -1,2592D-04 -1,9070D-04  2,0148D-04  1,4737D-04 -7,2907D-05
0COLUMN      5       ROWS       1 THRU       6
 ROW
      1)    6,2260D-05  8,5562D-07 -2,5128D-04 -3,6201D-05  2,8506D-04  1,0658D-05
0COLUMN      6       ROWS       1 THRU       6
 ROW
      1)    6,2781D-05 -7,6569D-05  2,9655D-05  1,0141D-04 -3,2138D-05 -1,7587D-04
```

MATRIX KRBF

```
0      MATRIX KRBF     (GINO NAME 101 ) IS A DB  PREC           6 COLUMN X           6 ROW SQUARE   MATRIX,
0COLUMN      1       ROWS       1 THRU       6
 ROW
      1)   -1,8375D-04  2,7738D-05 -1,4811D-05  1,0620D-05  9,9294D-05  2,7420D-05
0COLUMN      2       ROWS       1 THRU       6
 ROW
      1)    3,0692D-06 -1,4471D-04 -3,6000D-05 -1,8071D-04 -2,1191D-06 -5,8222D-05
0COLUMN      3       ROWS       1 THRU       6
 ROW
      1)   -8,2673D-05  9,7987D-05  3,3345D-05 -1,7058D-04  2,5355D-06  7,2068D-05
0COLUMN      4       ROWS       1 THRU       6
 ROW
      1)   -1,1676D-05 -1,2067D-04 -1,9258D-04  1,9908D-04  1,5417D-04 -6,6440D-05
0COLUMN      5       ROWS       1 THRU       6
 ROW
      1)    5,0289D-05 -3,0354D-06 -2,4191D-04 -2,3787D-05  2,5178D-04  9,9878D-07
0COLUMN      6       ROWS       1 THRU       6
 ROW
      1)    5,6951D-05 -6,0406D-05  2,1656D-05  1,1312D-04 -1,3285D-05 -1,4026D-04
```

Table 10: PPLM strain energy check

3.5.4.2 Free-free modes

With free boundary conditions, the first seven frequencies of the satellite model are described hereafter :

REAL EIGENVALUES

MODE NO.	EXTRACTION ORDER	EIGENVALUE	RADIANS	CYCLES	GENERALIZED MASS	GENERALIZED STIFFNESS
1	1	3.592250E-07	5.993538E-04	9.539012E-05	1.000000E+00	3.592250E-07
2	2	4.951627E-07	7.036780E-04	1.119938E-04	1.000000E+00	4.951627E-07
3	3	1.163635E-06	1.078719E-03	1.716834E-04	1.000000E+00	1.163635E-06
4	4	2.463147E-06	1.569442E-03	2.497844E-04	1.000000E+00	2.463147E-06
5	5	3.136540E-06	1.771028E-03	2.818678E-04	1.000000E+00	3.136540E-06
6	6	4.915792E-06	2.217159E-03	3.528717E-04	1.000000E+00	4.915792E-06
7	7	1.261733E+04	1.123269E+02	1.787738E+01	1.000000E+00	1.261733E+04

Table 11: free free modes

The distance between the last free – free mode and the first elastic mode is higher than a factor1 E+ 4 which is acceptable according to [RD 18].

3.5.4.3 Static check

The interface forces computed in the PPLM reference frame are described hereafter for a 1g static loading along the 3 PPLM axes.
Interface points are the 6 SVM I/F brackets plus the 2 bracing struts connections to the SVM subplatform (nodes 200000 and 200100).

FORCES OF SINGLE-POINT CONSTRAINT

POINT ID.	TYPE	T1	T2	T3	R1	R2	R3
49200	G	-5.337034E+02	2.345373E+01	5.475190E+01	9.326839E-02	-1.300459E+00	-1.727734E+00
49201	G	-8.088872E+02	-4.496633E+01	5.007025E+01	-2.865438E-01	8.814066E-01	-1.986412E+00
49202	G	-5.719158E+02	1.305241E+02	-1.036278E+02	1.298923E+00	-6.857715E-01	-2.951673E+00
49203	G	-5.452309E+02	-1.273288E+02	-1.002917E+02	-1.431689E+00	-6.308566E-01	2.542598E+00
49204	G	-7.934804E+02	4.393893E+01	4.346532E+01	2.862312E-01	8.317095E-01	1.913200E+00
49205	G	-5.334154E+02	-2.560792E+01	5.570000E+01	-1.015935E-01	-1.266987E+00	1.709970E+00
200000	G	-1.056488E+01	5.685371E-02	-3.359755E-02	4.111970E-04	-3.621952E-03	6.260519E-03
200100	G	-9.441480E+00	-7.058238E-02	-3.451951E-02	-4.242965E-04	-3.410519E-03	-8.003389E-03

1 PPLM MARCH 29, 2004 MSC/NASTRAN 7/17/97 PAGE 15

ANALYSE QS

0 Y SUBCASE 2

FORCES OF SINGLE-POINT CONSTRAINT

POINT ID.	TYPE	T1	T2	T3	R1	R2	R3
49200	G	2.968413E+01	-8.811996E+02	-4.606812E+02	1.058798E+00	-7.354142E+00	1.738161E-01
49201	G	-1.275531E+03	-1.144461E+02	8.012818E+00	5.050565E-01	-1.823340E+00	-1.146270E+01
49202	G	-1.278527E+03	-9.084083E+02	4.536402E+02	-2.076190E+00	3.503749E+00	-1.324375E+00
49203	G	1.278976E+03	-9.051414E+02	-4.542435E+02	-2.184447E+00	-3.182898E+00	-1.001543E+00
49204	G	1.274019E+03	-1.142285E+02	-7.301058E+00	5.444762E-01	1.815479E+00	-1.144898E+01
49205	G	-2.903861E+01	-8.809874E+02	4.605749E+02	1.055932E+00	7.340900E+00	1.632369E-01
200000	G	6.703978E+00	-1.111877E+00	-1.272931E-01	7.714457E-04	4.568610E-03	-1.538688E-01
200100	G	-6.186976E+00	-1.116192E+00	1.251244E-01	7.375096E-04	-4.498257E-03	-1.540268E-01

1 PPLM MARCH 29, 2004 MSC/NASTRAN 7/17/97 PAGE 16

ANALYSE QS

0 Z SUBCASE 3

FORCES OF SINGLE-POINT CONSTRAINT

POINT ID.	TYPE	T1	T2	T3	R1	R2	R3
49200	G	1.019538E+03	-5.700109E+02	-4.355695E+02	7.606128E-01	5.516358E+00	9.044878E+00
49201	G	1.661610E+02	4.627378E+00	-1.065927E+03	1.097106E+00	-3.101040E+00	-6.113295E-02
49202	G	-1.187267E+03	4.960278E+02	-4.120778E+02	1.339905E+00	7.606500E+00	-8.058428E+00
49203	G	-1.174792E+03	-4.890953E+02	-4.053111E+02	-8.660819E-01	7.304546E+00	8.002552E+00
49204	G	1.658966E+02	-4.402098E+00	-1.054572E+03	-1.849408E+00	-3.036530E+00	1.107635E-01
49205	G	1.007598E+03	5.629459E+02	-4.309645E+02	-7.242048E-01	5.521824E+00	-9.001347E+00
200000	G	1.386358E+00	-1.117427E-01	-1.110013E+00	-5.715572E-04	1.400635E-01	-6.432445E-03
200100	G	1.477604E+00	1.189914E-01	-1.107422E+00	6.212057E-04	1.403415E-01	7.717796E-03

1 PPLM MARCH 29, 2004 MSC/NASTRAN 7/17/97 PAGE 17

Table 12: I/F forces under 1g acceleration

For the 3 directions, the sum of the interface forces is coherent with the applied static acceleration.

3.5.4.4 Thermo-elastic check

CSAG approach is to have a unique FEM suitable for static, dynamic and thermo-elastic analyses. Here, the thermo-elastic checks are made only on the PPLM FEM without equipment. Indeed, interface loads at PR, SR and FPU FEMs are injected in CSAG FEM by equipment FEMs in line with the I/F requirement [RD 19]. That is to say : despite those models are not suitable for thermo-elastic check, they are designed in order to inject specified conservative interface loads on a rigid support once thermally loaded at cryo-temperature.

The 0 stress check results for PPLM are the following :

Stress max = 6.65*E3 Pa
Rotation max = 1.86*E-5 rad

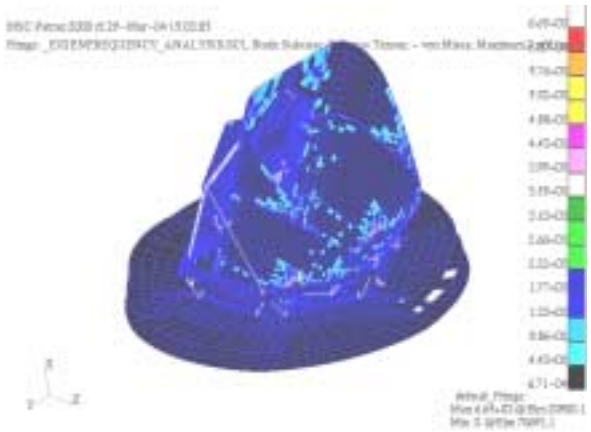

Figure 9: PPLM stresses

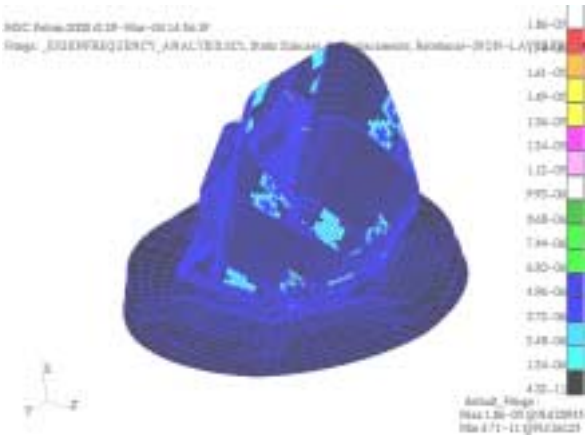

Figure 10: PPLM displacements

These results are not in line with the spec [RD 18) (1.*E3 Pa, 1.*E-z rad). However the only part that is not compliant is the baffle.
The results for the PPLM without baffle are the following :

Stress max = 3.52*E+2 Pa
Rotation max = 7.24*E-8 rad

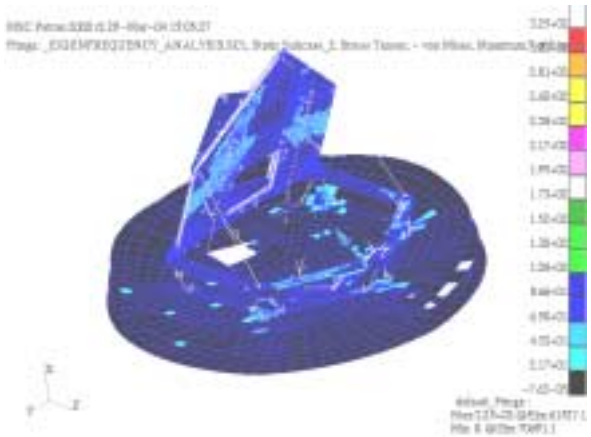

Figure 11: PPLM stresses without baffle

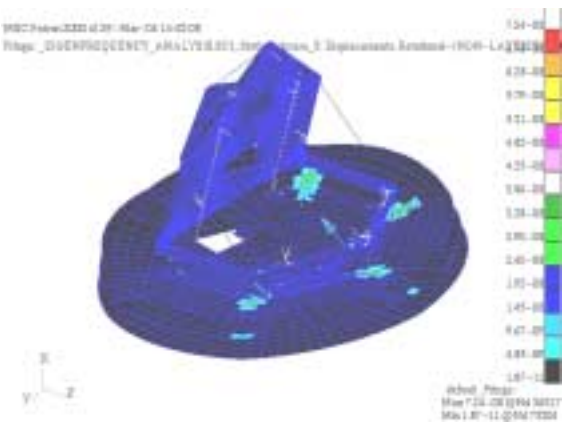

Figure 12: PPLM displacements without baffle

Concerning the baffle, a big effort has been asked to CSAG to reduce non compliance since PDR, and results are much better (seer [RD 1], §6.3.1). Higher improvements are unlikely for such non regular surface, subjected to warping effects, without degrading quality of the meshing.
Concerning the rotations issue, ALCATEL has asked CSAG to check only the rotations around in plane axes. Indeed, rotations around out of plane axes are not physical for QUAD elements and can be high on such surfaces. They will not affect the stability budget. Taking into account this request, results for baffle become :

Stress max = 6.65*E3 Pa
Rotation max = 6.82*E-7 rad

These results, below an exceed of a factor of 7 with respect to the spec are acceptable for such a surface, especially because the baffle is not in the direct load path for the stability. Moreover, CSAG have checked at their CDR that no sizing stresses appear in the out of spec elements (see CSAG CDR RID CDR-CSAG-3.1-0029).

4. PLANCK PLM DYNAMIC PROPERTIES

In order to ensure a satisfying dynamic behaviour with respect to Planck satellite, stiffness and frequency requirements have been derived separately to cryo-structure, V-grooves, baffle and telescope (see [RD 19] and [RD 20]).
This approach has remained unchanged since PDR, despite the evolution of sub-system testing boundary conditions since PDR, to a more "PPLM-like" configuration. As a consequence, most of the time, stiffness and frequency requirement cannot be checked directly during mechanical tests, but only after correlation of the FEMs. This choice has been made for the following reasons :

- cryo-structure and telescope + baffle are tested separately at subsystem level, despite evolution of B.C.
- Stiffness criteria are simple to check because B.C. are simple. Re-assessing stiffness specification taking into account tests B.C. evolution would have been risky, since in final cryo-structure and telescope tests B.C. are defined by CSAG dummies, under CSAG responsability
- having separated specification for each subsystem allows to have a better vision of the design evolutions impact on stiffness for each separated sub-system.
- The total of those specs is known by ALCATEL to ensure an acceptable and controlled dynamic behaviour for the whole PPLM. This is proved by the very similar PPLM dynamic behaviour wrt PDR, despite several design changes (see [RD 21]).

In §4.1 a status is made for each PPLM sub-system in order to check that no unjustified deviation exists at subsystem level, but what in final is important for the PPLM CDR, is the PPLM modal signature presented in §4.2.

4.1 PPLM sub-systems stiffness checks

Note : some results presented hereafter are extracted from CSAG document [RD 22] which has been issued between their Delta-PDR and CDR, and is the official CSAG CDR document. Slight changes have been implemented since this issue in CSAG PPLM FEM which has been delivered for our CDR analyses. The impact of these changes is low and is described in [RD 23] and [RD 24](mail EM-1019). Presented results remain valid.

4.1.1 V-Grooves and baffle frequencies

V-grooves and Baffle frequencies on rigid supports have been verified by CSAG for their CDR. Results are presented in [RD 22].

Lowest V-grooves mode is at 20.9Hz for V-groove 1 for a specification at 17Hz.
Lowest baffle mode is at 35.6Hz for a specification at 30Hz.

Slight MCI evolution on ALCATEL CDR V-grooves at instrument I/F have a very minor contribution on V-grooves modes. Baffle MCI is unchanged with respect to CSAG FEM. So V-grooves and baffle modes have not been re-verified for ALCATEL CDR FEM.

V-grooves and baffle are light and flexible structures with modes that are spread mainly between 20Hz and 80Hz. Possibilities of coupling with main PPLM modes are not avoidable. However, since these structures effective masses are distributed over a large frequency range, and no major coupling has been identified. Moreover, occurring couplings and resulting loading under sine environment have been taken into account through CSAG sine analyses, which cover system analyses as explained in § 6.3.11.

4.1.2 Cryo-structure stiffness

Results are presented in [RD 22], §5.2. Stiffness requirement is reached for the 3 directions.
These results correspond to the current cryo-struts design (50mm diameter, 1.55mm thickness).
The main consequence of this compliance is to ensure sufficiently high PPLM modes, especially lateral modes with respect to launcher requirements.

4.1.3 Telescope frequencies

Telescope frequencies specification corresponds to a particular configuration that has not evolved since PDR and is not fully flight representative (see §4 introduction).

Main differences with flight configuration are B.C. (simply supported at frame I/F points, with radial DoF free, instead of mounted on cryo-structure), and the fact that the baffle is represented by a lumped mass connected to telescope via RBE3 element, in order not to "mix" baffle and telescope modes.
Telescope modes description is given by CSAG in [RD 22], §4.1. There is a non compliance for the 2 first Z and Y lateral modes which are around 42Hz for a specification at 45Hz. An RFD [RD 25] has been issued and accepted, since it has been verified at PPLM level that it did not have an impact on PPLM main modes.

In order to take into account updates on ALCATEL CDR telescope FEM, and mainly the effect of the presence of the baffle FEM with corresponding inertia, first telescope main modes with baffle in ALCATEL configuration are given hereafter for information, and are not directly comparable to the spec because of the baffle (B.C. remain identical to those specified to CSAG for this calculation) :

Frequency [Hz]	Mx [Kg]	My [Kg]	Mz [Kg]	Mode description
36.9	0.0	68.8	0.0	Y lateral main mode
47.3	0.0	31.0	0.0	2nd Y lateral mode
48.8	2.7	0.0	55.7	Z lateral main mode
51.5	27.7	0.0	2.1	X longitudinal first mode
61.3	13.7	0.0	47.5	2nd Z lateral mode
72.9	47.2	0.0	5.5	X longitudinal main mode

Table 13: Telescope main modes – ALCATEL configuration

Total mass of telescope in ALCATEL configuration is 223.6Kg.
The differences with CSAG modes computation are mainly due to the baffle.

Comments:

PLANCK Telescope+baffle Lateral main modes are located at 37Hz and 47Hz for the Y axis and at 49 Hz and 61Hz for the lateral Z axis. The frequency of these modes are correctly located compared to the frequencies of the PPLM which are at 19 Hz (Y axis) and 26 Hz (Z axis).
PLANCK Telescope longitudinal modes are located at 51 Hz and 73 Hz. They are de-coupled from telescope Y main modes. Coupling possibility with telescope Z mode is identified around 50Hz, but would be due to unrealistic B.C. with respect to flight configuration : it disappears with the PPLM configuration (see §4.2), which in final should be considered.
So, the telescope dynamic behaviour is acceptable.

4.2 PPLM Modal analysis

The following results are given for CDR ALCATEL FEM.

Analysis has been performed up to 140Hz.

The PPLM is clamped at the 6 SVM brackets location. V-groove 1 bracing struts are also clamped at the SVM subplatform I/F.

Main modes are listed in the following table (Meff > 10%).

Frequency (Hz)	Mx [Kg]	My [Kg]	Mz [Kg]	Mode description
18.6	0.0	160.3	0.0	First Y lateral mode
25.7	3.5	0.0	217.3	First Z lateral mode
33.1	0.6	105.9	6.3	Second Y lateral mode
33.3	11.7	7.8	88.8	Second Z lateral mode
53.7	35.6	0.0	4.1	First longitudinal mode
64.9	69.6	0.0	1.5	Main longitudinal mode

Table 14: PPLM main modes

Secondary modes are listed in the following table.

Frequency (Hz)	Mx [Kg]	My [Kg]	Mz [Kg]	Mode description
30.4	17.1	0.0	0.0	V-groove 1 out of plane mode
32.3	0.	29.6	0.0	V-groove 2 Y mode
34.3	26.9	0.0	1.9	V-groove 3 out of plane mode
35.6	0.0	17.4	0.0	Cryo-structure + baffle Y mode
36.4	9.5	0.0	0.0	V-groove 2 out of plane mode
40.5	0.0	4.1	0.0	Torsion mode around X axis (Ix = 167.6 Kg.m2)
42.0	25.5	0.0	0.0	Secondary longitudinal global mode
47.3	17.6	0.0	0.3	Baffle + V-groove 3 mode
68.1	9.2	0.0	5.22	Secondary global X-Z mode
72.3	8.8	0.0	0.3	Secondary global longitudinal mode

Table 15: PPLM secondary modes

Main modes deformed shapes are given hereunder :

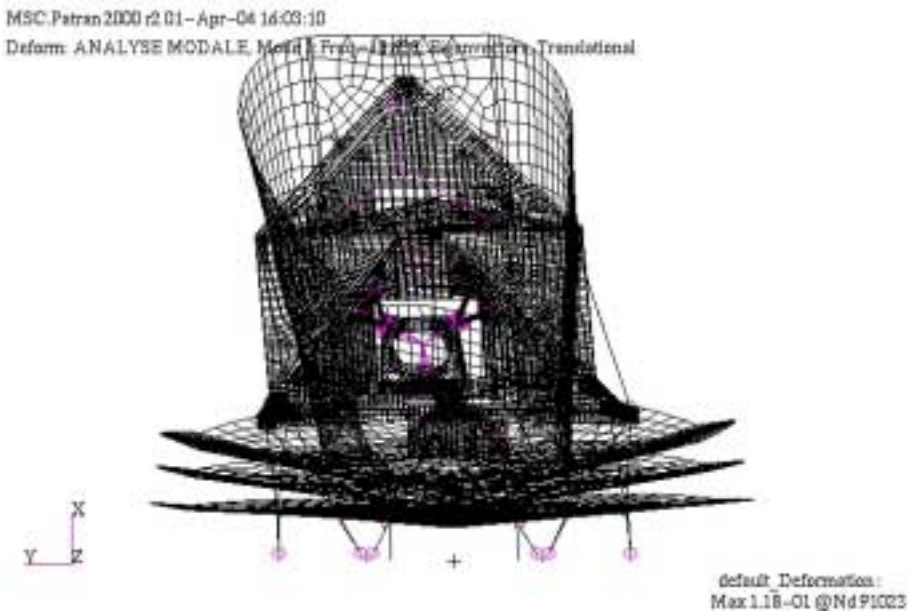

Figure 13: PPLM Y first lateral mode 18.6Hz

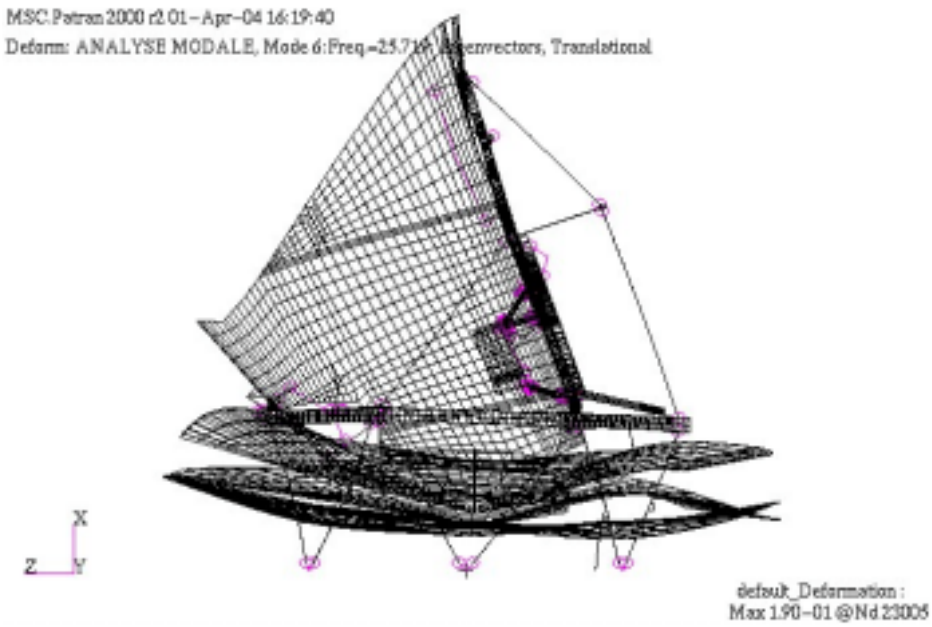

Figure 14: PPLM Z first lateral mode 25.7Hz

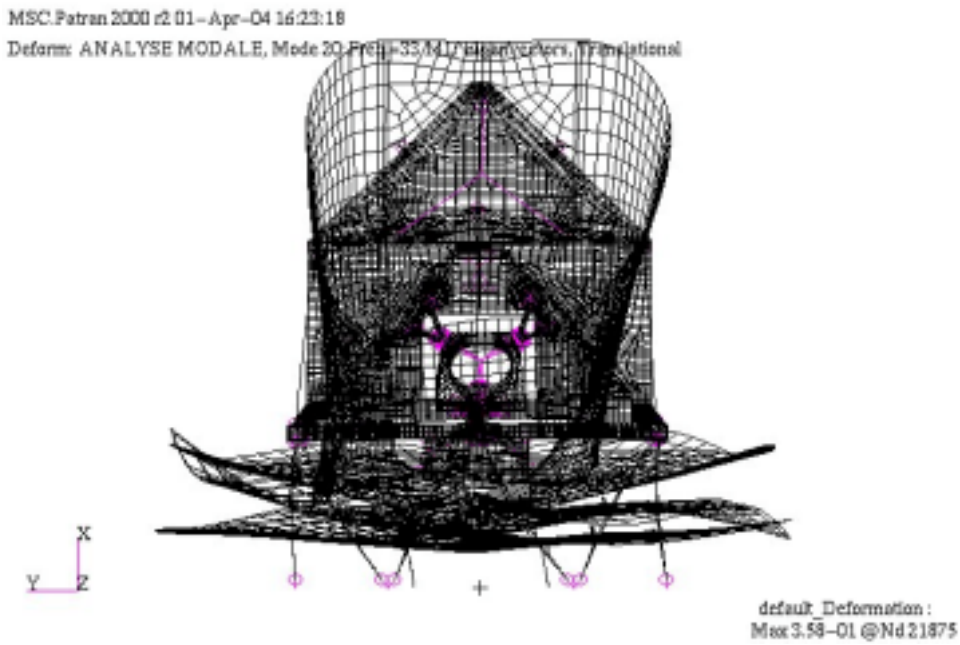

Figure 15: PPLM Y second lateral mode 33.1Hz

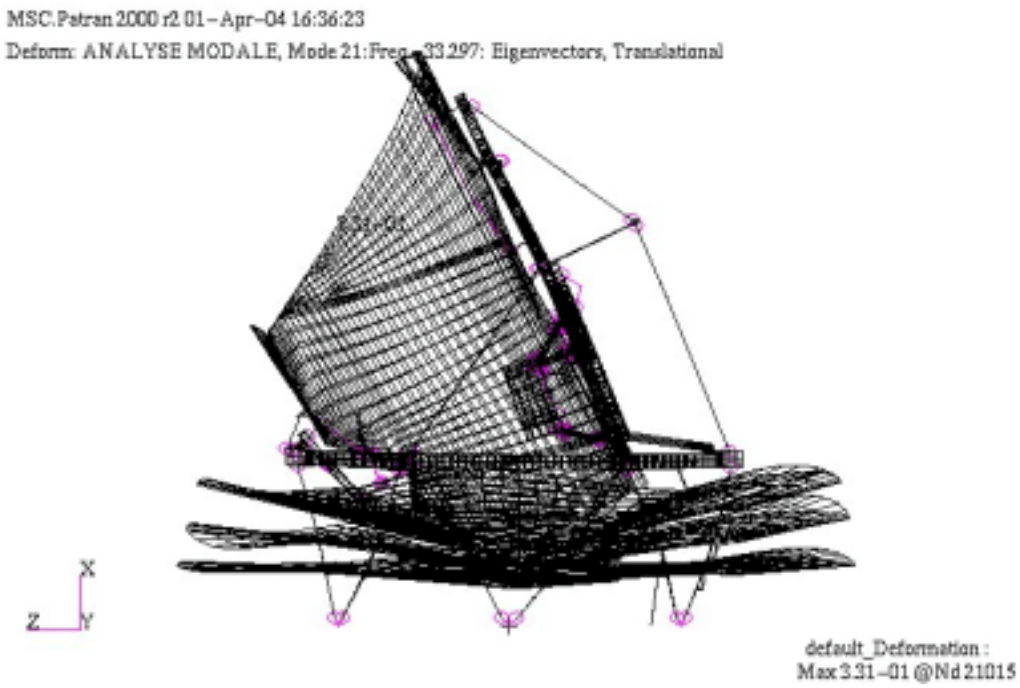

Figure 16: PPLM Z second lateral mode 33.3Hz

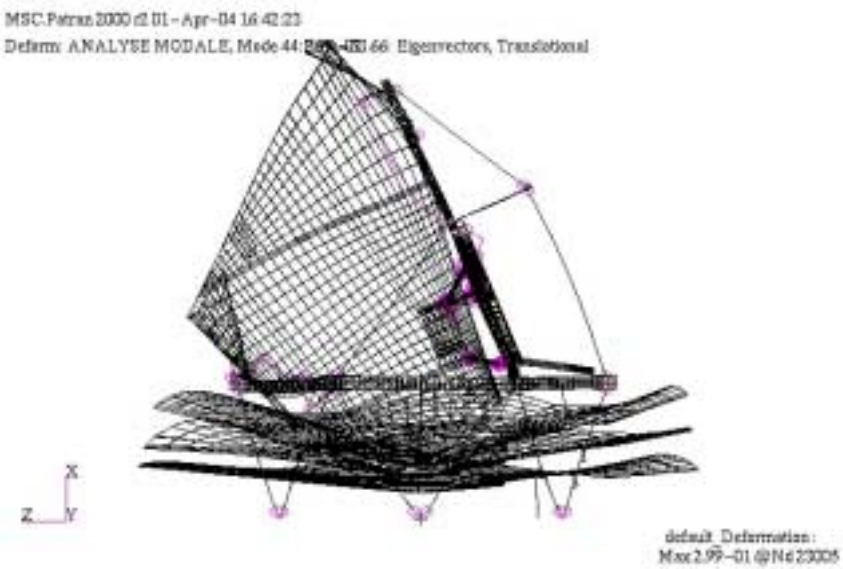

Figure 17: PPLM first longitudinal mode 53.7Hz

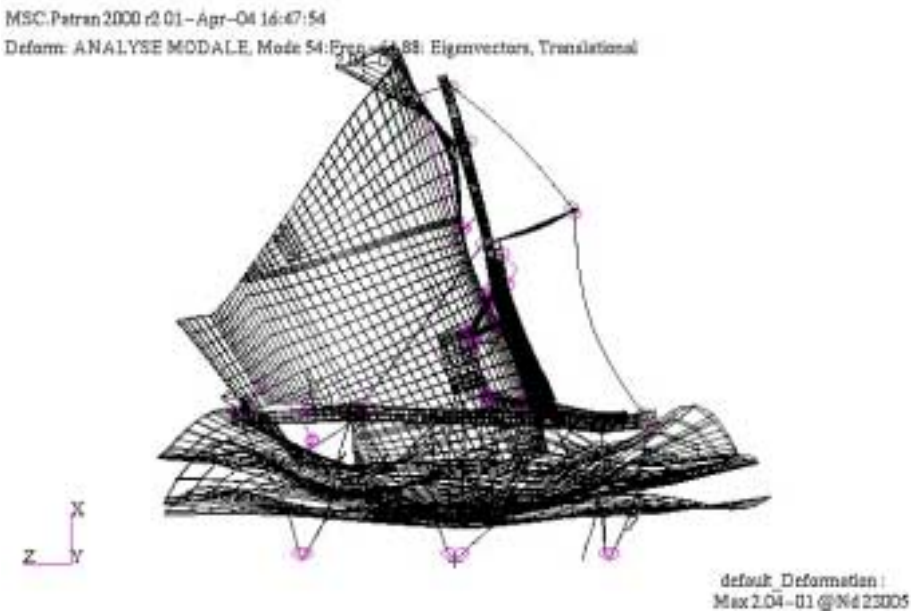

Figure 18: PPLM main longitudinal mode 64.9Hz

Comments :

Generally speaking, PPLM dynamic behaviour is close to PDR one. There are 2 well defined lateral modes for Y and Z axes, at similar frequencies as PDR ones, slightly higher (19Hz and 33Hz for Y, 26Hz and 33 Hz for Z). Those modes are well identified and de-coupled from launcher and SVM lateral modes.

Longitudinal main modes are higher than PDR ones, especially because of the increase of cryo-struts and frame stiffness, due to sizing constraints. They are de-coupled from lateral main modes.
PDR longitudinal mode at 60Hz has shifted up to 65Hz, but, as for PDR, is still very sensitive for equipment response, especially the SR. Since PDR, it has become obvious that this mode, whatever its frequency

(always around 60Hz), is linked to the PPLM design concept, and that it is hard to control its deformed shape (many parts of the structure are involved). This mode is a global mode mainly due to stiffness coupling between cryo-structure and telescope interfaces. Some design changes, such as telescope struts diameter and thickness modifications, have been decided in order to limit equipment response on this mode, but despite these changes, recent integration of SR simplified FEM with up to date ISMs stiffness has modified the SR response with a high increase of in plane SR response. This is detailed in § 6.3 and § 9.1.

As a conclusion :

- PPLM lateral dynamic behaviour is safe with no risk of coupling with launcher, SVM or longitudinal PPLM modes.
- PPLM longitudinal behaviour still shows a global mode at 65Hz that cannot be avoided, and cannot be perfectly controlled in term of deformed shape and instrument response. Moreover, SVM modes around that frequency can slightly couple with PPLM response (actually, it is not a strong coupling between the 2 structures, as strain energy study shows – see § 5.2). This effect is taken into account in following system sine analyses. Equipment response on that mode is likely to lead to the necessity of a secondary notching down to a minimum of 0.6g as base input. This possibility has already been discussed with Arianespace and agreed in principle, as explained in § 9.1.
- Concerning secondary modes, they mainly concern V-grooves and baffle modes, which are spread between 20Hz and 80Hz (most of them are below 50Hz), and can show high displacements at their edges. Coupling effects on these structures remain limited due to the distribution of the modes between 20Hz and 70Hz, and have been taken into account in CSAG analyses.

5. PLANCK SATELLITE PROPERTIES

Since PPLM CDR analyses are performed at satellite level, a short overview of Planck CDR FEM behaviour is given here.

5.1 Planck overview

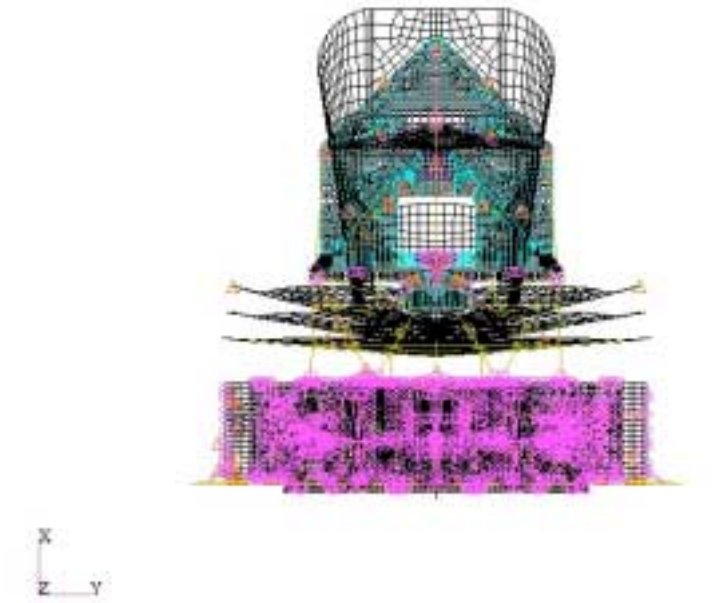

Figure 19: view of CDR PLANCK satellite FEM

PPLM FEM is the one described in § 3.
The detailed Planck and SVM CDR FEM descriptions are given in [RD 26].
Planck CDR FEM checks are described in [RD 26] (FEM description). The model is compliant for sine analyses.

Planck CDR FEM mass is 1925.6kg.

5.2 Planck modal analysis

The modal analysis is performed up to 140Hz.

The boundary conditions applied at the interface of the spacecraft are simply supported boundary conditions.
Only main modes are given.

Mode Nr	Frequency Hz	Mxx Kg	Myy Kg	Mzz Kg	Mode Description
7	18.039	0.000	181.173	0.008	1st PLM Y-Lateral Mode
11	24.637	2.422	0.031	264.462	1st PLM Z-Lateral Mode
24	31.667	0.018	43.665	0.036	PLM Groove#1 (Bending about 3 in-plane local axes)
25	31.992	0.070	76.956	0.189	In-phase Opposition Coupling between PLM Groove#1 (Bending about 3 in-plane local axes) & PLM Groove#2 (Bending about 3 in-plane local axes) – second Y lateral mode
27	32.830	2.626	74.123	23.792	PLM Baffle (Combined Bending and Torsion Mode) + PLM Groove#2 (Bending about 3 in-plane local axes)+ Inner SA Breathing Mode
28	32.919	8.843	21.797	98.093	PLM Baffle (Breathing Mode) + PLM Groove#2 (Bending about 3 in-plane local axes) + Outer SA Bending Mode – second Z lateral mode
29	34.292	34.441	0.019	0.395	PLM Groove#3 (Breathing Mode)
33	37.016	20.337	76.460	2.276	SVM Panel +Y (Out-of-plane Bending Mode)
40	41.881	73.444	21.973	3.134	PLM Baffle (Bending about local Y and Z axes in CORD20000) + PLM Primary_Reflector (Bending about global Y-axis) + SVM Octogonal Box (Bending Mode about global Z-axis) + SVM Panel+Y (Out-of-plane Bending Mode)
41	42.135	50.615	0.362	0.481	PLM Baffle (Bending about local Y and Z axes in CORD20000) + PLM Primary_Reflector (Bending about global Y-axis)
45	45.089	190.015	0.248	41.365	1st SVM Longitudinal Mode
47	47.734	17.169	0.044	4.440	Coupling between PLM Baffle (Bending about global Y-axis on the reflector I/F side) + PLM Groove3 (Bending about 3 in-plane local axes) + PLM Primary_Reflector (Bending about global Y-axis)
50	49.231	2.381	2.523	21.605	PLM Groove#1 (Bending about 3 in-plane local axes)
51	49.504	0.113	38.444	7.487	SVM Panel -Y+Z (Out-of-plane Bending Mode)

Mode Nr	Frequency Hz	Mxx Kg	Myy Kg	Mzz Kg	Mode Description
52	50.293	65.173	2.798	206.181	1st SVM Z-Lateral Mode
54	51.176	0.093	52.753	1.832	PLM Baffle (Bending about local Y and Z axes in CORD20000) + PLM Primary_Reflector (Torsion about local X-axis in CORD20000) + PLM Groove#2 (Bending about 3 in-plane local axes) + In-Phase Opposition SVM Tanks#2&3 Bending Mode
55	52.109	0.004	27.136	26.770	SVM Tank#2 (1st Lateral Mode)
56	52.246	0.104	87.525	13.981	SVM Tank#3 (1st Lateral Mode)
58	53.706	72.189	0.856	14.098	PLM Baffle (Breathing Mode)
59	53.971	0.043	2.519	27.238	SVM Octagonal Box (Combined Bending about global Y and Z axes)
61	55.666	4.203	4.201	53.518	SVM Panel +Z (Out-of-plane Bending Mode)
64	57.707	23.181	0.117	0.029	PLM Groove#1 (Bending about 3 in-plane local axes)
69	61.731	0.000	161.179	3.369	SVM Octagonal Box (Combined Bending about global Y and Z axes)
70	62.048	0.860	76.308	2.607	1st SVM Y-Lateral Mode
71	62.712	36.494	54.163	36.802	SVM Shear Panels +Y +Z (Bending about Out-of-plane local axes) + PLM Baffle (Breathing Mode)
72	62.973	171.954	4.855	18.850	1st PLM Longitudinal Mode
73	63.147	24.385	29.756	13.113	SVM Panel -Y (Out-of-plane Bending Mode) + PLM Groove#3 (Bending about 3 in-plane local axes)
74	63.539	4.764	32.076	7.276	PLM Struts_Blades_Brace (Bending about global Z-axis) + PLM Grooves In-phase Bending Mode
75	64.219	5.260	20.153	82.517	PLM Baffle (Bending about global Y-axis) + PLM Primary_Reflector (Bending about global Y-axis)
76	64.435	21.268	19.494	8.217	PLM Baffle (Bending about global Y-axis) + PLM Primary_Reflector (Bending about global Y-axis)
78	66.483	4.637	10.506	117.458	SVM Shear Panels +Y +Z (Bending about global X-axis)
79	67.522	2.519	13.661	82.040	SVM Shear Panel +Y +Z (Bending about global X-axis)
80	68.269	18.715	0.054	53.612	SVM Shear Panel -Y -Z (Bending about global X-axis) + SVM Shear Panel +Y +Z (Bending about global X-axis)
85	70.645	15.428	5.819	1.824	SVM Lower_Closing_Panel (Local Bending -Y+Z due to Equipments and Connector Brackets resonance)

Mode Nr	Frequency Hz	Mxx Kg	Myy Kg	Mzz Kg	Mode Description
87	71.312	61.904	9.512	7.250	SVM Lower_Closing_Panel (Local Bending - Y+Z due to Equipments and Connector Brackets resonance)
88	71.478	14.341	4.458	1.602	PLM Groove#1 (Bending about 3 in-plane local axes) + PLM Baffle (Bending about local Y and Z axes in CORD20000 + Torsion about local longitudinal axis in CORD20000)
90	72.113	7.362	11.852	2.732	SVM Inner Solar Array (Bending about global Z-axis)
96	74.414	106.927	6.091	0.238	SVM Tank#3 (Longitudional Mode)
97	75.091	17.024	1.985	0.313	PLM Baffle (Bending about local Y and Z-axes in CORD20000)
98	75.866	41.770	14.058	15.942	PLM Groove#1 (Bending about global Y-axis)
99	76.319	5.087	22.108	18.999	PLM Groove#1 (Bending about 3 in-plane local axes)
100	77.191	112.098	16.758	4.819	SVM Octagonal Box (Combined Bending about global Y and Z axes)
101	77.433	15.814	39.193	0.482	SVM Shear Panel -Y +Z (Bending about global X-axis)
102	77.589	10.258	10.096	1.675	PLM Groove#3 (Bending about 3 in-plane local axes)
104	79.074	16.968	31.188	1.765	SVM Tank#1 (Longitudinal mode)
111	82.350	0.021	37.005	77.095	SVM Payload Subplatform (Longitudinal Mode)
113	83.778	2.285	8.205	26.512	SVM Outer Solar Array (Bending about global Z-axis)
114	84.448	2.306	8.949	11.399	SVM Lower_Closing_Panel (Panels +Y-Z & -Y-Z Local Bending)
119	87.088	0.698	22.207	0.486	SVM Lower_Closing_Panel (Panel +Y+Z Local Bending)
122	87.853	0.005	30.117	0.610	SVM Shear Panel -Y +Z (Bending about global X-axis)
129	89.964	10.404	14.137	1.400	PLM Groove#2 (Breathing Mode)
132	91.405	19.512	0.185	10.178	SVM Lower_Closing_Panel (Panel +Y+Z Local Bending)
236	131.802	0.074	26.018	0.234	SVM Inner Solar Array (Bending about global Y and Z-axes)
249	136.827	0.146	0.035	19.229	SVM Inner Solar Array (Bending about global Y and Z-axes)

Table 16: Planck main modes

A closer look to longitudinal mode at 63Hz, generating high equipment responses, has been done in order to assess the risk of coupling between SVM and PPLM :
Strain energy calculation on this mode shows that PPLM participation is about 70%, and SVM 30%. Participation factor for this mode is 2.3, which shows that no strong coupling occur between the 2 structures (usual minimum value for identifying high coupling is 3). As a consequence, impact of SVM

modes around 60Hz on PPLM equipment responses on this mode is rather low, and this issue can be treated at PPLM level.

6. PPLM SINE ANALYSES

PPLM CDR sine analyses have been performed at satellite level, with the inputs described hereafter. Only primary notchings on satellite interface loads have been used, and if necessary, envisaged secondary notchings are explained case by case. Indeed, they cannot be taken for granted until they are formally accepted by Arianespace. At that stage, only obvious necessary secondary notching is for the 63Hz longitudinal mode on equipment response.

6.1 Methodology

The dynamic response analysis is performed using the input qualification levels specified by ARIANE5 user's manual.

***Longitudinal axis :** ±1.25g from 5Hz to 100Hz,
***Lateral axis :** ±1.00g from 5Hz to 25 Hz,
±0.80g from 25Hz to 100Hz.

These qualification levels are applied at the base of the spacecraft .
The reduced damping factor considered in this analysis is 2% for all the whole spacecraft except that for SVM propellant tanks which have a 5% damping in longitudinal direction.

6.2 Primary notching

Analyses and primary notching level evaluation have been performed from the main ARIANE V qualification quasi-static loads (7.5g longitudinal and 2.5g lateral) which are summarised in the following table.

Flight Event	Long. Flight Level [g]	Lat. Flight Level [g]	Long. Qualif Level [g]	Lat. Qualif Level [g]
Max Dynamic Pressure	-3.2	±2.0	-4.0	±2.5
SRB End of Flight	-6.0	±1.0	-7.5	±1.25
Max Tension Case	2.5	±0.9	3.13	±1.13

Table 17: Ariane V quasi-static loads

The following table presents the qualification maximal loads at the launcher interface due to the dynamic response (with qualification factor of 1.25), the maximum quasi-static loads at the interface and the foreseen notching values.

Load	Launcher Quasi-Static Loads [g]	Launcher Quasi-Static I/F Loads [N/Nm]
Fx	7.5	141677
Fy	2.5	47226
Fz	2.5	47226
My	2.5	37544
Mz	2.5	37544

Table 18: Predicted notching levels

The notched levels to be applied at S/C interface are presented on the following figures.

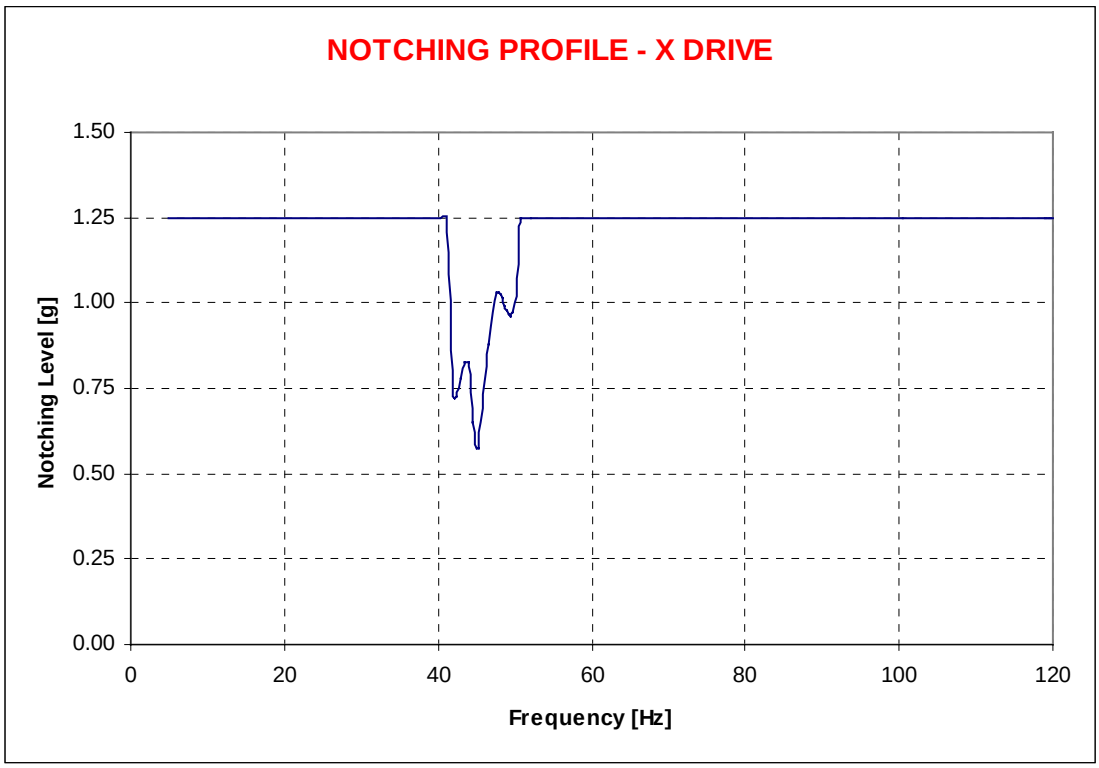

Figure 20 : Qualification notching level along X Axis

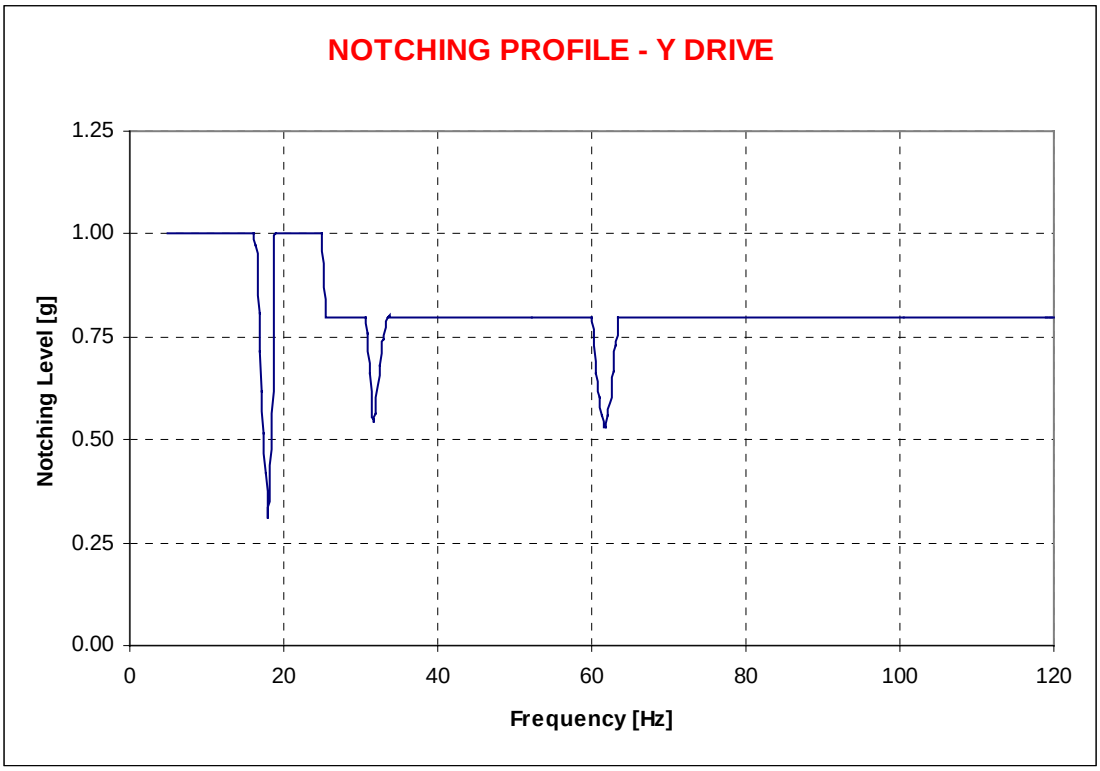

Figure 21: Qualification notching level along Y Axis

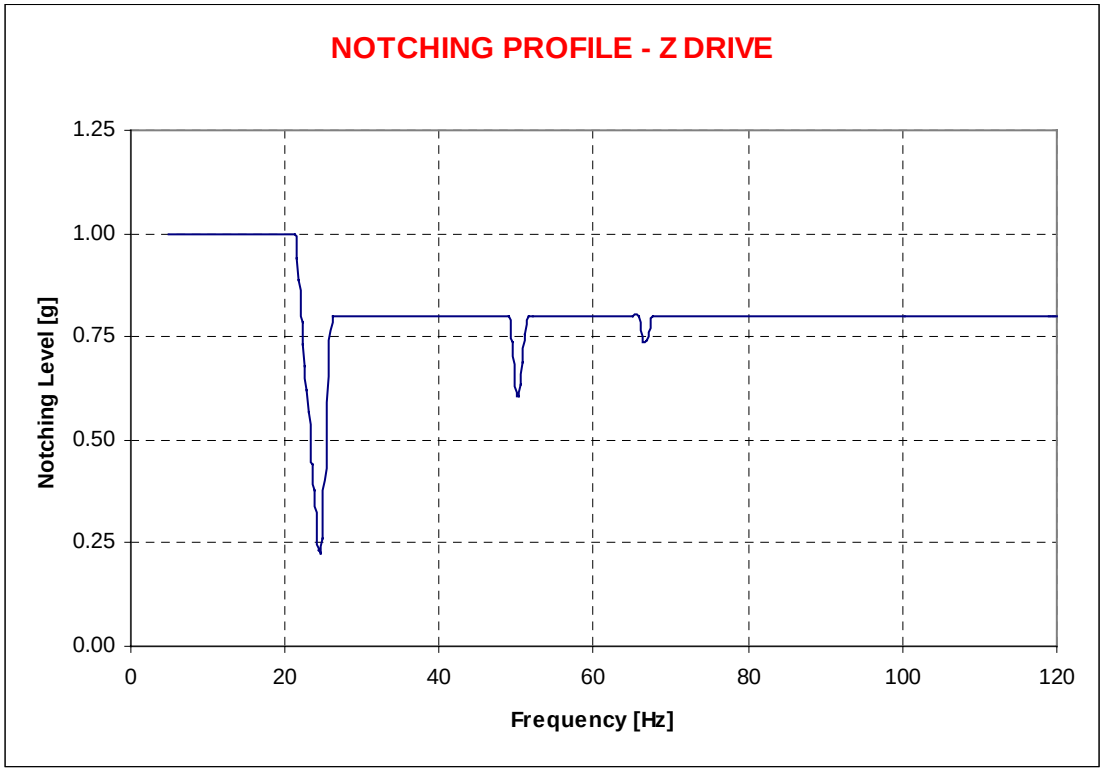

Figure 22: Qualification notching level along Z Axis

6.3 P-PLM Substructures Quasi static loads and mechanical environment

This chapter provides status on CDR PPLM analyses results with respect to current sine and QS specifications.
For sub-systems with high frequency modes (like PR, SR, FPU and JFET), only QS loads generated by satellite sine environment must be checked. For the FPU, which is the only equipment with its first mode close to 100Hz, it has been verified by sensitivity analyses that no risk of coupling at high frequencies exist (once mounted on the PR panel, almost all its mass participate to lower frequency PR panel modes). However, for such sub-systems, a sine specification has been specified as the QS loads applied at the base of the equipment (see [RD 27] for FPU and JFET box), the goal of which is to pass the QS loads at low frequencies during tests.

6.3.1 P-PLM quasi static loads

The quasi static loads applied to the P-PLM structure are defined in the following table. These loads have been evaluated from the cryo-struts/ SVM interface forces.
For the longitudinal axis, QSL is obtained by dividing the sum of I/F longitudinal forces by PPLM mass.
For the lateral axes, QSL are defined as the maximum between :
- lateral forces sum divided by PPLM mass
- base momentum divided by the mass times the CoG height.

These results include an uncertainty factor of 1.2.

Load Case	X axis [g]	Y axis [g]	Z axis [g]
X axis, 63.0 Hz	14.0	/	0.7
X axis, 24.6 Hz	1.9	/	3.7
Y axis, 18.8 Hz	/	8.3	/
Z axis, 32.9 Hz	2.4	/	6.5
Z axis, 25.7 Hz	/	/	7.8

Table 19: P-PLM quasi static design loads

These loads are expressed in the global satellite coordinate system.
They must be compared to cryo-structure QS spec [RD 20] :

Load cases	X (g)	Y (g)	Z (g)
1	16	/	+/-1
2	10	/	6
3	/	11	/
4	2	/	10
5	2	/	-10

Note : For each load cases, the force combination can have a reverse sign.

Sizing qualification QS loads

Table 20: Cryo-structure QS specification

Comments :
Above QSL are covered by cryo-structure QS spec, except for cases 4 and 5, with slight exceed for X value (2.4 g instead of 2 g). This is not considered as a problem since longitudinal contribution is small for this QS loading, and because this load case is not mentioned as a sizing load case by CSAG in [RD 28].

For the PPLM CDR, it has also been verified that cryo-structure QS loads cover launcher QS loads (qualification loads = 7.5g longitudinal, 2.5g lateral conservatively combined), by comparing interface forces for each 6 feet at the SVM/PPLM I/F, with the PPLM mounted on a rigid support. Same verification has been made for transport load cases.

Moreover, it has been verified that the maximum loads seen at each strut end fitting for the PPLM CDR sine analyses, are largely covered by CSAG sizing loads remembered hereafter.
For information, as stated in [RD 28], appendix A.1, struts ends are sized with following maximum load cases:

Load case	S1(N)	S2(N)	M1(Nm)	M2(Nm)	F(N)
Element 40542 Sine Y, 33.8 Hz	828	335	115	53	9305
Element 40642 Sine Y, 18.3 Hz	94	13	17	11	18823
Element 40542 Static 105 (Y)	453	220	66	35	17865

Table 21: Cryo-struts end fitting maximum sizing loads

6.3.2 Telescope quasi static loads

The quasi static loads applied to the telescope structure are defined in the following table. These loads have been evaluated from the cryo-struts/ telescope frame interface forces.
For the longitudinal axis, QSL is obtained by dividing the sum of I/F longitudinal forces by telescope mass.
For the lateral axes, QSL are defined as the maximum between :

- lateral forces sum divided by telescope mass
- base momentum divided by the mass times the CoG height.

These results include an uncertainty factor of 1.2.

Load Case	X axis [g]	Y axis [g]	Z axis [g]
X axis, 63.0 Hz	17.1	/	6.1
Y axis, 18.8 Hz	/	13.1	/
Z axis, 32.9 Hz	4.1	/	10.6

Table 22: Telescope quasi static design loads

These loads are expressed in the global satellite coordinate system.
They must be compared to telescope QS spec [RD 19] :

Load Cases	X (g)	Y (g)	Z (g)
1	16.5	/	6
2	16.5	/	-6
3	/	13	/
4	5	/	13
5	5	/	-13

Table 23: Telescope QS specification

Comments :
Above QSL are covered by telescope QS spec for Z axis, and almost covered for X and Y axes:
For X axis, exceed is less than 4%, which is acceptable since results include 1.2 uncertainty factor, and since secondary notching will occur at that frequency (see § 9.1).
For Y axis, exceed is less than 1%, which is acceptable with regard of the 1.2 uncertainty factor (this factor could be reduced on this mode since it is a well identified global lateral mode).

6.3.3 P-PLM Sine environment

The following curves represent the accelerations calculated at the 6 interface points between PPLM and SVM, for the 3 axes. These curves are without uncertainty factor (cannot be included in the dedicated post-processing software).

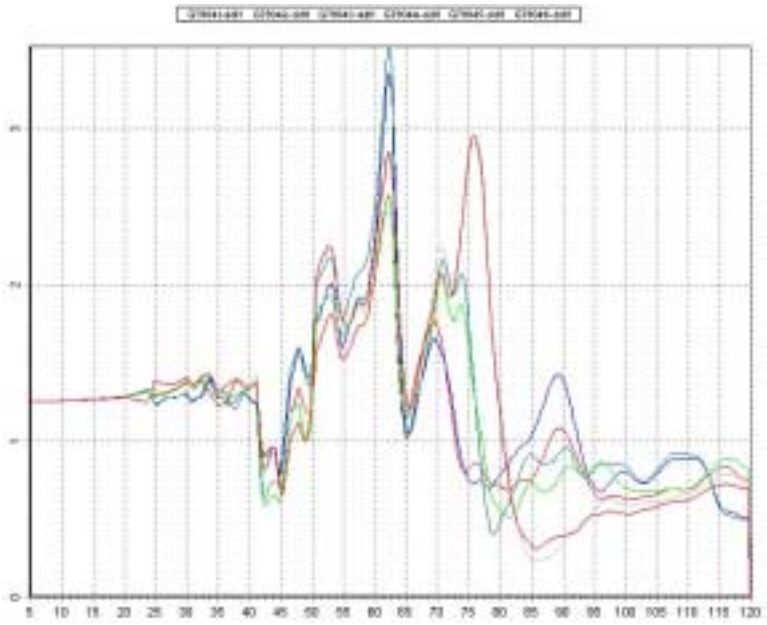

Figure 23 : PPLM base accelerations, X axis

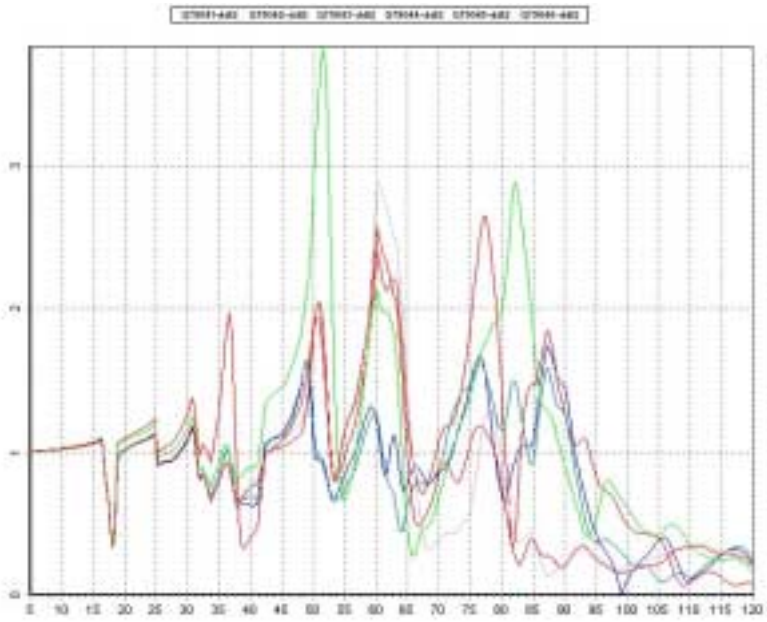

Figure 24 : PPLM base accelerations, Y axis

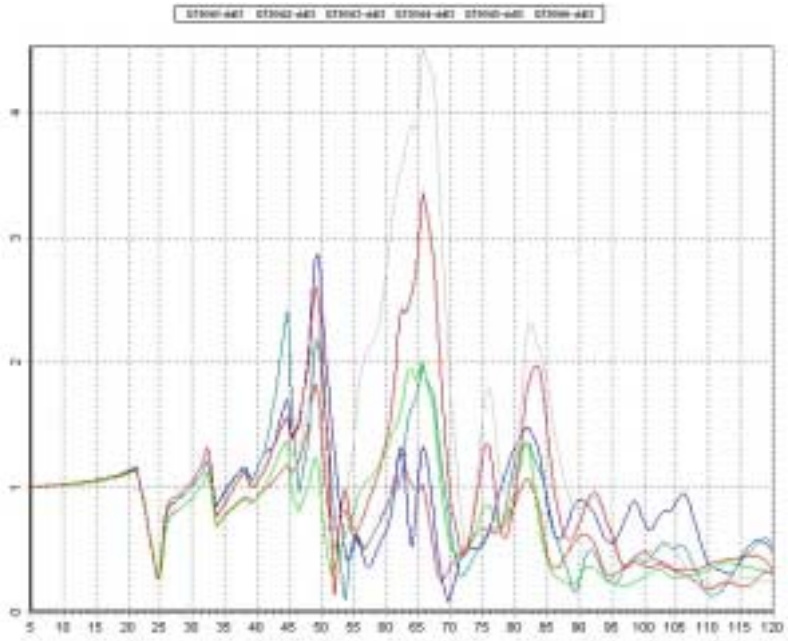

Figure 25 : PPLM base accelerations, Z axis

This environment has to be compared to cryo-structure and telescope sine specifications [RD 19] and [RD 20]. These 2 specifications are identical since the decision to test the telescope on a cryo-structure dummy, at the base of which cryo-structure sine levels are applied.

Freq (Hz)	Long (X axis)	Freq (Hz)	Lat (Y or Z axis)
5-10	10 mm	5-10	10 mm
10-50	2 g	10-40	1.875
50-100	3.5 g	40-70	5g
		70-100	2.5g

Table 24 : cryo-structure and telescope sine specification

Note : a slight modification has been brought to this specification, which has been formalised in [RD 29]. It consists, for lateral axes, in changing 40Hz frequency to 42Hz.

Comments :
The average acceleration (including phase) has been computed from the 6 curves presented above, for each axis, with a 1.2 uncertainy factor has been added. Cryo-structure and telescope sine environment are covered by specification.

6.3.4 PR and SR QSL

PR and SR are very stiff structures that are mounted on flexible blades called ISMs. As described in § 3.3 ISMs have been modelled with up to date values from Astrium, so that interface stiffness coupling with PR and SR panels are taken into account. Due to important stiffness, reflectors themselves do not deform under sine environment. As a consequence, they are represented by a rigid mass representative in term of MCI (nodes 91000 for PR and 92000 for SR). QSLs are extracted directly from these rigid masses responses.

Results are expressed in RDP coordinate system (Z axis perpendicular to panel).

These results include an 1.2 uncertainty factor.

Load Case	X axis [g]	Y axis [g]	Z axis [g]
X axis, envelop	14.2	1.5	13.2
Y axis, 18.8 Hz	1.0	*17.4**	1.3
Z axis, envelop	8.2	2.1	11.6

Table 25 : PR QS loads

These results must be compared to the PR QS specifcation [RD 30] :

PR	X (g)	Y (g)	Z (g)
Case 1	**20**	4	**20**
Case 2	3	**13**	3

Table 26 : PR QS specification

* The 17.4g along Y axis are generated by the first Y global mode. Notching is applied on the satellite interface loads on this mode. The exceed with respect to the specification is due to the fact that peak shapes output from analysis, of the interface moment that drives the notching, and the Y SR response, are slightly different. Actually, without notching, PR has a maximum response of 35.1g at 18.0Hz, exactly at the same frequency as the maximum interface moment. At 18.0Hz, notching factor is 0.31, which leads to a PR response of 35.1*0.31=10.88g, thus, including 1.2 uncertainty factor, 13.0g. So, the PR QS specification is still valid provided the primary notch shape is adjusted to the PR response shape. One possibility would be to use accelerometer on PR to pilot the notching.

Load Case	X axis [g]	Y axis [g]	Z axis [g]
X axis, 63.0Hz	54.3	2.1	35.8
Y axis, 18.8 Hz	2.6	10.4	1.6
Z axis, envelop	14.6	3.5	10.4

Table 27 : SR QS loads

These results must be compared to the SR QS specification [RD 30] :

SR	X (g)	Y (g)	Z (g)
Case 1	16	8	**37**
Case 2	**26**	12	27
Case 3	8	**18**	3

Table 28 : SR QS specification

An obvious out of spec response appears along X SR axis, on the longitudinal mode at 63.0Hz. This issue has been studied in more detailed, as presented in § 9.1.
SR response for Y and Z excitation axes is covered by QS specification.

6.3.5 FPU QSL

In order to check FPU QSLs, accelerations are directly extracted at the FPU CoG location (node 102000).
Results are presented in the RDP coordinate system (Z perpendicular to panel – out of plane).
These results include an 1.2 uncertainty factor.

Load Case	X axis [g]	Y axis [g]	Z axis [g]
X axis, 63.0Hz	18.9	1.3	14.9
Y axis, 18.8 Hz	1.4	10.0	1.4
Z axis, envelop	5.7	1.4	6.3

Table 29 : FPU QS loads

These results must be compared to the FPU QS specification [RD 27] (combined levels) :
- 15g out of plane
- 25g in plane

FPU response is covered by specification.

6.3.6 JFET box QSL

In order to check JFET box QSLs, accelerations are directly extracted at the JFET box CoG location (node 93000).
Results are presented in the RDP coordinate system (Z perpendicular to panel – out of plane).
These results include an 1.2 uncertainty factor.

Load Case	X axis [g]	Y axis [g]	Z axis [g]
X axis, 63.0Hz	10.8	1.1	19.3
Y axis, 18.8 Hz	1.1	9.4	1.0
Z axis, envelop	5.2	1.0	7.6

Table 30 : JFET QS loads

These results must be compared to the JFET QS specification [RD 27] (combined levels) :
- 30g out of plane
- 15g in plane

JFET response is covered by specification.

6.3.7 Pipes sine environment

Despite pipes have high frequency modes, (spec : >130Hz), a sine environment has been defined for 0.1K, 4K and 20K pipes, so that sub-contractors can take into account low frequency effects such as inner pipe hitting the outer pipe (free inner pipe have low frequency modes).
Specification [RD 27] is 25g for all axes, except for out of plane directions on V-grooves in the frequency range 50-65Hz, for which the spec is 60g.

All pipes interface points have been checked, with the following results :

Only 3 I/F points acceleration exceed slightly specification, for an X satellite excitation : node 30115 (20K I/F on V-groove 1), with 36.1 g out of plane including 1.2 uncertainty factor, at 72Hz, for a specification at 25g. Also, nodes 36278 and 36066 (0.1K and 4K I/F on V-groove 3) see around 26.5g out of plane including 1.2 uncertainty factor at 63Hz, for a specification at 25g.
These exceeds are not considered as an issue since inner pipe modes should be at lower frequencies (to be checked with sub-contractors), and pipes can see much more QS loads than these levels. No secondary notching should be necessary.

6.3.8 Pipes dynamic displacements

Relative displacements between pipes attachment points are induced by PPLM sine environment. These displacements are taken into account in the pipes sizing through a dedicated specification [RD 27]. Only dimensioning load cases have been checked during CDR analyses.
Note : for the 0.1K and 4K I/F points on frame and lower beam, dynamic displacements, less important than between V-grooves, are covered by a QS spec (50g combined for 2 axes, see [RD 27]).

Concerning 20K pipe, according to the JPL analysis [RD 48], some cases are clearly not dimensioning. As a consequence, only load cases for which MoS computed by JPL are below 50% have been checked, which covers largely possible spec evolution.
Only 1 exceed has been identified with respect to the spec, from CDR analyses:
- 0.9mm including 1.2 factor along Z axis factor instead of 0.4mm for the load case [RD 27]: “sine Z, between last cone support and H.E. I/F (+Y side)”. However this displacement is negligible with respect to the 2 other directions (2.3mm X and 3.9mm Y specified) and should not be dimensioning. This shall be checked with JPL.

Concerning the 0.1K and 4K pipes, following exceeds have been identified :
- 0.4mm Y including 1.2 factor instead of 0.2mm for the load case [RD 27] : “sine X, between subplatform and V-groove 1”
- 0.5mm Y including 1.2 factor instead of 0.2mm for the load case [RD 27] : “sine Z, between subplatform and V-groove 1”

For those 2 load cases, Y component is the smallest contribution of the 3 directions and should not be dimensioning.

- 0.7mm X including 1.2 factor instead of 0.5mm for the load case [RD 27] : "sine Z, between V-groove 1 and V-groove 2". Here also, this should not be dimensioning because pipes are attached to V-grooves with flexible supports along longitudinal direction.

In any case, those 3 exceeds correspond to load cases with MoS higher than 80% in Air Liquide 0.1K pipe sizing [RD 43]. RAL analyses for 4K pipe are still not available but same type of margins can be expected to be reached, TBC with RAL analyses results.

Conclusion : despite some exceeds with respect to the spec [RD 27], dynamic displacements are in a correct range and exceeds concern not dimensioning directions. No notching should be necessary, which shall be checked with sub-contractors.

6.3.9 Bellow sine environment.

The Bellow is a flexible pipe with low frequency modes. A sine environment has been specified for each interface area as described in [RD 27].

- Since the sizing of the Bellow on cryo-strut is currently being performed by IAS, cryo-strut sine environment has been updated with the CDR PPLM analyses, and so is compliant by definition. It consists of the envelop of the levels seen by the 3 cryo-strut I/F points (nodes 40473, 40464, 40455), including a 1.2 factor. Note that for this spec update, bellow mass on cryo-strut has been adjusted to a more realistic value of 0.5kg for each 3 I/F points, instead of 0.7kg in the initial CDR FEM MCI. This recent update has been accepted by IAS.

- JFET+PR panel interface (nodes 93000, 68218, 68021, 68198, 68239, 68171) :
  For the PR panel and JFET I/F, tests have already been performed successfully by IAS with input levels [RD 27] of JFET I/F (test report still expected). This spec has not been changed since issue 3.1 of [RD 27].
  The status of CDR analysis with respect to this spec is the following :
  10.8g along X RDP including 1.2 factor instead of 3g appears in the 50-70Hz range because of the main longitudinal mode. However this level should be divided by almost a factor of 2 with the secondary notching on the main longitudinal mode presented in § 9.1. Moreover, it is very likely that the bellow, which has seen 25.5g along Z RDP during tests in that frequency range without difficulty, can sustain such levels fro X RDP. This issue shall be addressed to IAS in order to confirm this assumption.
  Also, peak at 73Hz in CDR analyses along Z RDP axis induces 9.6g level including 1.2 factor. This is slightly out of the frequency range 75-90Hz of the spec for which sine level is 11g, but is very close, and should not cause any problem for Bellow qualification. This also shall be checked with IAS.
  To finish with, Peak of 4.8g along Y RDP axis including 1.2 factor appears at 51Hz for an Y excitation, which exceeds the spec but is also a low level for Bellow sizing and should be accepted by IAS.
  Other responses at JFET – PR panel I/F issued from CDR analyses are covered by spec.

- PAU interface (node 140659) :

Here also some slight exceeds appear with respect to the spec [RD 27] :

4.8g including 1.2 factor instead of 3.5g along X satellite axis in the 35-55Hz frequency range.
5.7g including 1.2 factor instead of 4.7g along X satellite axis in the 55-65Hz frequency range.
7.8g including 1.2 factor instead of 6.3g in the 70-90Hz frequency range.

Conclusion : CDR results show some exceeds with respect to the Bellow spec, but :
- results presented here are conservative since they include 1.2 uncertainty factor.
- Bellow is a robust and highly damped structure, and exceeds do not seem dimensioning, which shall be checked with IAS.

No secondary notching on Bellow should be necessary (TBC with IAS response).

6.3.10 LFI wave guides and support structures sine environment

This environment [RD 27] has been updated following RAA / Planck satellite coupled analyses, performed in the frame of CDR analyses, and is compliant by definition. This update is detailed in § 9.2. It consists mainly of a release of sine inputs, and should help LABEN solving sizing problems on wave guides under this environment.

6.3.11 Subsystem / system sine analyses comparison

In order to secure PPLM structure qualification approach, a verification has been made on July 2003, with the PPLM FEM [RD 31] (similar to CDR PPLM FEM, no important design change, see [RD 23]), mounted on an SVM FEM received from Alenia beginning of June 2003. Internal responses at critical locations have been compared between CSAG configuration (PPLM alone – CSAG sine specification notched levels) and ALCATEL configuration (PPLM mounted on SVM – Ariane 5 qualification levels with primary notchings). CSAG configuration results have been delivered by CSAG [RD 32].
As expected, this comparison shows that system responses are covered by CSAG configuration responses. Especially, no unfortunate coupling concerning baffle and V-grooves structures appear (few peaks that are not covered are covered by peaks at other frequencies).
Examples of typical plots are shown hereafter for an X excitation (baffle and V-grooves maximum responses). Results are in m/s2.
This coverage effect is observed globally on the structure. For Y and Z excitations, system responses are even more covered.
Red curve is CSAG response, purple one is ALCATEL response.

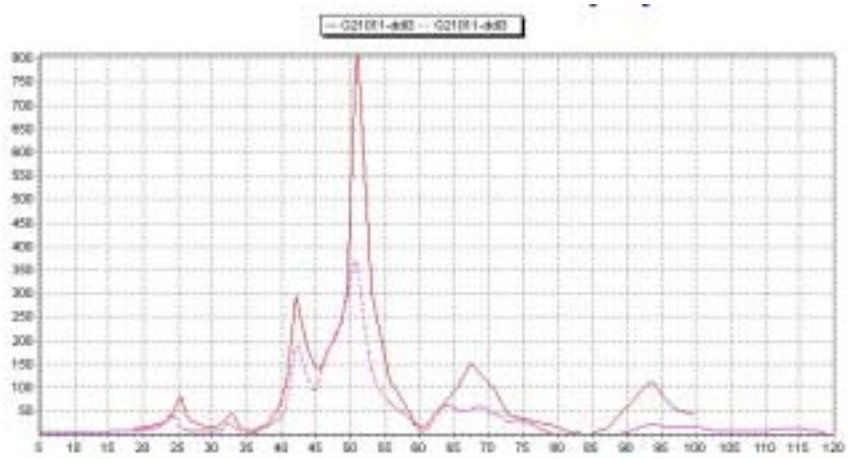

Figure 26 : baffle edge max response, m/s2, X excitation

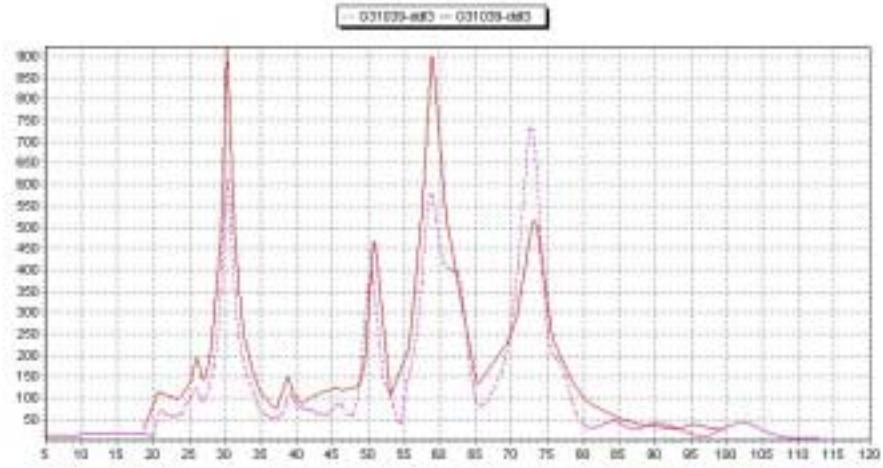

Figure 27 : V-groove 1 edge max response, m/s2, X excitation

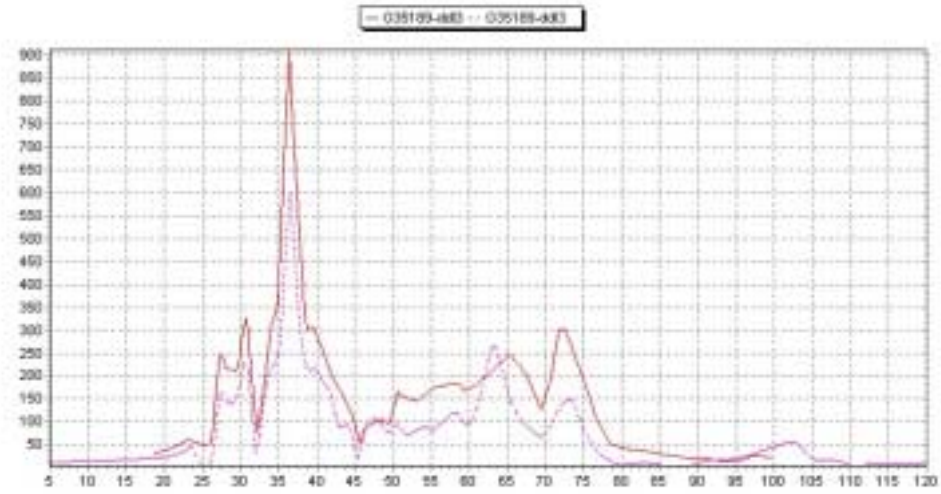

Figure 28 : V-groove 2 edge max response, m/s2, X excitation

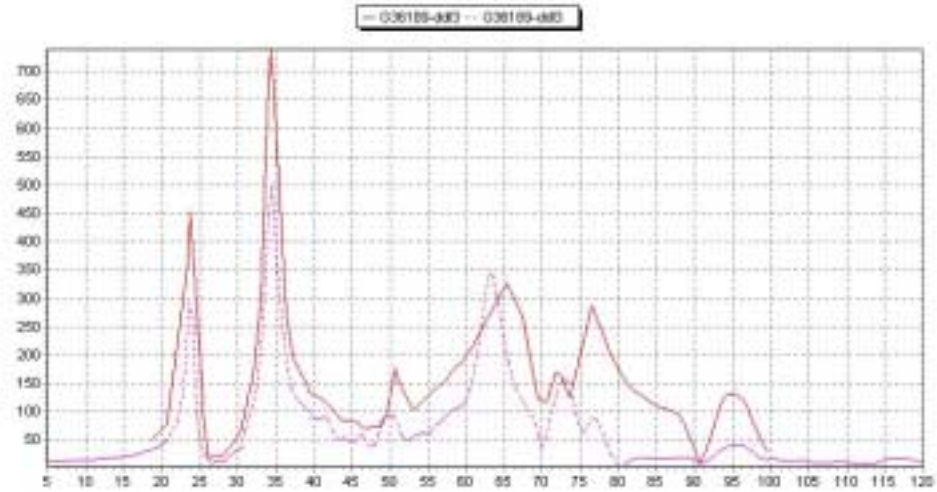

Figure 29 : V-groove 3 edge max response, m/s2, X excitation

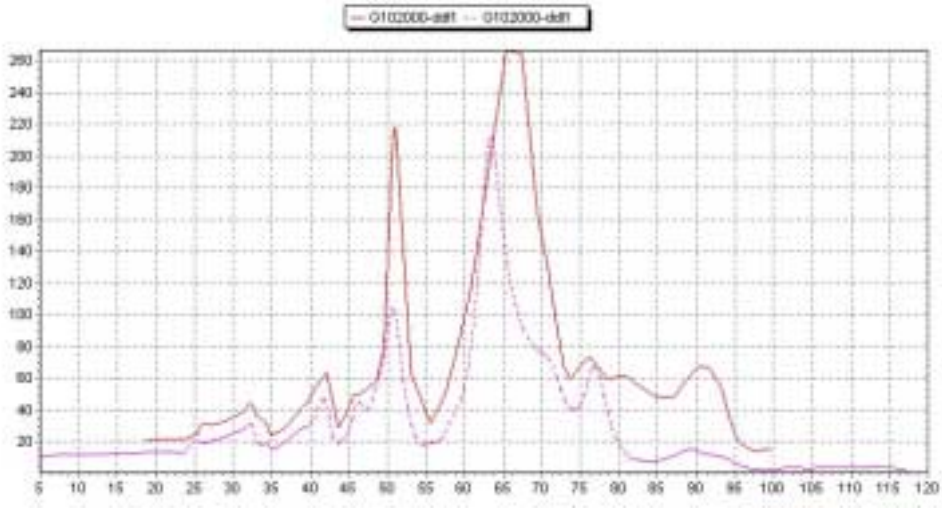

Figure 30 : FPU in plane response, m/s2, X excitation

Note : since those intermediate analyses, FPU response has decreased at system level, due to an evolution of the 63Hz mode deformed shape.

6.3.12 Conclusion on sine analyses

No blocking issue has been identified from the PPLM CDR sine analyses. Remaining open points are :

- Necessity of secondary notching at satellite on equipment response the 63Hz longitudinal mode (see dedicated chapter 9.1) down to a minimum of 0.6g as base input (topic already discussed with Arianespace and agreed in principle).
- Local exceeds with respect to sine and dynamic displacements specification [RD 27] for pipes and Bellow, which were to be expected because of necessary design evolutions since PDR. However,

necessity of secondary notching on those sub-systems is unlikely since no dimensioning exceed appears (TBC with sub-contractors).

7. PPLM ACOUSTIC ANALYSES

7.1 PPLM acoustic environment

Cryo-structure and telescope acoustic environment are defined in [RD 19] and [RD 20] as the Ariane 5 qualification acoustic specification [AD 01]].
CSAG has performed acoustic analyses on PPLM with ASTRYD software up to 710Hz, in order to check the integrity of PPLM structure, especially V-grooves and baffle, that are affected by acoustic pressure. Results are presented in [RD 22], dated 07/05/2003. Two configurations have been analysed : with and without open honeycomb, which cover the mass and design evolutions of baffle and V-grooves up to now (no significant design change has been performed on these structures since this analysis – see [RD 23]).
These analyses show that acoustic environment is not sizing for PPLM (high MoS), which has already been verified for cryo-structure through cryo-structure QM acoustic test showing no damage and good correlation with analyses.

7.2 Equipment random environment

This chapter deals with FPU, JFET, RAA and pipes random environment generated by acoustic loads on PPLM structure. PR and SR are sized by acoustic loads and are not part of these CDR analyses.

7.2.1 FPU, JFET and RAA random environments

These environments have been derived from ASTRYD analysis performed at PPLM level in January 2003, and summarised in [RD 34], dated 14/02/2003.
In order to have realistic acoustic loading, SVM geometry is represented (same for CSAG acoustic analysis [RD 22]).

Looking only at the interface levels, these analyses are still considered as valid, since telescope main panel design has not changed since, and FPU, JFET and RAA masses are similar.

The resulting random spec are included in [RD 27].

7.2.2 Pipes random environment

Following design changes on the V-grooves, and especially the bracing struts concept addition, random levels at pipes interface have been re-assessed through CSAG acoustic analysis [RD 22], dated 07/05/2003.

The resulting random spec are included in [RD 27].

QM acoustic tests results on cryo-structure were well in line with these spec, as reported during ESA progress meeting PM 20 :

More relevant comparison (because closest to flight configuration, even if conservative) is for 20 K pre-cooler locations on V-grooves 1,2,3 :
Max peak of 8g2/Hz out of plane after applying -3dB rule, instead of 6g2/Hz specified for V-grooves 1 and 2 ; max peak of 11g2/Hz out of plane after applying -3dB rule, instead of 10g2/Hz specified for V-groove 3.

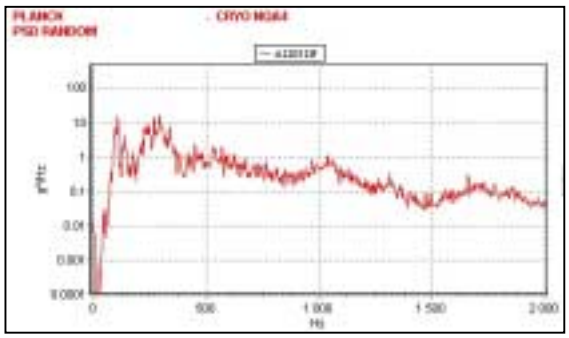

Figure 31 : 20K pipe I/F out of plane test results, Groove 1

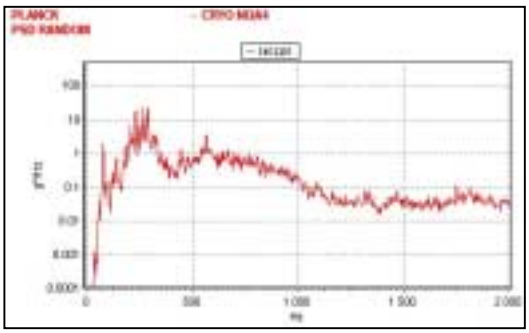

Figure 32 : 20K pipe I/F out of plane test results, Groove 3

8. PPLM THERMO-ELASTIC ANALYSES

Thermo-elastic analyses have been performed by CSAG in the frame of their CDR, both for PPLM structure sizing ([RD 22] and [RD 28]) and stability budget.
As shown in [RD 22], global thermo-elastic loads are not dimensioning for cryo-structure and telescope.
Thermo-elastic loads can be sizing locally for certain I/F, which is presented in [RD 28].

In order to consolidate the PPLM stability budget, contribution of specific load cases not taken into account in CSAG budget (because not available at this date) have been analysed for PPLM CDR. The chosen approach is to proceed by delta with respect to reference computations issued from CSAG CDR (i.e. with CSAG CDR FEM [RD 1].
For that purpose, the following loads cases have been analysed :

- Cool down of the PPLM to the operational temperature as defined in [RD 22] when PPLM is mounted onto the SVM instead of rigid support (coupled analyses)

- Cool down of the PPLM to the operational temperature as defined in [RD 22] with updated PR, SR and FPU FEMs (CSAG CDR FEMs includes PR, SR, FPU and JFET FEMs introducing thermoelastic loads coherent with the specified ones in [RD 22] but not in line with the last instrument definition)

- Cool down of the PPLM to the operational temperatures updated on the basis of the PPLM CDR thermal analyses (see [RD 54])

The purpose of this chapter is not to re-assess the stability budget, but only to provide inputs to be included in the optical budget if necessary.

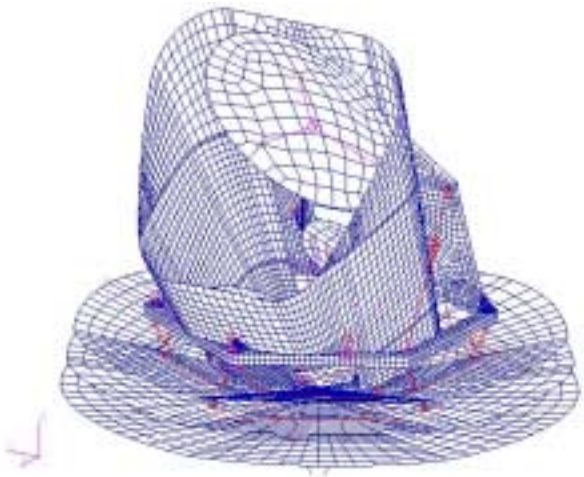

Figure 33 : Reference configuration for CDR thermo-elastic analyses

0 stress checks presented in § 3.5.4.4 are valid for this FEM without PR, SR and FPU FEMs : for those 3 equipment, it is not requested to inject realistic I/F loads (ie, it is not necessary to pass thermo-elastic checks), but conservative I/F loads defined in [RD 19] as loads seen at each I/F point once cooled down on a rigid support.

2 reference thermal maps are used for these analyses : cold case and hot case. These maps have been created by CSAG from data sent by Alcatel [RD 38].

The deformed shape of the reference configuration - cold case - is shown here under (despite the other PPLM parts are present for calculation , only the telescope deformation is shown) :

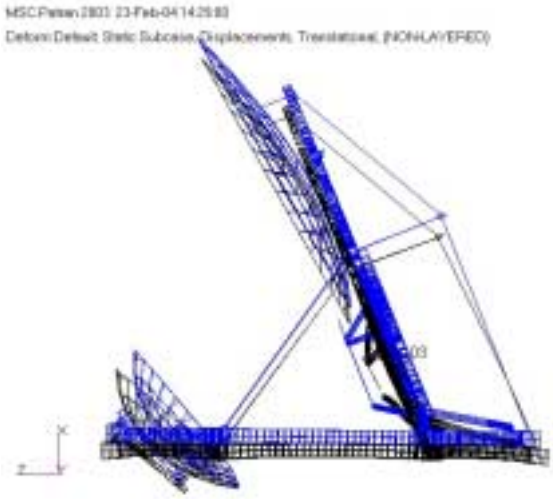

Figure 34 : Reference configuration deformed shape (telescope)

8.1 Description of outputs

For SVM stiffness impact analysis (§8.2), and thermal loading sensitivity analyses (§8.3), displacements are output at the PR, SR and FPU I/F centre, as the average displacement computed at each I/F point. I/F

points are located at the bottom of ISMs for the reflectors, and at the bottom of the bipods for the FPU (interface with telescope structure). They represent CSAG structure contribution to the stability budget. The delta are then calculated as the difference between studied configuration and reference configuration displacements, in the equipment coordinate frames described hereafter.

Corresponding output coordinate systems are described hereafter :

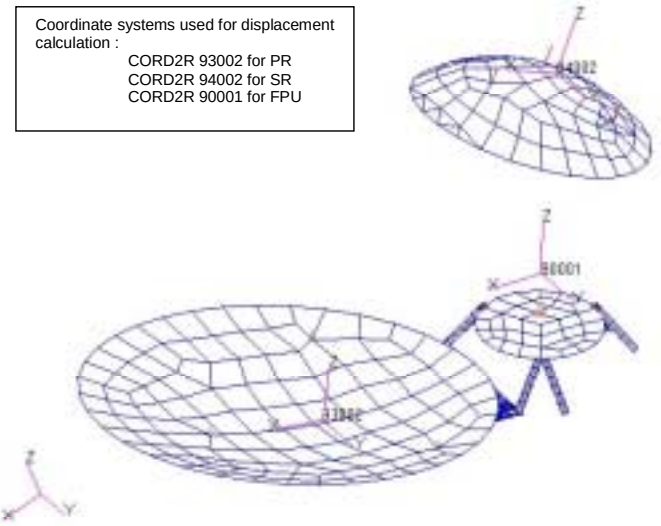

Figure 35 : Equipment output coordinate systems

These coordinate systems are defined by the following NASTRAN cards :

PR COORDINATE SYSTEM (for I/F centre displacements output)

```
CORD2R*       93002          60001       1.484790000         0.0
*         0.077840000    1.001660400         0.0       0.953388860
*         1.484790000         0.0        0.953388860
```

SR COORDINATE SYSTEM (for I/F centre displacements output)

```
CORD2R*       94002          60001       -0.02864000         0.0
*         0.895070000    -0.70987211         0.0       1.627137500
*             0.0            0.0         1.627137500
```

FPU COORDINATE SYSTEM (for I/F centre displacements output)

```
CORD2R*       90001          60001       0.381320000         0.0
*         0.040660000    0.233832546         0.0       0.394645351
*         0.735305351         0.0        0.188147454
```

Those systems are defined with respect to coordinate system 60001 defined hereafter :

```
CORD2R*        60001        40000    0.853000000          0.0
*                0.0    0.853000000          0.0    0.853000000
*          1.706000000          0.0          0.0
```

FPU coordinate system corresponds to ORDP coordinate system.
PR and SR coordinate systems correspond to OM1C and OM2C coordinate systems orientation, with a translation of the center.

FPU I/F centre is linked to the 6 I/F points by the following RBE3 element :

```
RBE3    93999        93999  123456   1.0      123    90392  90393
          90394  1.0    123     90395  90396  90397
```

PR I/F centre is linked to the 3 I/F points by the following RBE3 element :

```
RBE3    91999        91999  123456   1.0      123    91136  91137
          91138
```

SR I/F centre is linked to the 3 I/F points by the following RBE3 element :

```
RBE3    92999        92999  123456   1.0      123    92109  92110
          92111
```

For the analyses concerning the implementation of equipment FEMs delivered by sub-contractors (§8.4), on top of here-above mentioned mean displacements, displacements at each I/F points (6 for FPU and 3 for PR and SR) are output (here again they consist in delta with respect to nominal configuration).

These displacements are expressed in the following coordinate systems :

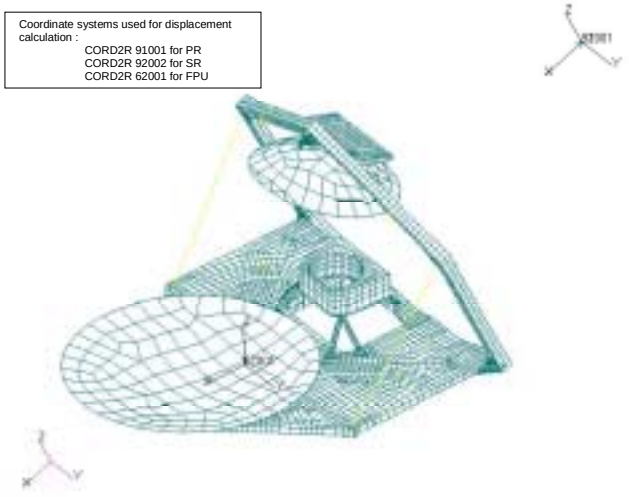

Figure 36 : Equipment I/F points output coordinate systems

Definition of these coordinate systems is given hereafter :

PR REFLECTOR

```
CORD2R*        91001         60001    -1.838500000          0.0
*              0.0    -1.838500000          0.0     1.838500000
*              0.0           0.0           0.0
```

SR REFLECTOR

```
CORD2R*        92001         60001    -1.838500000          0.0
*              0.0    -1.838500000          0.0     1.838500000
*              0.0           0.0           0.0
```

FPU

```
CORD2R*     62001         60001       1.25865002633   0.0
*       -0.079140       0.874044065676  0.0           0.843940849671
*        2.181730876    0.0           0.305465960654
```

8.2 SVM interface stiffness contribution

In order to assess the SVM interface stiffness impact on the budget (with respect to CSAG specified clamped B.C. at the PPLM base), PPLM FEM (reference configuration wtih cold case thermal loading) has been mounted on the CDR SVM FEM [RD 26]. This SVM FEM is not suitable for thermo-elastic use, but it has been loaded at its reference temperature, so that no thermo-elastic deformation is generated, only its stiffness participates to the calculation.

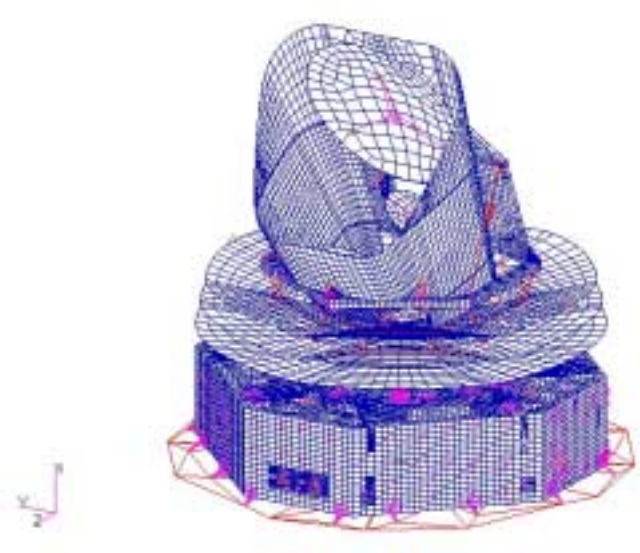

Figure 37 : PPLM mounted on SVM

This configuration has been tested with iso-static B.C. applied at the PPLM/SVM interface, in order to be flight representative. In order to make relevant comparison with the reference configuration, the displacements at the instrument I/F are computed relatively to the PPLM/SVM I/F mean motion.

The delta on the mean I/F displacements with respect to reference configuration – cold case – (PPLM clamped) are the following :

	tx (µm)	ty (µm)	tz (µm)	rx (µrad)	ry (µrad)	rz (µrad)
FPU Δ displ. *	+34	-6	+27	+4	-13	-3
PR Δ displ. *	+40	-10	+47	+6	+27	-3
SR Δ displ. *	+8	0	+53	+5	-5	+1

Table 31 : Delta displacements – SVM stiffness contribution

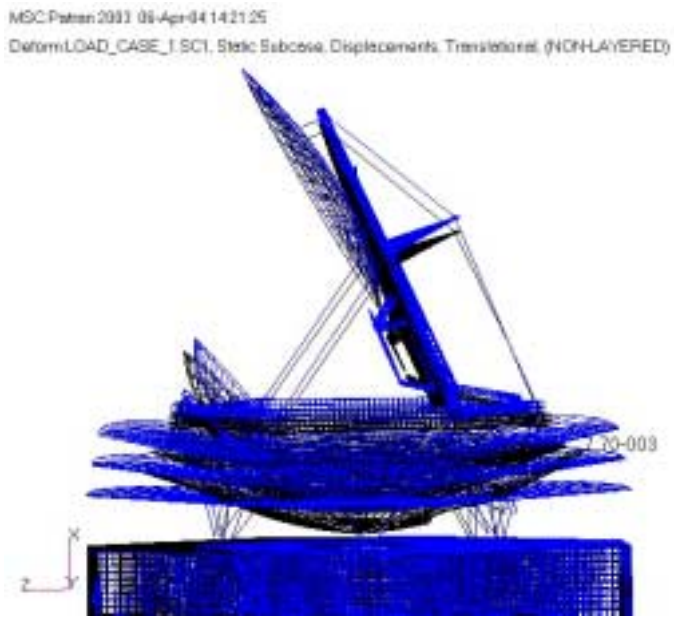

Figure 38 : deformed shape of PPLM mounted on SVM (isostatic B.C.)

8.3 Local thermal loading updates

Sensitivity analyses have been performed in order to assess the impact on stability of new CDR thermal loading on well identified PPLM parts.

8.3.1 PR panel thermal map update – cold case

Dimensioning case is cold case for the PR panel thermal loading.
Description of thermal loading areas is given hereafter. Panels are divided into 33 parts on which is applied a constant temperature (see table 3.1).
The triangle panel is also considered for that thermal load update.

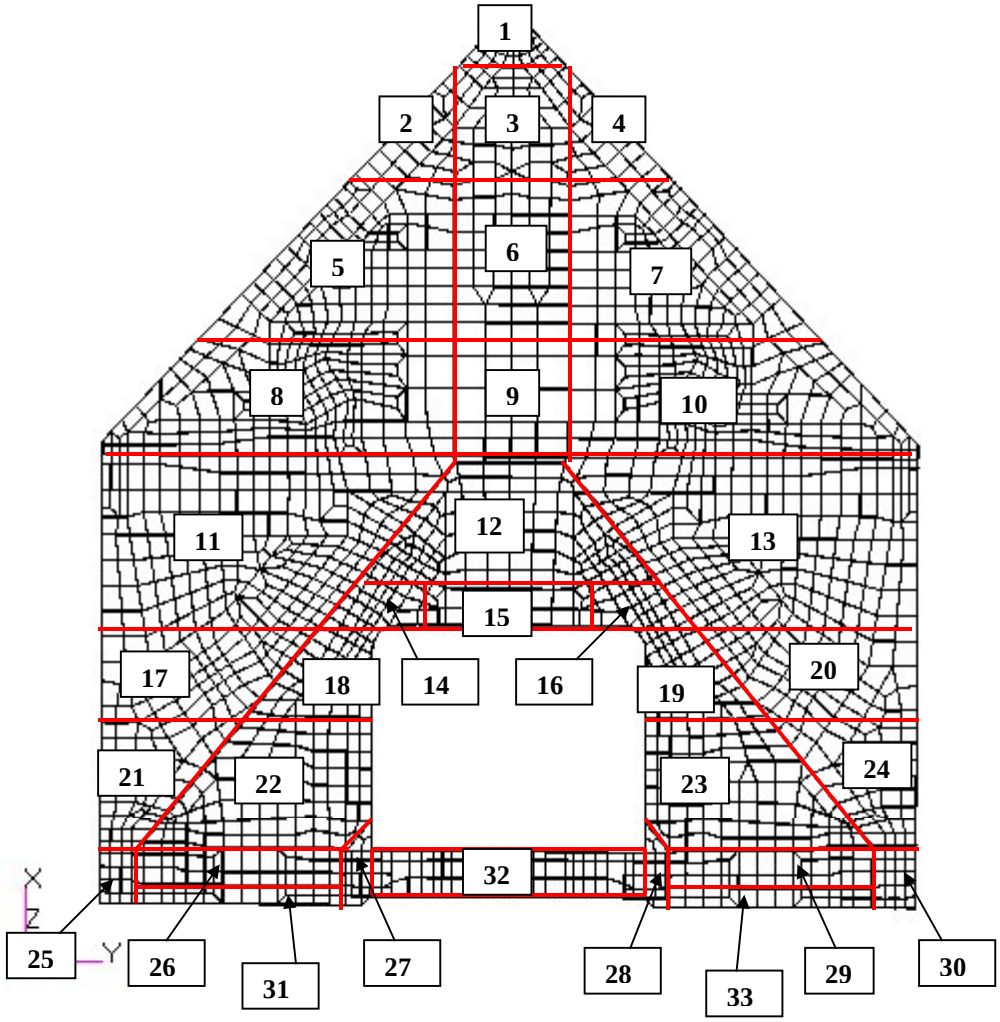

Figure 39- View of telescope main panel thermal loading areas

The updated thermal map on telescope main panel & doubler with respect to reference cold case is described hereafter.(Temperature in °K)

Loading area	+ Z side (main panel)	- Z side (main & doubler panels)	Interface main / doubler panels
1	39.1	39.1	
2	39.7	39.7	
3	39.4	39.4	
4	39.6	39.6	
5	40.2	40.2	
6	40	40	
7	40.1	40.1	
8	41.4	41.4	
9	41.4	41.4	
10	41.4	41.4	
11	43.7	43.6	
12	47	47.2	47.1
13	43.7	43.6	
14	44.9	44.9	44.9
15	46.3	46.3	46.3
16	44.8	44.8	44.8
17	43.1	43.1	
18	43.5	43.5	43.5
19	43.6	43.6	43.6
20	43.2	43.2	
21	42.8	42.8	
22	43.1	43	43.1
23	43.4	43.4	43.4
24	43.3	43.3	
25	43.5	43.5	
26	43	43	43
27	42.6	42.6	
28	42.7	42.6	
29	43.6	43.6	43.6
30	46.6	46.8	
31	43	43	
32	42.6	42.5	
33	43.7	43.7	

Table 32 – Temperatures applied on Telescope main panel

Temperature of triangle panel : 41.4 °K

The delta on the mean I/F displacements with respect to reference configuration – cold case – are the following :

		Δ tx (µm)	Δ ty (µm)	Δ tz (µm)	Δ rx (µrad)	Δ ry (µrad)	Δ rz (µrad)
CS 90001	FPU grid 93999	0	0	-4	0	-9	0
CS 93002	PR grid 91999	1	0	-2	0	6	0
CS 94002	SR grid 92999	0	0	1	0	0	0

Table 33 : Delta displacements induced by updated thermal map on the PR panel

8.3.2 Bellow supporting cryo-strut thermal map update – hot case

Dimensioning case is hot case for the Bellow cryo-strut thermal loading.
Description of thermal loading areas is given hereafter.

Thermal node	T (°K)
32101	248,09
32102	220,53
32103	221,51
32104	229,82
32105	233,73
32106	230,49
32107	218,35
32108	198,87
32109	163,74
32110	155,95
32111	144,98
32112	138,59
32113	129,51
32114	122,23
32115	115,21
32116	107,06
32117	97,13
32118	93,95
32119	92,02
32120	84,61
32121	77,50
32122	70,01
32123	61,34
32124	51,01
32125	50,28
32126	49,57
32127	48,91
32128	48,31
32129	47,79
32130	47,37

FEM grid	T (°K)
49004	248,09
40442	223,44
40443	221,01
40444	226,96
40445	230,92
40446	232,97
40447	230,20
40448	220,62
40449	206,63
40450	185,13
40451	162,33
40410	156,19
40452	149,86
40453	144,08
40454	140,34
40455	135,76
40456	130,45
40457	126,00
40458	121,76
40459	117,64
40460	113,26
40420	108,49
40461	102,91
40462	97,10
40463	95,21
40464	93,57
40465	92,43
40466	89,20
40467	84,80
40468	80,58

40469	76,30
40430	71,86
40470	65,87
40471	59,24
40472	51,74
40473	50,53
40474	50,01
40475	49,50
40476	49,15
40477	48,57
40478	48,10
40479	47,79
49104	47,37

Table 34– Temperatures applied on Bellow cryo-strut

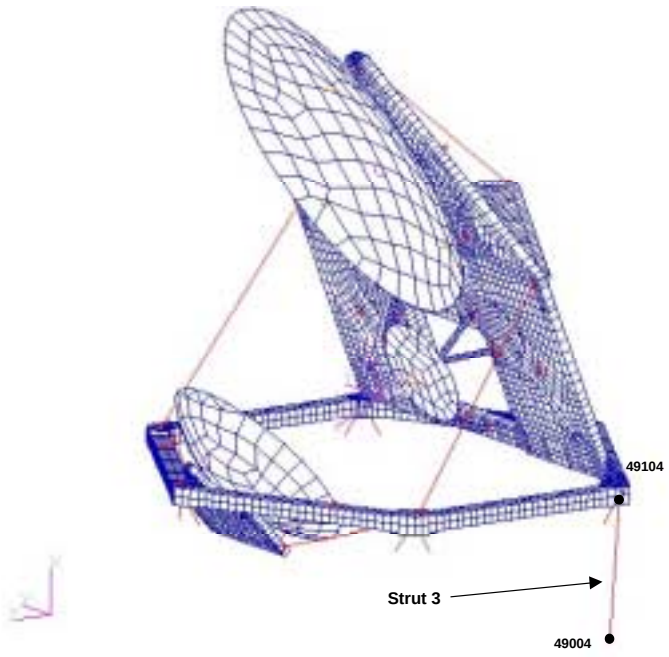

Figure 40- View of Bellow cryo-strut

The delta on the mean I/F displacements with respect to reference configuration – hot case – are the following :

		Δ tx (µm)	Δ ty (µm)	Δ tz (µm)	Δ rx (µrad)	Δ ry (µrad)	Δ rz (µrad)
CS 90001	FPU grid 93999	-15	0	-15	12	8	-13
CS 93002	PR grid 91999	-18	-15	-18	17	-5	-15
CS 94002	SR grid 92999	-4	4	-3	10	7	-4

Table 35 : Delta displacements induced by the Bellow strut updated thermal map

8.3.3 Frame updated thermal map– hot case

Dimensioning case is hot case for the frame thermal loading. This loading is described hereafter.

Beam face	upper	lower	inner	outer
Beam n°	T (°K)	T (°K)	T (°K)	T (°K)
1	44.39	44.37	44.39	44.30
2	44.38	44.40	44.42	44.32
3	44.39	44.47	44.12	44.75
4	44.01	44.10	44.06	44.03
5	45.06	45.08	45.09	45.00
6	44.68	44.67	44.68	44.60

Connection face	upper	lower	inner	outer
Connection n°	T (°K)	T (°K)	T (°K)	T (°K)
C1	46.02	46.12	45.96	45.84
C2	43.74	44.30	44.05	43.94
C3	48.05	47.16	47.37	47.27
C4	44.24	44.17	43.74	44.13
C5	48.05	47.23	47.43	47.32
C6	44.50	45.16	44.82	44.73

Table 36– Temperatures applied on telescope frame

Nota : at junction between two beam faces or two connection faces is applied the average temperature as following.

$$T_{up/out} = (T_{up} + T_{out})/2 \quad ; \quad T_{lo/out} = (T_{lo} + T_{out})/2$$
$$T_{up/in} = (T_{up} + T_{in})/2 \quad ; \quad T_{lo/in} = (T_{lo} + T_{in})/2$$

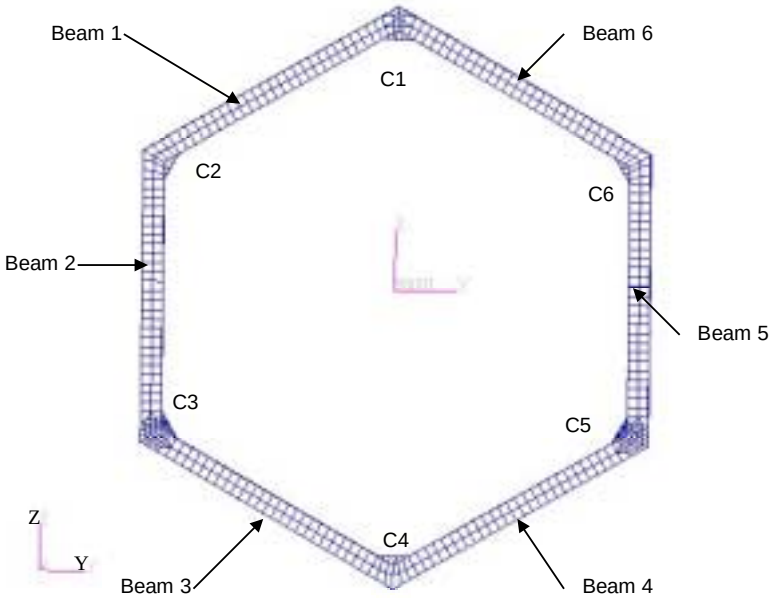

Figure 41 - View of frame

The delta on the mean I/F displacements with respect to reference configuration – hot case – are the following :

		Δ tx (µm)	Δ ty (µm)	Δ tz (µm)	Δ rx (µrad)	Δ ry (µrad)	Δ rz (µrad)
CS 90001	FPU grid 93999	-3	1	-3	0	-12	0
CS 93002	PR grid 91999	-3	1	1	1	4	0
CS 94002	SR grid 92999	4	0	-1	-2	-19	-3

Table 37 – Delta displacements induced by the updated frame thermal map

8.4 PR, SR and FPU thermo-elastic FEMs updates

In order to assess the impact of more realistic equipment I/F loads, it has been decided to perform thermo-elastic analyses with available equipment thermo-elastic FEMs.

8.4.1 Thermo-elastic FEMs status

- FPU :

This model has been delivered by LABEN on 16/01/2004 (see [RD 39] for description).
This FEM has been created with IDEAS software, which has a tendency to degrade FEMs quality.
However, 0 stress checks are much better than previous delivery thanks to simplification of the meshing : Max stress = 6.9*E3 Pa, which exceeds the specification of 1*E3 Pa, but is acceptable since it only concerns an interface plate at the bottom of a bipod. If not considering the interface plates, all the FPU is

within spec, which means that the global load (in opposition to local loads at the 4 screws locations for each I/F plate) generated by FPU global deformation, at the bipods feet, are not affected by the out of spec. Since only the global load at each bipod feet is injected on PR panel I/F, the situation is acceptable (rotations are not considered since stability of FPU is not checked, the purpose of this FEM being only to inject realistic I/Floads).

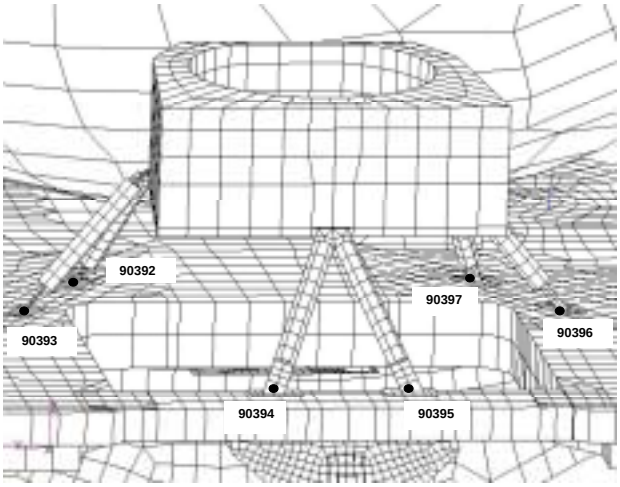

Figure 42 – LABEN FPU thermo-elastic FEM mounted on PR panel

- PR and SR :

These models have been delivered by ASED on 09/03/2004 on Alcatel request following the problems encountered for SR response under sine environment. They are described in [RD 37].
Unfortunately, high discrepancy with respect to the 0 stress spec is observed at the ISMs / reflectors interface (around 800*E3 Mpa). This is slightly better than the previous FEMs delivered by ASED in May 2002 [RD 40], but is still too high to have good confidence on reflectors thermo-elastic behaviour.
In the absence of correct ASED thermo-elastic FEMs, computed results can only be taken as orders of magnitude, and reliable results would necessitate the delivery of correct thermo-elastic FEMs by ASED. However, interface loads on a rigid support seem logical with respect to the conservative spec [RD 19] (important decrease). This is an indication that the implementation of the ASED reflectors FEMs should give a correct tendency with respect to previous FEMs.

Force	Blade	PR - spec	SR - spec	PR – FEM ASED	SR – FEM ASED
F radial	upper	340 N	170 N	62 N	31 N
F tangential	lower	110 N	55 N	21 N	9 N
F radial	lower	160 N	90 N	25 N	14 N

Table 38 – comparison between spec and reflectors FEM I/F loads

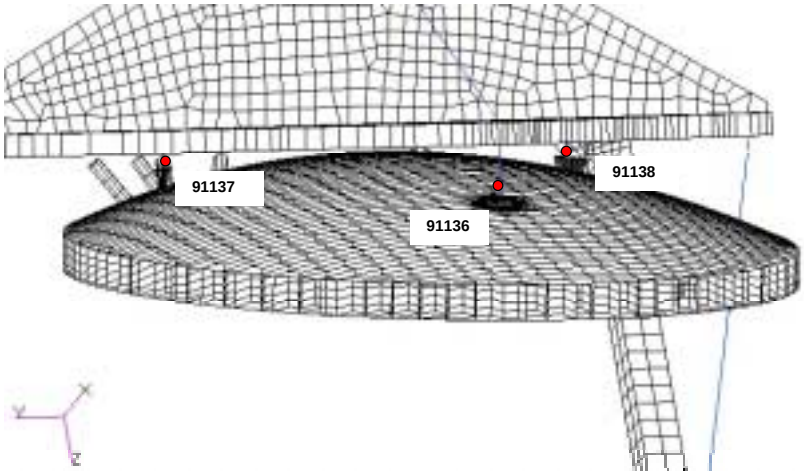

Figure 43 – ASED PR FEM mounted on PR panel

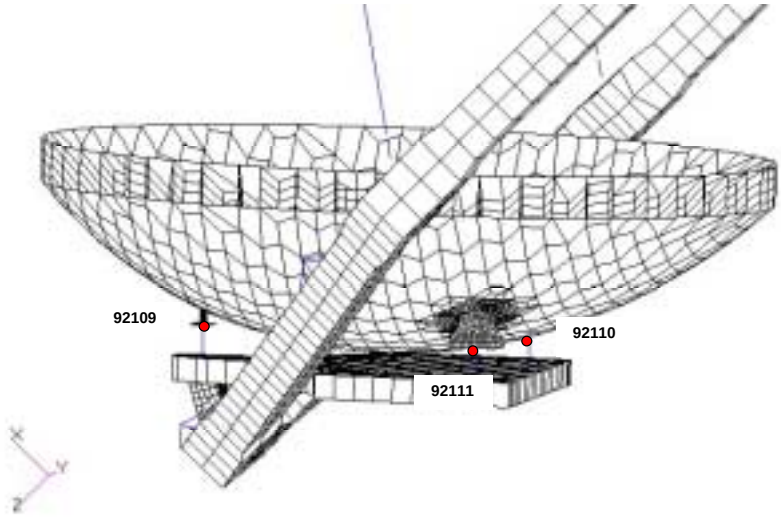

Figure 44 – ASED SR FEM mounted on SR panel

- Computation :

The PPLM FEM has been checked after the implementation of these FEMs. It has been checked by a 0 stress check that on panel side, no stress higher than 1.*E3 appears in the equipment I/F area, which means that the equipment connections are correct. Also, usual FEMs checks have been performed succesfully.
The approach is still an approach by delta. Each new equipment FEM is mounted one at a time, and impact on displacements of the 3 equipment is computed with respect to the reference configuration – cold case.

8.4.2 FPU FEM contribution

Impact of the change of FPU FEM is important, which is logical since with the current FPU design, interface loads are filtered by the bipods blades, and are much lower than specified ones (reduction factor around 20). For instance, local tilt on the lower beam I/F is highly decreased, which generates a big delta for the Y rotation.

Delta at the I/F centres are given hereafter :

	Δ tx (µm)	Δ ty (µm)	Δ tz (µm)	Δ rx (µrad)	Δ ry (µrad)	Δ rz (µrad)
FPU grid 93999	-89	0	121	0	50	0
PR grid 91999	-23	0	7	0	-71	0
SR grid 92999	-3	0	-9	0	-4	0

Table 39 – Delta displacements at I/F centre location

Delta at the I/F points are given hereafter :

	Δ tx (µm)	Δ ty (µm)	Δ tz (µm)	Δ rx (µrad)	Δ ry (µrad)	Δ rz (µrad)
FPU grid 90392	4	43	105	-1476	1187	-66
FPU grid 90397	4	-43	106	1469	1180	66
FPU grid 90393	12	43	121	-1655	878	71
FPU grid 90396	13	-43	121	1652	875	-71
FPU grid 90395	-266	10	136	98	-3482	410
FPU grid 90394	-266	-11	136	-83	-3473	-422
PR grid 91136	-47	0	26	0	-88	0
PR grid 91137	-12	2	-21	4	9	-4
PR grid 91138	-12	-2	-21	-4	9	4
SR grid 92109	3	0	-8	0	-2	0
SR grid 92110	4	0	-9	0	-5	0
SR grid 92111	4	0	-9	0	-5	0

Table 40 – Delta displacements at I/F points location

8.4.3 PR FEM contribution

Delta at the I/F centres are given hereafter :

	Δ tx (µm)	Δ ty (µm)	Δ tz (µm)	Δ rx (µrad)	Δ ry (µrad)	Δ rz (µrad)
FPU grid 93999	2	0	-1	0	-6	0
PR grid 91999	12	0	0	0	23	0
SR grid 92999	-1	0	0	0	1	0

Table 41 – Delta displacements at I/F centre location

Delta at the I/F points are given hereafter :

	Δ tx (µm)	Δ ty (µm)	Δ tz (µm)	Δ rx (µrad)	Δ ry (µrad)	Δ rz (µrad)
FPU grid 90392	2	0	1	-1	-5	0
FPU grid 90397	2	0	1	2	-5	0
FPU grid 90393	2	0	0	1	-4	0
FPU grid 90396	3	0	0	-1	-4	0
FPU grid 90395	2	0	-4	-1	-5	0
FPU grid 90394	2	0	-3	0	-7	0
PR grid 91136	36	0	6	-2	256	-1
PR grid 91137	-3	2	6	-47	-75	-14
PR grid 91138	-3	-2	6	48	-78	14
SR grid 92109	0	0	-1	0	1	0
SR grid 92110	0	0	-1	0	0	0
SR grid 92111	0	0	-1	0	0	0

Table 42 – Delta displacements at I/F points location

8.4.4 SR FEM contribution

Delta at the I/F centres are given hereafter :

	Δ tx (µm)	Δ ty (µm)	Δ tz (µm)	Δ rx (µrad)	Δ ry (µrad)	Δ rz (µrad)
FPU grid 93999	0	0	1	0	-2	0
PR grid 91999	0	0	-1	0	3	0
SR grid 92999	5	0	3	0	2	0

Table 43 – Delta displacements at I/F centre location

Delta at the I/F points are given hereafter :

	Δ tx (µm)	Δ ty (µm)	Δ tz (µm)	Δ rx (µrad)	Δ ry (µrad)	Δ rz (µrad)
FPU grid 90392	1	0	1	-1	2	0
FPU grid 90397	1	0	1	2	2	0
FPU grid 90393	0	0	1	-1	1	0
FPU grid 90396	0	0	1	1	1	0
FPU grid 90395	0	0	0	0	-5	0
FPU grid 90394	0	0	0	0	-6	0
PR grid 91136	2	0	-3	0	0	0
PR grid 91137	1	0	0	1	3	0
PR grid 91138	1	0	0	-1	3	0
SR grid 92109	9	0	11	-1	-178	-1
SR grid 92110	-2	-4	2	-59	79	-56
SR grid 92111	-2	4	2	62	80	58

Table 44 – Delta displacements at I/F points location

9. PPLM SPECIFIC ANALYSES

9.1 Sine analysis check with Astrium PR and SR FEMs

In order to have a better assessment of the equipment response on the 63Hz longitudinal mode, It has been asked to ASED to deliver up to date PR and SR FEMs for our CDR analyses. These FEMs have been delivered on 09/03/2004, and are described in [RD 37]. They are representative of current PR and SR design and MCI.
First lateral modes of these FEMs are : 123.7Hz (+7.5% with respect to simplified FEM) for PR and 185.1Hz (-2% with respect to simplified FEM) for SR.
These FEMs have been introduced in the CDR Planck FEM, replacing simplified FEMs.

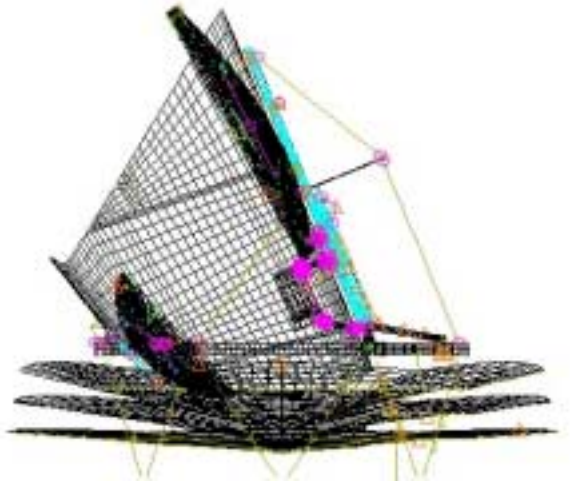

Figure 45 : ASED PR and SR FEMs mounted on PPLM

Planck FEM checks with this configuration are compliant, with a slight exceed for the strain energy check (4*E-3 for Y rotation) which is acceptable given the high number of DoF in this FEM (PR and SR meshing is very detailed).

Verification of sine response at 63Hz has been made for PR, SR and also FPU and JFET, since the change of deformed shape can affect the 4 equipment responses.
For PR and SR, a node is created at the location of the CoG, linked to the top of the 3 ISMs by RBE3 elements, from which responses are extracted.
Output coordinate frame are the same as those described in § 6.3.

Results are the following, including 1.2 uncertainty factor :

Equipment	X (g)	Y (g)	Z (g)
PR	27.4 – 66.4Hz	1.7 – 42.1Hz	18.7 – 66.4Hz
SR	37.3 – 66.4Hz	2.8 – 42.3Hz	29.8 – 62.7Hz
FPU	23.8 – 66.7Hz	1.7 – 42.3Hz	19.2 – 62.7Hz
JFET	9.7 – 62.7Hz	1.7 – 42.3Hz	15.1 – 62.7Hz

These results confirm that the longitudinal modes between 60Hz and 70Hz are very sensitive to small design parameters changes, and difficult to control in term of deformed shape. With this new configuration, effective masses of longitudinal modes between 60 Hz and 70 Hz are distributed on 2 modes instead of one : a mode at 62.7 Hz and a mode at 66.5Hz, whereas with the CDR configuration, effective masses are more concentrated at 63 Hz. However, this transfer of effective masses only concerns longitudinal modes between 60Hz and 70Hz, as comparison on effective masses shows, and do not affect other PPLM modes.

The deformed shapes of the 62.7 Hz and 66.5 Hz modes with this new configuration are shown hereunder (only PPLM is shown despite it is mounted on SVM).

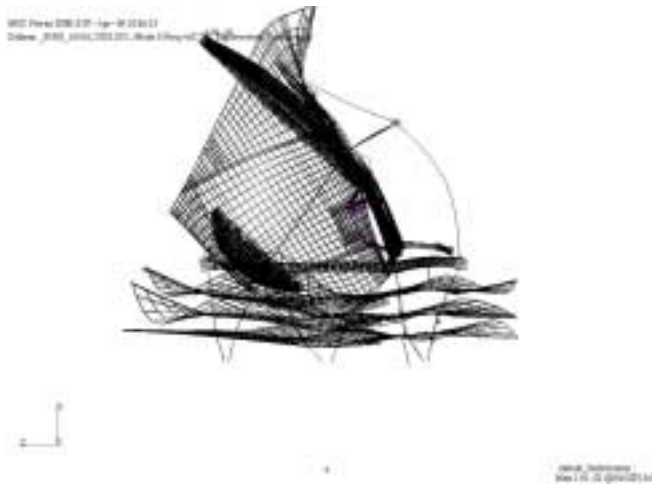

Figure 46 : 62.7Hz mode

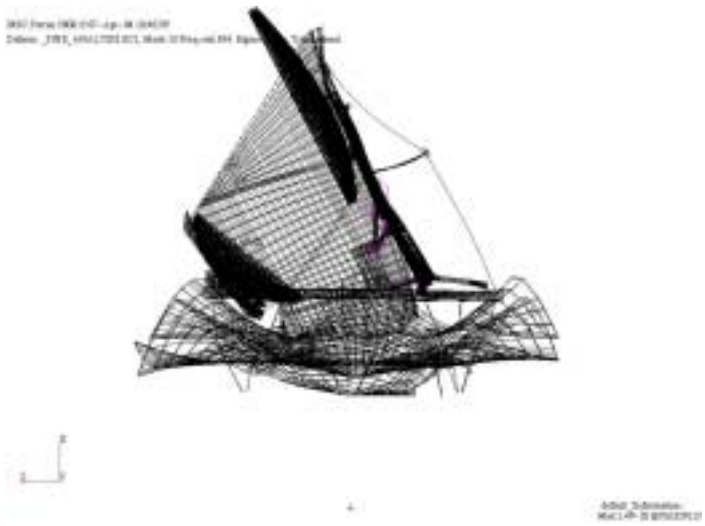

Figure 47 : 66.5Hz mode (high in plane motion of PR and SR)

Situation improves with respect to SR response presented in §6.3, but exceeds with respect to spec [RD 27] appear for other equipment. This is due to the different deformed shapes between the 2 configurations which generates transfers between equipment responses.
With this configuration, a secondary notching is necessary on PR (X response), SR (X response) and FPU (Z response).
Minimum notching factors are the following :

Equipment	Notching factor	Frequency
PR	0.73	66.4Hz
SR	0.70	66.4Hz
FPU	0.78	62.6Hz

This corresponds to a minimum input level of 0.7*1.25=0.875g. This is an improvement with respect to the situation presented in §6.3, where SR response induced a necessity of notching down to 0.6g.
Of course, the situation during tests is liable to evolve because, as it has been shown, deformed shape is complex and sensitive to small design parameters.

However, the situation is considered as not worrisome for the following reasons :

- 1.2 factor is used in the presented results to cover uncertainties. The most realistic configuration, that is to say with ASED reflectors FEMs, shows a good improvement of the notching factor. CDR configuration with simplified FEMs can be considered as a worst case.
- It has already been discussed with Arianespace at system level possibilities of notchings in that frequency range. It should be feasible down to 0.6g – 0.7g as base input according to first Ariane 5 / Planck coupled loads analysis, to be confirmed with final coupled loads analysis. The corresponding notched inputs shall be presented for Planck system CDR.

9.2 RAA / satellite coupled analyses

This analysis has been performed with the following objectives :

- Assess dynamic behaviour of RAA once mounted on satellite, and especially the risks of couplings since first modes on rigid support are around 80Hz
- Verify correct sizing of RAA interfaces with realistic loads
- Verify that implementation of RAA FEM in the Planck CDR FEM does not modify satellite global dynamic behaviour
- Update LABEN sine specification by taking into account the CDR date dynamic environment

9.2.1 Status on RAA FEM

RAA dynamic FEM [RD 41] has been delivered by LABEN in July 2003.

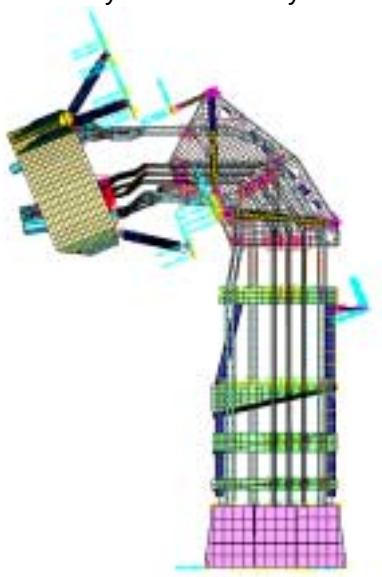

Figure 48 : LABEN RAA FEM

This FEM has been generated under NASTRAN format by IDEAS software, which obligatorily leads to slight differences between IDEAS and NASTRAN FEMs, especially for such complex FEMs.

- strain energy, static and free-free checks performed on NASTRAN FEM are compliant with respect to [RD 18]

- IDEAS and NASTRAN FEMs MCI are identical
- Clamped modes comparison (20 first modes) is given hereunder :

MODE	FREQUENCY
1	78.7920
2	82.9924
3	83.3407
4	86.8788
5	87.4671
6	89.0887
7	90.8749
8	92.3530
9	93.6877
10	93.8680
11	94.8983
12	96.5083
13	97.3551
14	97.7962
15	98.7349
16	98.8229
17	101.9299
18	103.6076
19	104.3793
20	106.1258

Table 45 – IDEAS FEM clamped modes

MODE N	FREQUENCE (HZ)
1	79.791
2	83.121
3	84.310
4	87.718
5	88.445
6	90.131
7	91.661
8	92.964
9	93.022
10	94.046
11	94.905
12	95.204
13	95.326
14	96.314
15	98.687
16	100.304
17	103.535
18	105.344
19	105.757
20	107.898

Table 46 – NASTRAN FEM clamped modes

There are 2 modes with effective mass more than 3% of total mass, all others are much below and comparing their effective mass would not be relevant (wave guides local modes).

Mode	Frequency IDEAS	Frequency NASTRAN	Eff. mass IDEAS	Eff. mass NASTRAN
Y mode	83.3Hz	83.1Hz	3.4%	3.4%
Z mode	94.9Hz	94.0Hz	3.4%	2.8%

In order to secure the reliability of the NASTRAN FEM, max wave guide responses under 1g longitudinal sine acceleration up to 120 Hz applied on the 2 FEMs mounted on rigid support have been checked :

Node	IDEAS max WG response	NASTRAN max WG response
324144	64g, 104 Hz	65g, 106 Hz
324161	61g, 105 Hz	71g, 107 Hz

So, the NASTRAN FEM is acceptable despite minor discrepancies that tend to be conservative.

Since this FEM delivery, an important design change has occurred : the lower support structure, which was interfaced with the BEU box, is now interfaced directly with the SVM subplatform, via 4 very stiff feet in order not to degrade the RAA modal behaviour. As a consequence, the RAA FEM has been modified this way : BEU box is removed from the FEM, since the BEU is already represented in the SVM FEM. Lower structure columns are extended down to 4 I/F on sub-platform via RBE2 rigid elements.

9.2.2 Planck with RAA FEM description

The Planck FEM is the CDR FEM described in §5, on which the following modifications have been performed :

- Remove the rigid masses representing the RAA
- Remove FPU FEM described in §3.2
- Integration of the RAA+FPU FEM with RBE2 and I/F CELAS elements. HFI is represented in the new FPU as described in §3.2.

The corresponding Planck FEM properties are described hereafter :

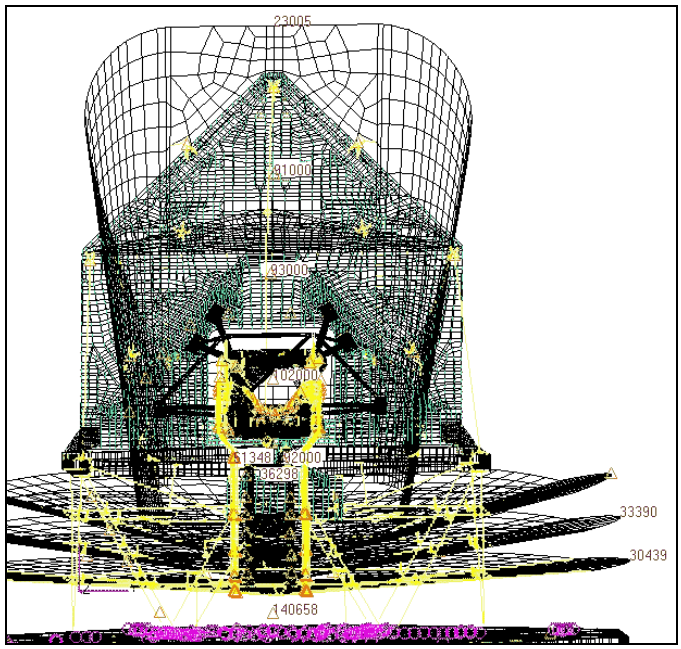

Figure 49 : Planck + RAA FEM – view 1

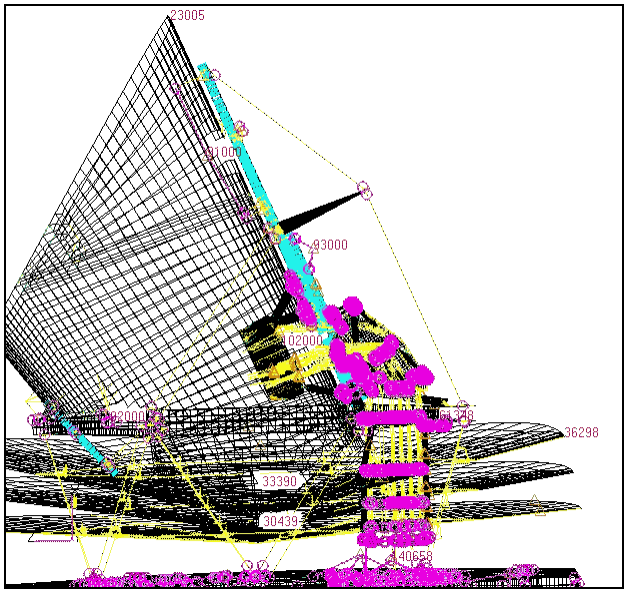

Figure 50 : Planck + RAA FEM – view 2

Strain energy check results are given hereafter :

```
MATRIX KRBG     (GINO NAME 101 ) IS A DB  PREC          6 COLUMN X          6 ROW SQUARE   MATRIX.
COLUMN      1      ROWS      1 THRU      6     ---------------------------------------------
      1)    1.0202D-04 -3.4308D-05  6.0967D-06  2.7741D-05  9.1346D-06 -7.1326D-05
COLUMN      2      ROWS      1 THRU      6     ---------------------------------------------
      1)   -1.6083D-05 -2.0052D-05 -3.1172D-05  1.4942D-04  6.4225D-05  2.9344D-05
COLUMN      3      ROWS      1 THRU      6     ---------------------------------------------
      1)    4.7222D-05  7.8835D-06 -7.4643D-05 -5.8019D-05  9.9142D-05 -4.9951D-06
COLUMN      4      ROWS      1 THRU      6     ---------------------------------------------
      1)    7.8922D-06  1.0672D-04 -4.9587D-05  3.9450D-04  9.0302D-05  1.2325D-04
COLUMN      5      ROWS      1 THRU      6     ---------------------------------------------
      1)   -1.1204D-04  7.1546D-05 -7.1431D-05 -1.4399D-04  1.4349D-04  3.2667D-04
COLUMN      6      ROWS      1 THRU      6     ---------------------------------------------
      1)   -7.5938D-05 -3.3471D-04 -8.0880D-05 -4.9984D-05  2.4934D-04 -2.7260D-04
```

```
MATRIX KRBN     (GINO NAME 101 ) IS A DB  PREC          6 COLUMN X          6 ROW SQUARE   MATRIX.
COLUMN      1      ROWS      1 THRU      6     ---------------------------------------------
      1)    2.7018D-05 -4.0720D-05 -2.9604D-05  3.0140D-05  1.2791D-04 -1.0389D-04
COLUMN      2      ROWS      1 THRU      6     ---------------------------------------------
      1)   -2.1352D-05 -6.6583D-05 -4.7780D-05  1.3348D-04  8.9027D-05 -6.5037D-05
COLUMN      3      ROWS      1 THRU      6     ---------------------------------------------
      1)    3.5188D-05  2.2646D-05  3.1978D-06 -5.9432D-05 -9.5251D-05  1.3898D-05
COLUMN      4      ROWS      1 THRU      6     ---------------------------------------------
      1)    4.3437D-06  8.8571D-05 -6.1481D-05  3.4013D-04  1.2101D-04  6.8179D-05
COLUMN      5      ROWS      1 THRU      6     ---------------------------------------------
      1)   -2.6934D-05  5.3341D-05 -7.0530D-05 -1.2921D-04  1.4067D-04  3.1278D-04
COLUMN      6      ROWS      1 THRU      6     ---------------------------------------------
      1)   -8.6669D-05 -1.6516D-04 -6.8761D-05  3.0708D-05  1.9552D-04  2.0019D-04
```

```
MATRIX KRBF     (GINO NAME 101 ) IS A DB  PREC          6 COLUMN X          6 ROW SQUARE   MATRIX.
COLUMN      1      ROWS      1 THRU      6     ---------------------------------------------
      1)    2.7018D-05 -4.0720D-05 -2.9604D-05  3.0140D-05  1.2791D-04 -1.0389D-04
COLUMN      2      ROWS      1 THRU      6     ---------------------------------------------
      1)   -2.1352D-05 -6.6583D-05 -4.7780D-05  1.3348D-04  8.9027D-05 -6.5037D-05
COLUMN      3      ROWS      1 THRU      6     ---------------------------------------------
      1)    3.5188D-05  2.2646D-05  3.1978D-06 -5.9432D-05 -9.5251D-05  1.3898D-05
COLUMN      4      ROWS      1 THRU      6     ---------------------------------------------
      1)    4.3437D-06  8.8571D-05 -6.1481D-05  3.4013D-04  1.2101D-04  6.8179D-05
COLUMN      5      ROWS      1 THRU      6     ---------------------------------------------
      1)   -2.6934D-05  5.3341D-05 -7.0530D-05 -1.2921D-04  1.4067D-04  3.1278D-04
COLUMN      6      ROWS      1 THRU      6     ---------------------------------------------
      1)   -8.6669D-05 -1.6516D-04 -6.8761D-05  3.0708D-05  1.9552D-04  2.0019D-04
```

Table 47 – Strain energy check

All diagonal values are below 1.*E-3.

The free-free modes verification results are given hereafter :

MODE NO.	EXTRACTION ORDER	EIGENVALUE	RADIANS	CYCLES
1	1	1.401362E-07	3.743477E-04	5.957928E-05
2	2	1.814773E-07	4.260016E-04	6.780025E-05
3	3	3.290925E-07	5.736658E-04	9.130175E-05
4	4	1.052284E-06	1.025809E-03	1.632626E-04
5	5	2.526911E-06	1.589626E-03	2.529968E-04
6	6	3.962715E-06	1.990657E-03	3.168229E-04
7	7	1.558202E+02	1.248280E+01	1.986699E+00
8	8	1.558342E+02	1.248336E+01	1.986788E+00
9	9	1.558871E+02	1.248547E+01	1.987125E+00
10	10	1.596362E+02	1.263472E+01	2.010879E+00

Table 48 – free-free modes

6 free-free modes are clearly identified.

Mass properties are given hereafter :

```
            O U T P U T   F R O M   G R I D   P O I N T   W E I G H T   G E N E R A T O R
                                    REFERENCE POINT =        0
                                              M O
          *  1.923671E+03 -2.997602E-15 -1.909584E-14  6.217249E-15  2.635907E+01 -4.904328E+01 *
          * -2.997602E-15  1.923671E+03 -1.989520E-13 -2.635908E+01 -6.039613E-14  1.527544E+03 *
          * -1.909584E-14 -1.989520E-13  1.923671E+03  4.904328E+01 -1.527544E+03  5.551115E-14 *
          *  6.217249E-15 -2.635908E+01  4.904328E+01  3.199694E+03 -1.889506E+01 -9.307518E+00 *
          *  2.635907E+01 -6.039613E-14 -1.527544E+03 -1.889506E+01  3.775122E+03  6.002530E+01 *
          * -4.904328E+01  1.527544E+03  5.551115E-14 -9.307518E+00  6.002530E+01  3.955536E+03 *
                                                S
                                *  1.000000E+00  0.000000E+00  0.000000E+00 *
                                *  0.000000E+00  1.000000E+00  0.000000E+00 *
                                *  0.000000E+00  0.000000E+00  1.000000E+00 *
                                              DIRECTION
               MASS AXIS SYSTEM (S)     MASS              X-C.G.        Y-C.G.        Z-C.G.
                  X            1.923671E+03      3.231970E-18  2.549462E-02  1.370248E-02
                  Y            1.923671E+03      7.940776E-01 -3.139629E-17  1.370248E-02
                  Z            1.923671E+03      7.940776E-01  2.549462E-02  2.885688E-17
                                              I(S)
                                *  3.198083E+03 -2.004911E+01 -1.162363E+01 *
                                * -2.004911E+01  2.561772E+03 -6.069732E+01 *
                                * -1.162363E+01 -6.069732E+01  2.741297E+03 *
                                              I(Q)
                                *  2.542796E+03                             *
                                *                2.759237E+03               *
                                *                                3.199118E+03 *
                                                Q
                                *  2.409979E-02  3.861080E-02  9.989637E-01 *
                                * -9.564080E-01 -2.900144E-01  3.428245E-02 *
                                *  2.910375E-01 -9.562431E-01  2.993840E-02 *
```

Table 49 – mass properties

9.2.3 Planck with RAA FEM dynamic behaviour verification

In order to check that Planck global behaviour does not evolve because of the RAA FEM replacing rigid masses in CDR FEM (which ensures reliability of results presented in this document), responses of relevant PPLM nodes (on equipment, baffle and grooves) are compared between the 2 configurations, for an un-notched 1g base input. Corresponding curves are given hereafter :

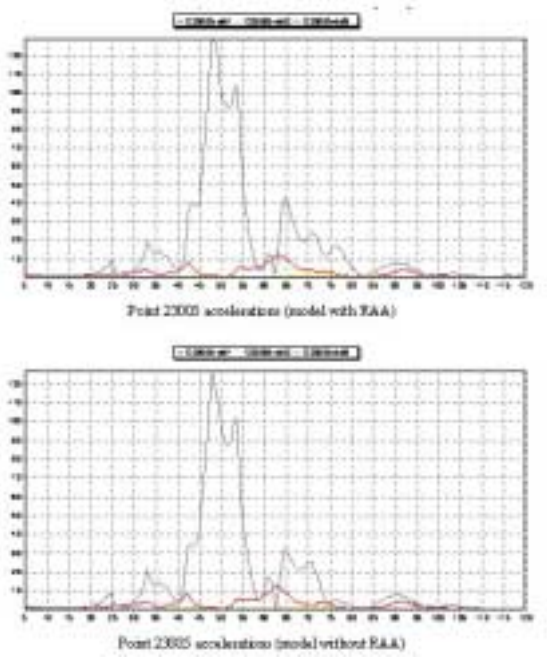

Figure 51 : Baffle response comparison – X input

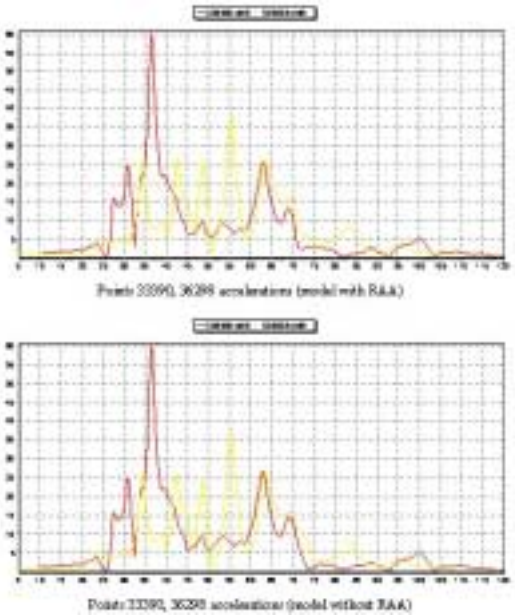

Figure 52 : Grooves response comparison – X input

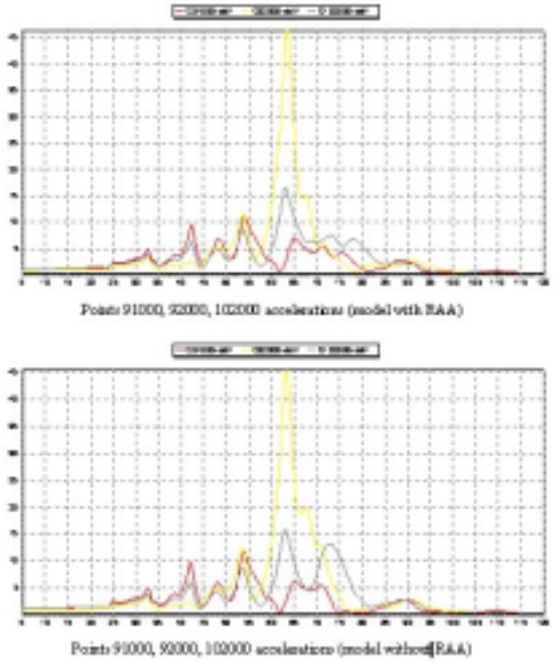

Figure 53 : Equipment responses comparison – X input

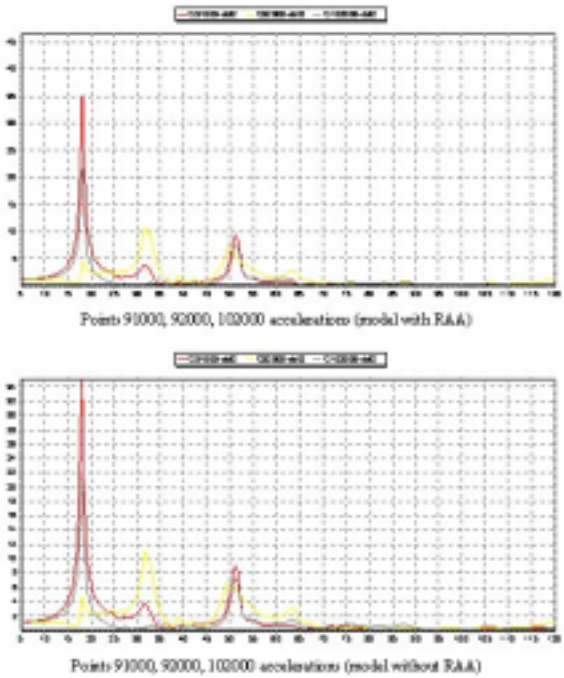

Figure 54 : Equipment responses comparison – Y input

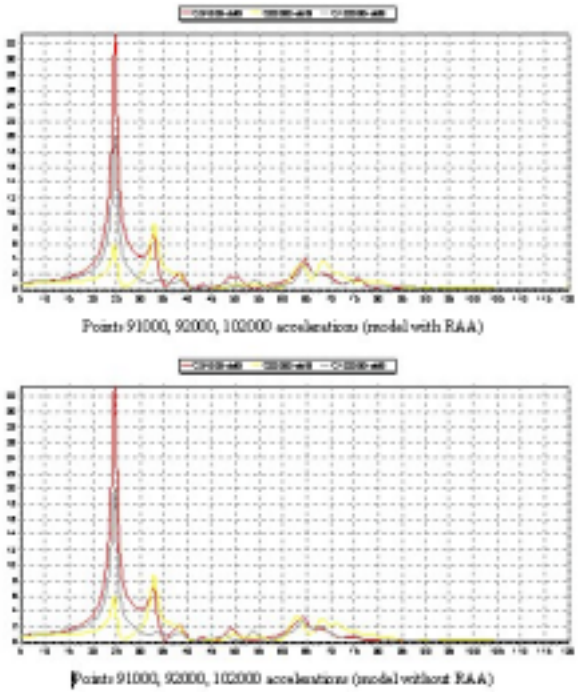

Figure 55 : Equipment responses comparison – Z input

It is seen that the Planck global dynamic behaviour is almost not impacted by presence of RAA FEM.

9.2.4 Dynamic analysis of RAA mounted on spacecraft

9.2.4.1 Description

A sine analysis (with un-notched inputs) is performed in order to check the RAA dynamic behaviour once mounted on satellite. This analysis will serve as reference for the sensitivity analyses, and is called "nominal".
Some representative points are chosen in order to show RAA structure dynamic behaviour, as shown hereunder.
Note that all these points are defined in a local coordinate system 90001:

- Y(90001) = Y(global coordinate system),
- Z(90001) perpendicular to PR panel.

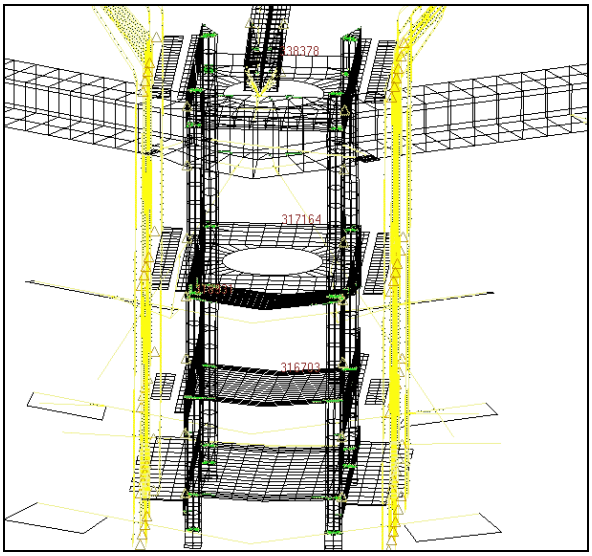

Figure 56: Lower structure representative points

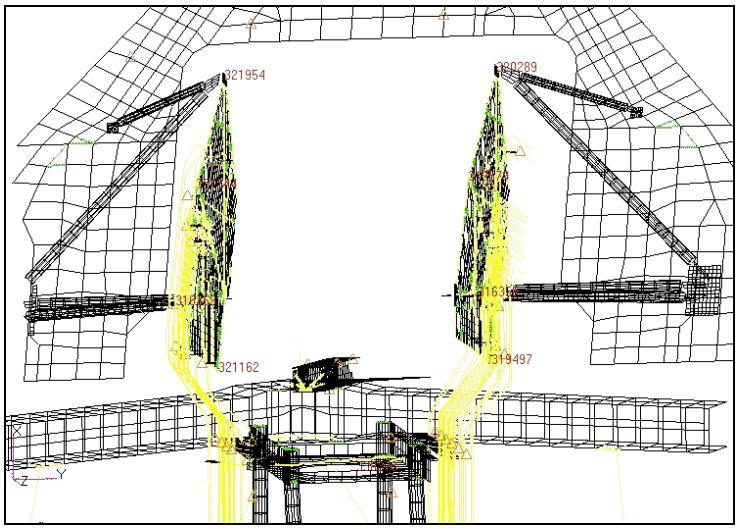

Figure 57: Upper structure representative points

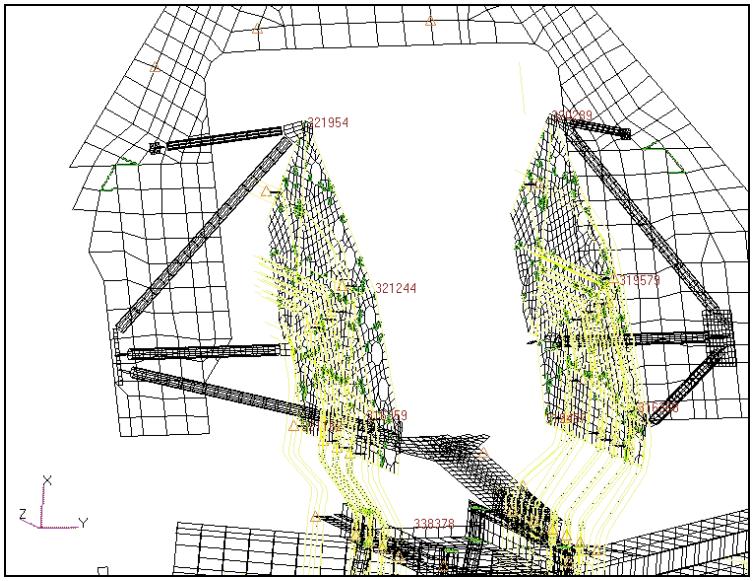

Figure 58: Upper structure representative points

Only the most representative results are presented in following paragraphs.

9.2.4.2 Representative points accelerations (drive X)

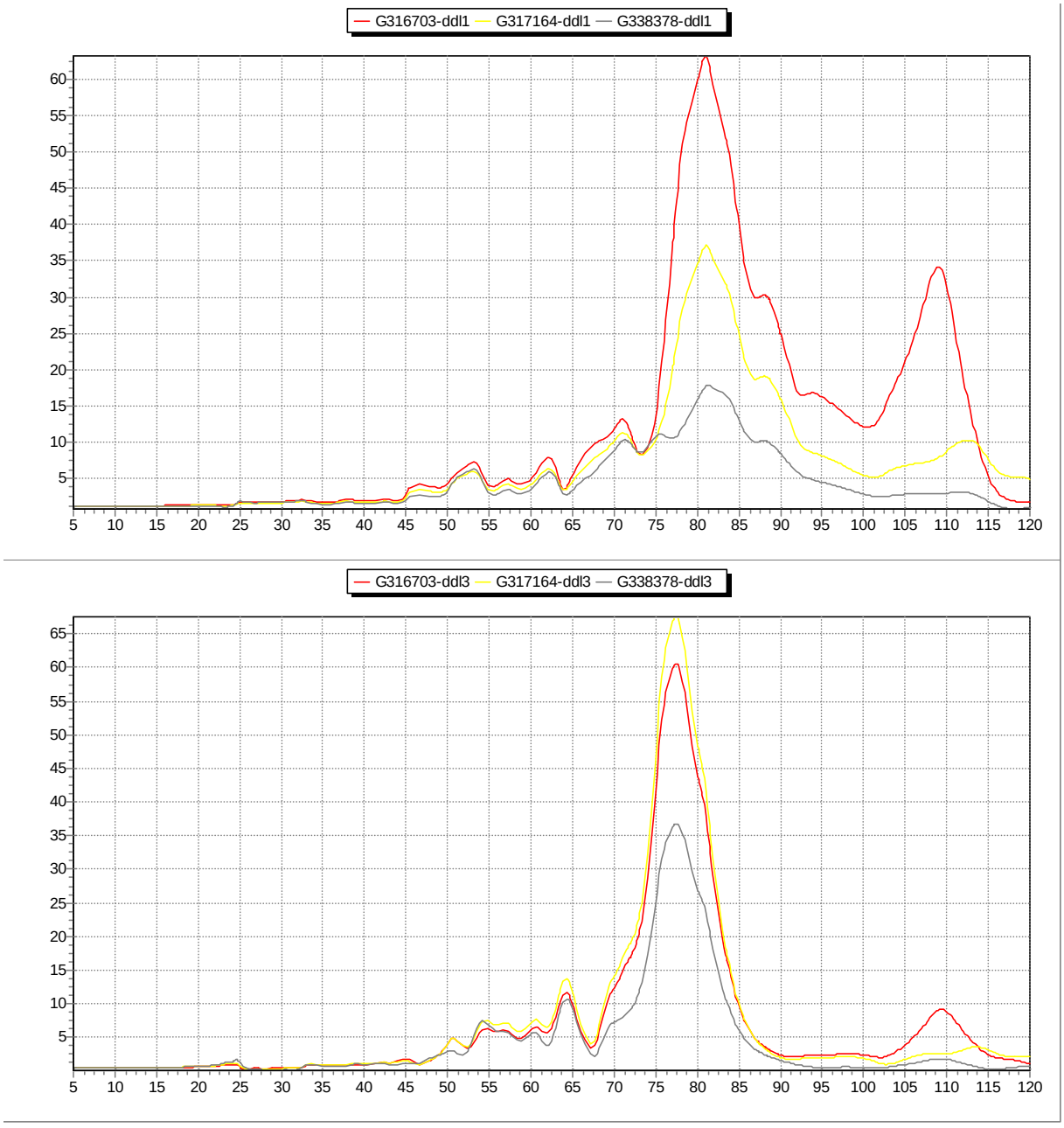

Figure 59: Accelerations of representative points (X drive)

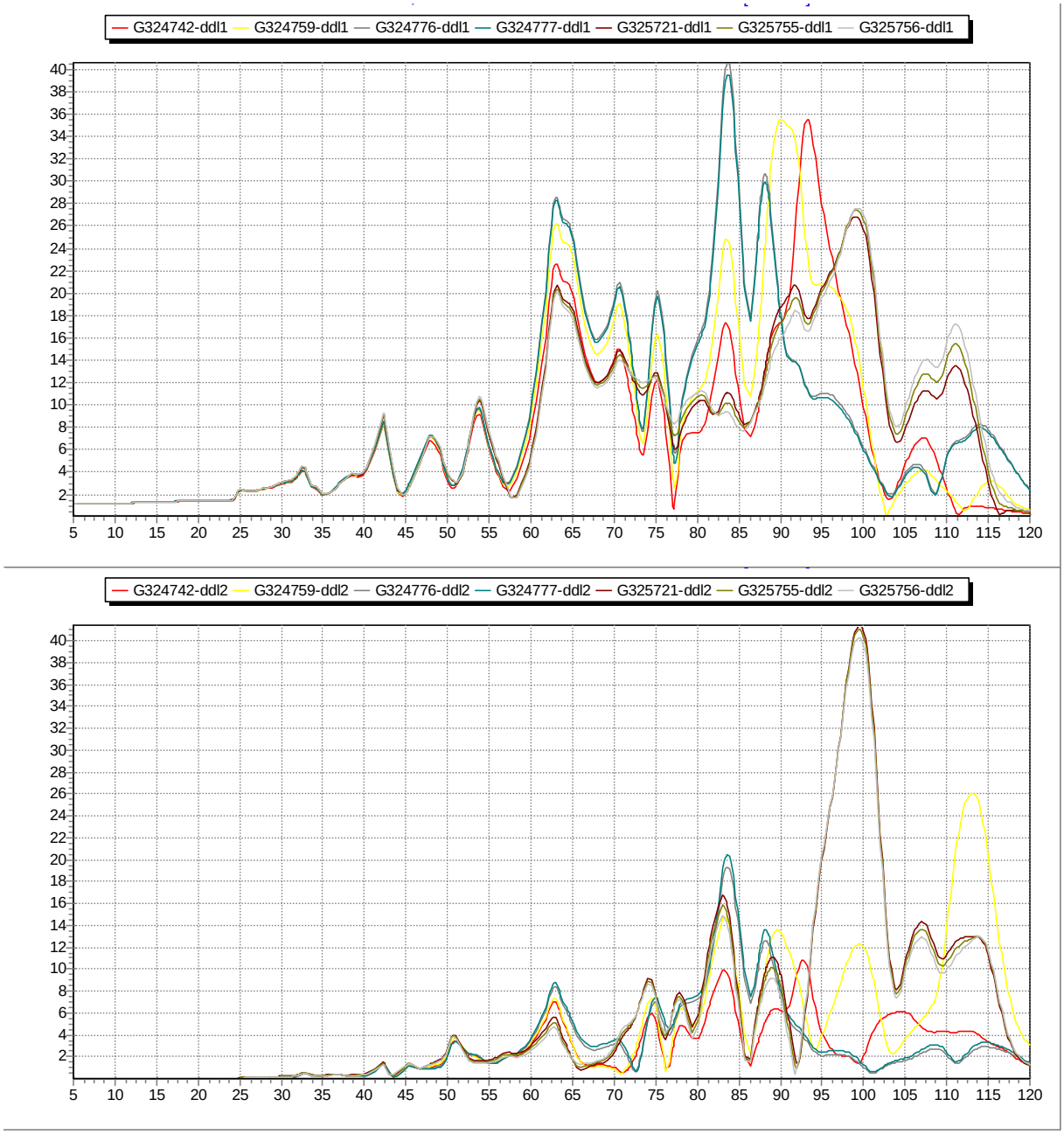

Figure 60: Accelerations of representative points (X drive)

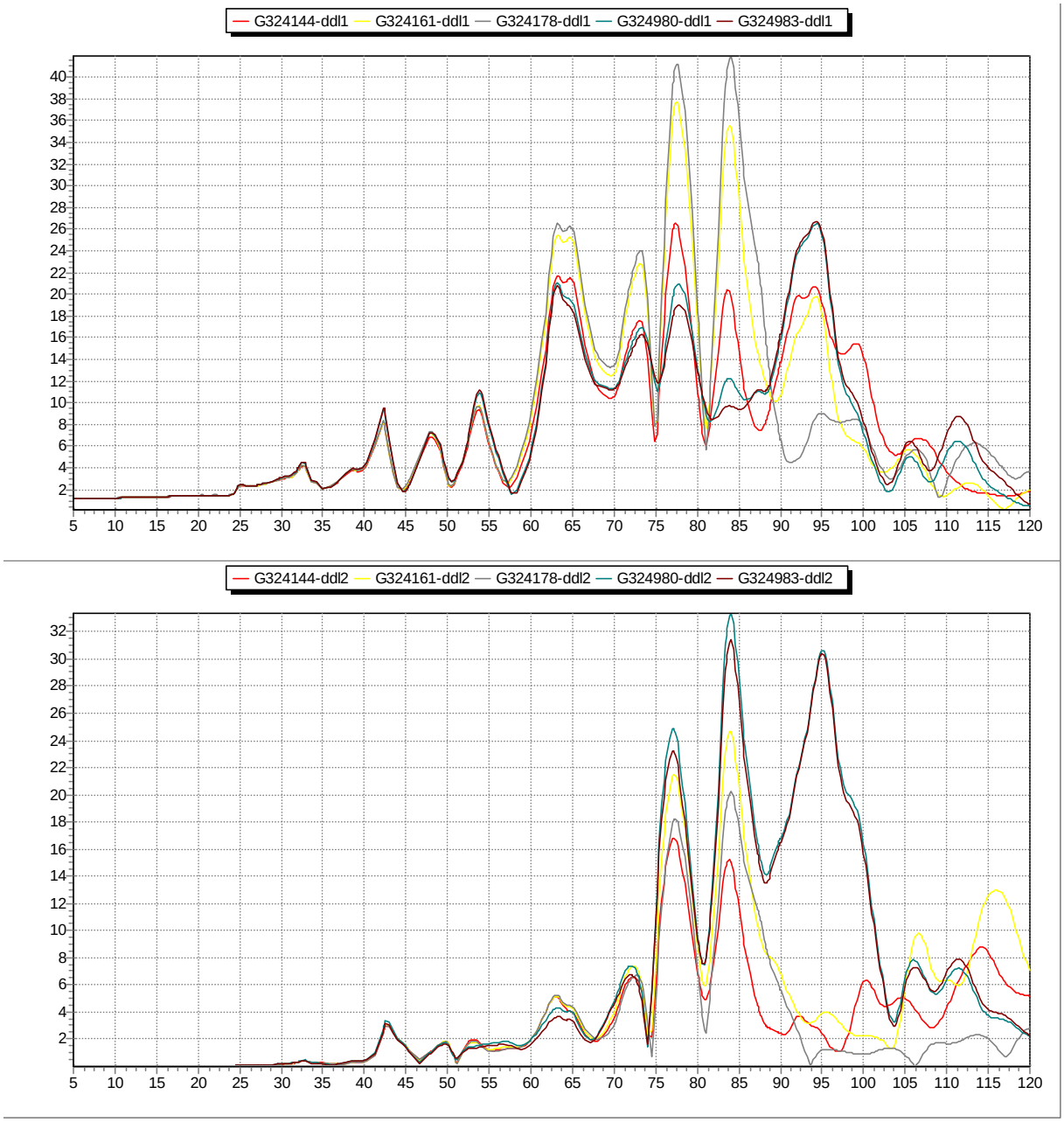

Figure 61: Accelerations of representative points (X drive)

9.2.4.3 Representative points accelerations (drive Y)

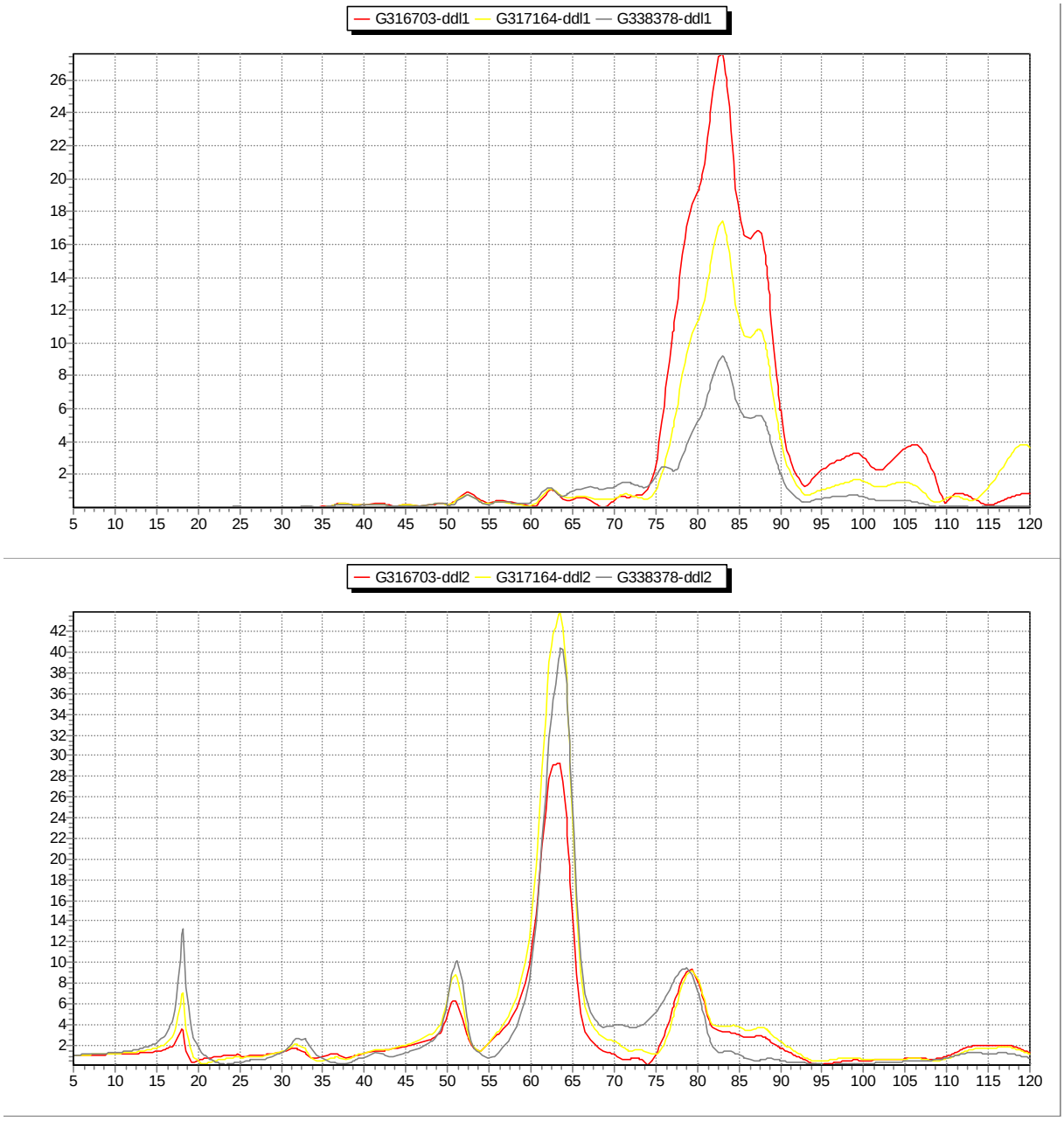

Figure 62: Accelerations of representative points (Y drive)

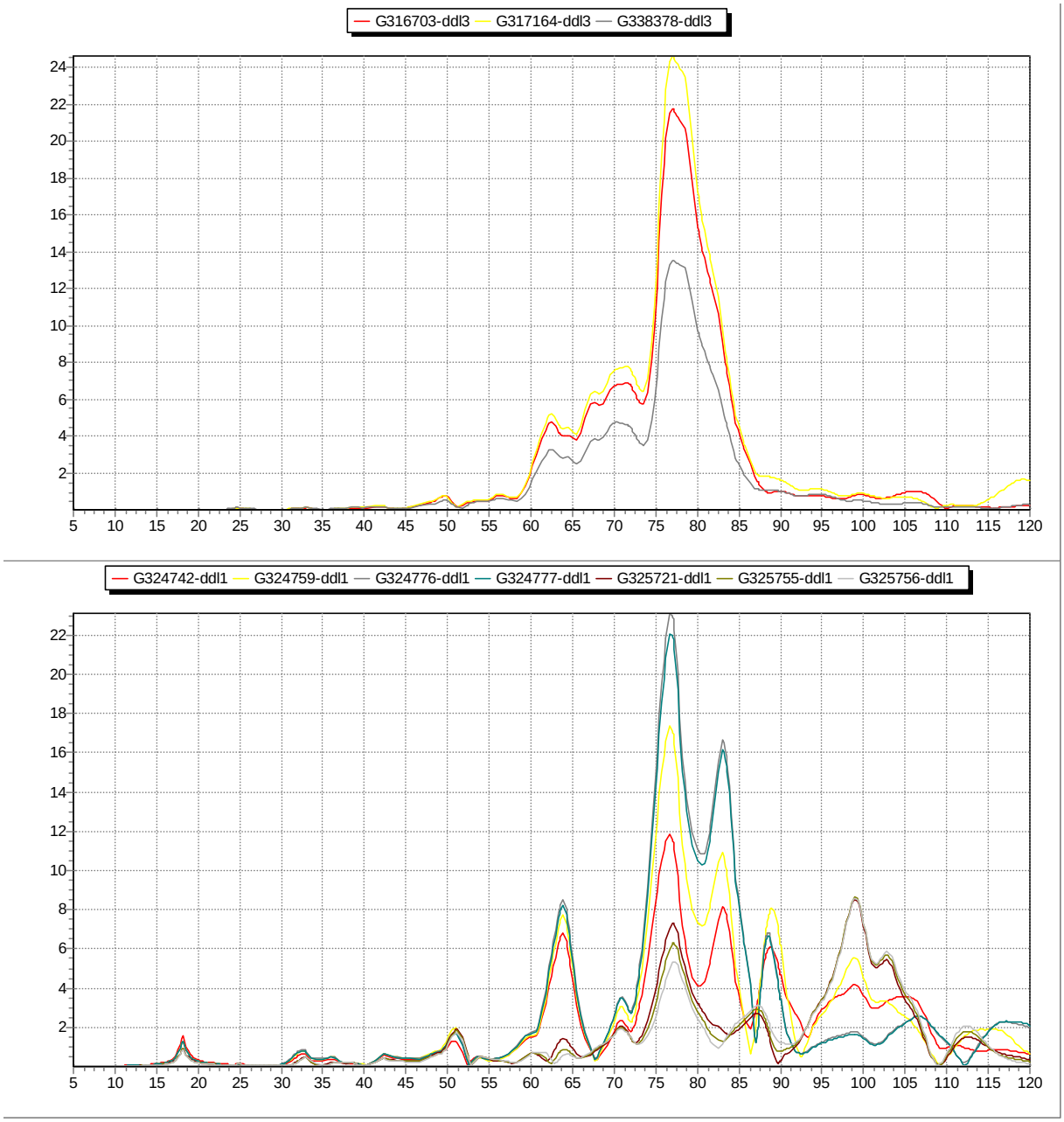

Figure 63: Accelerations of representative points (Y drive)

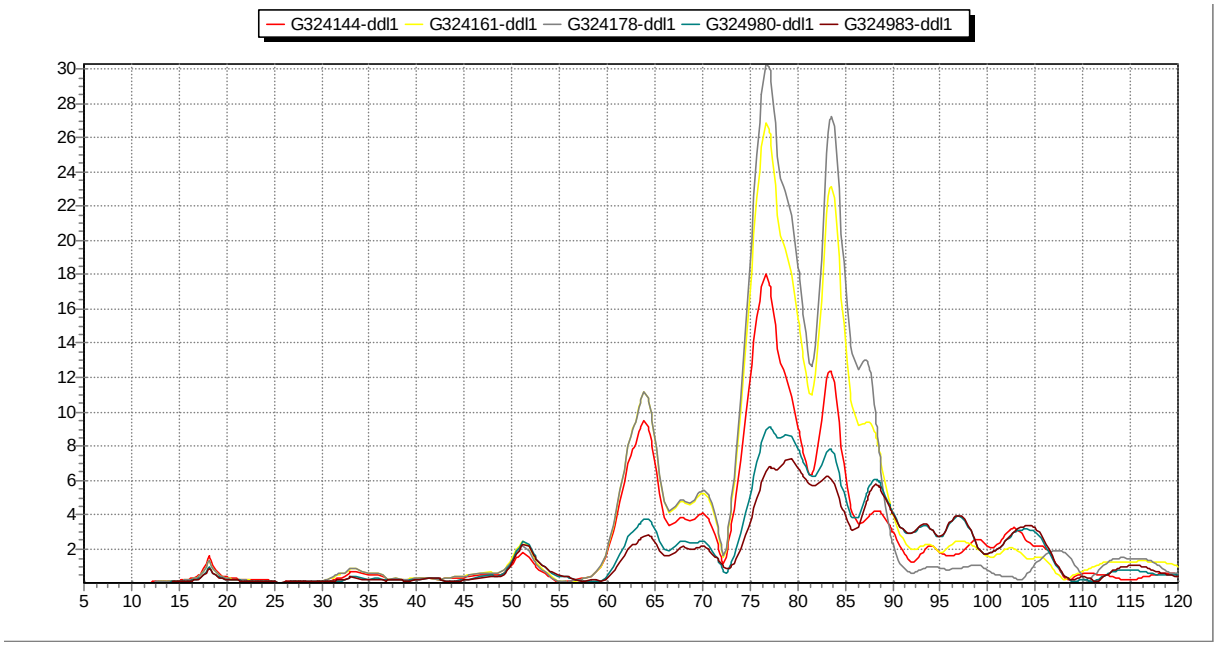

Figure 64: Accelerations of representative points (Y drive)

9.2.4.4 Representative points accelerations (drive Z)

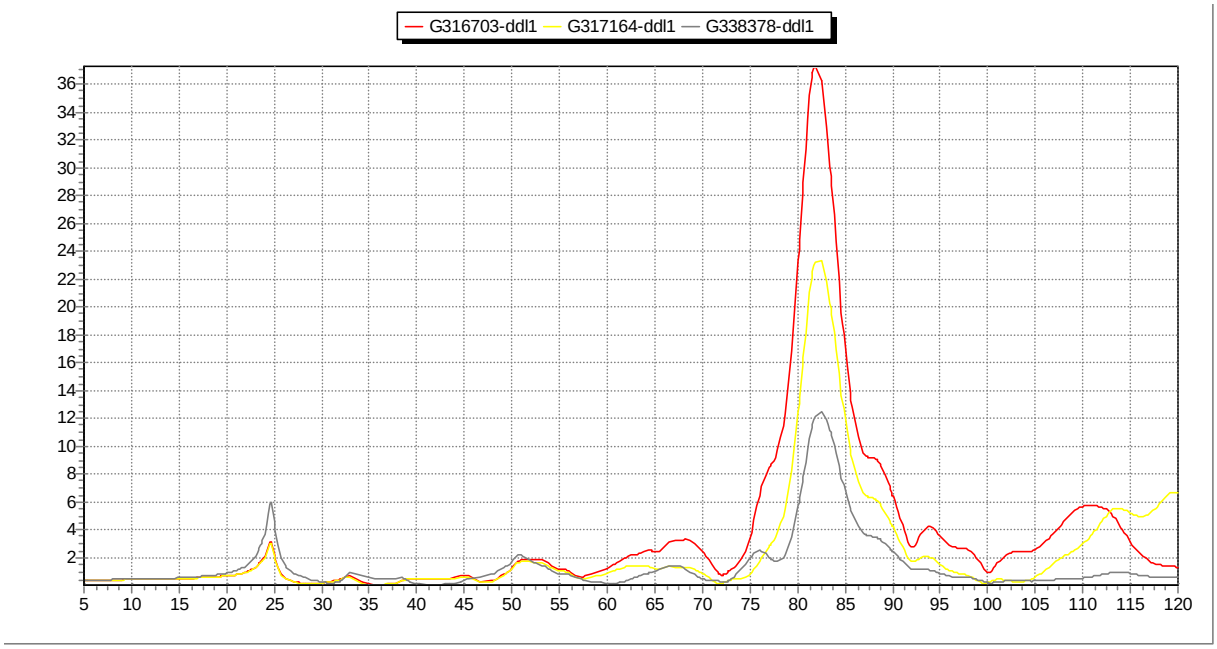

Figure 65: Accelerations of representative points (Z drive)

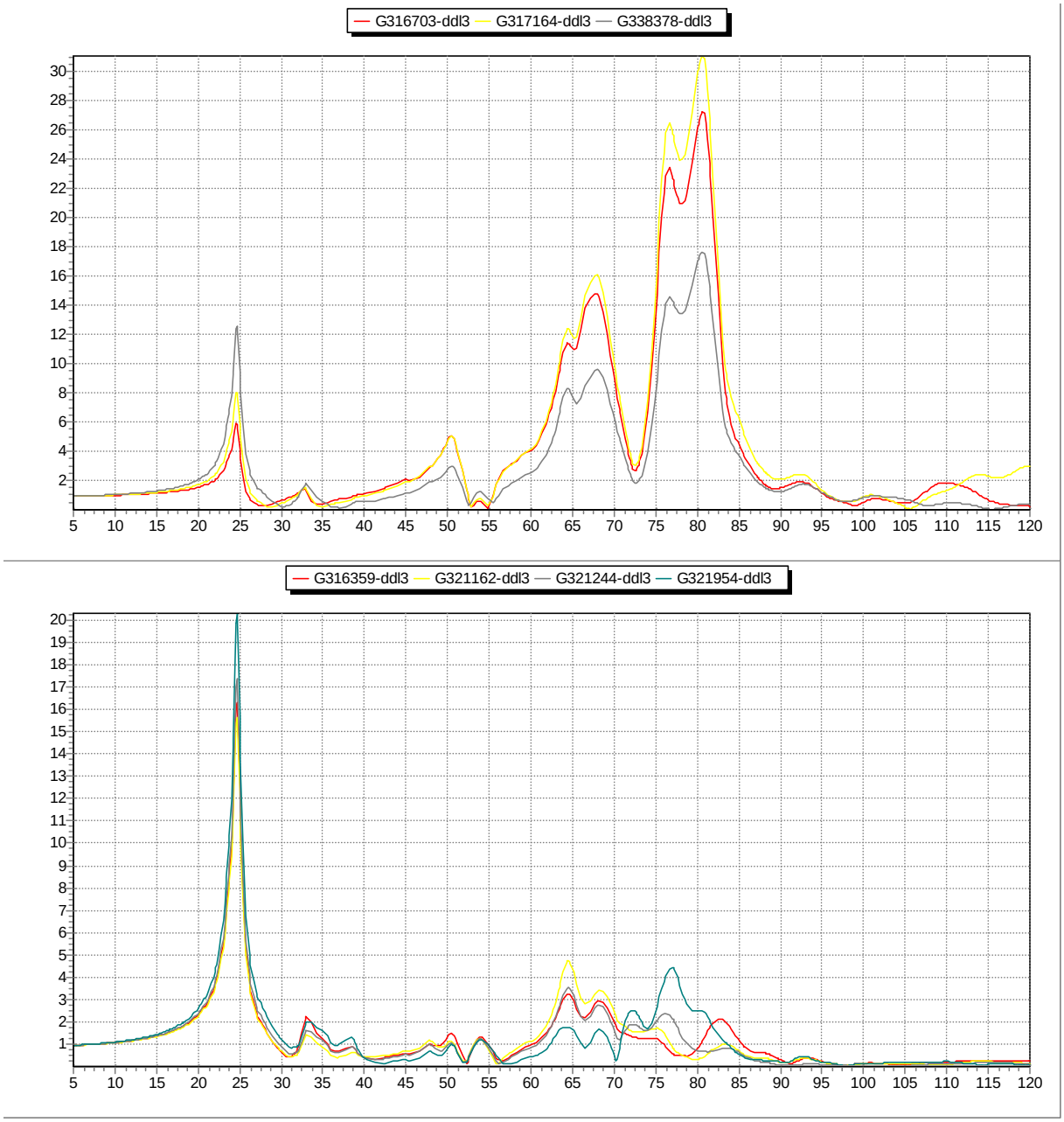

Figure 66: Accelerations of representative points (Z drive)

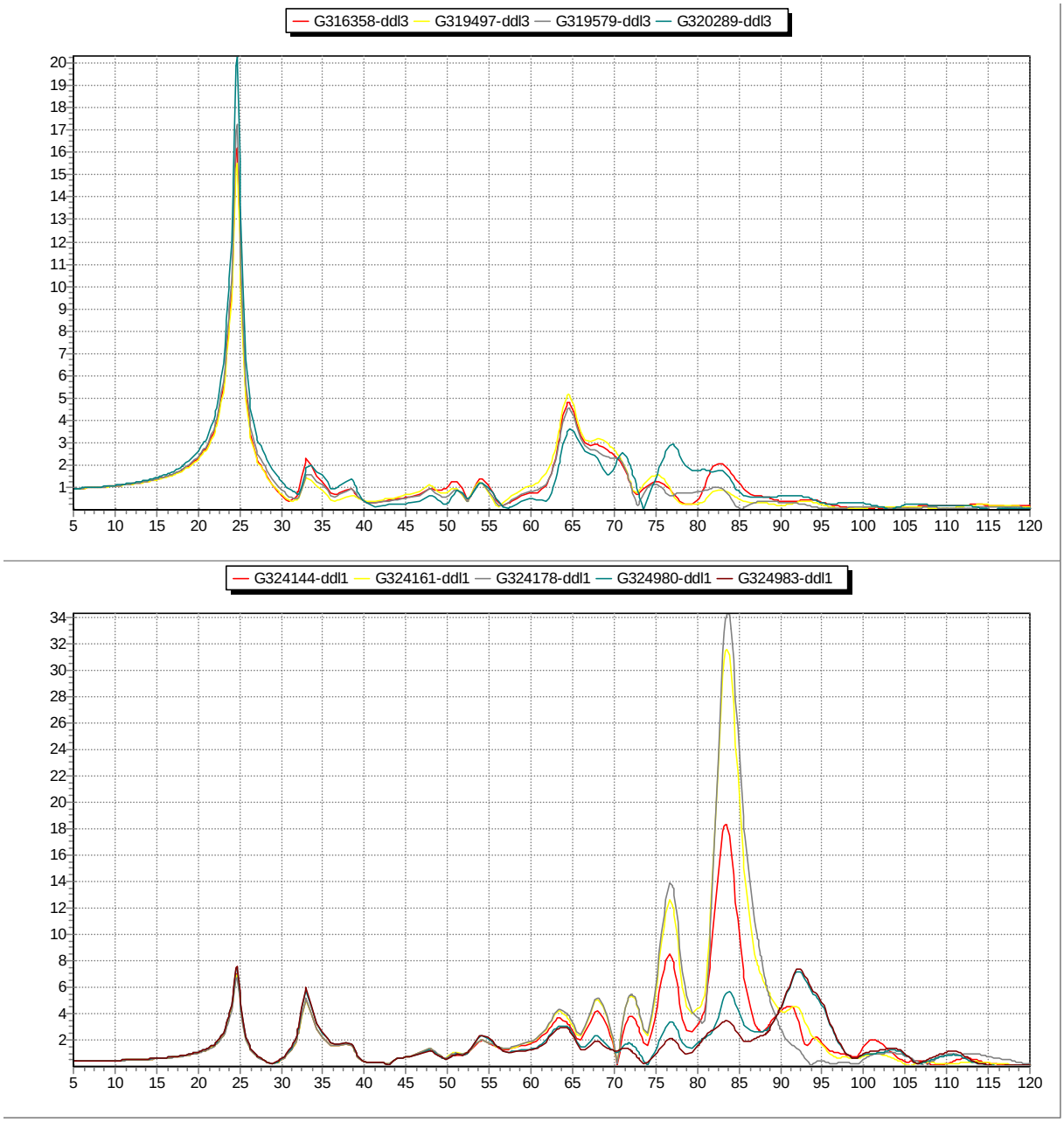

Figure 67: Accelerations of representative points (Z drive)

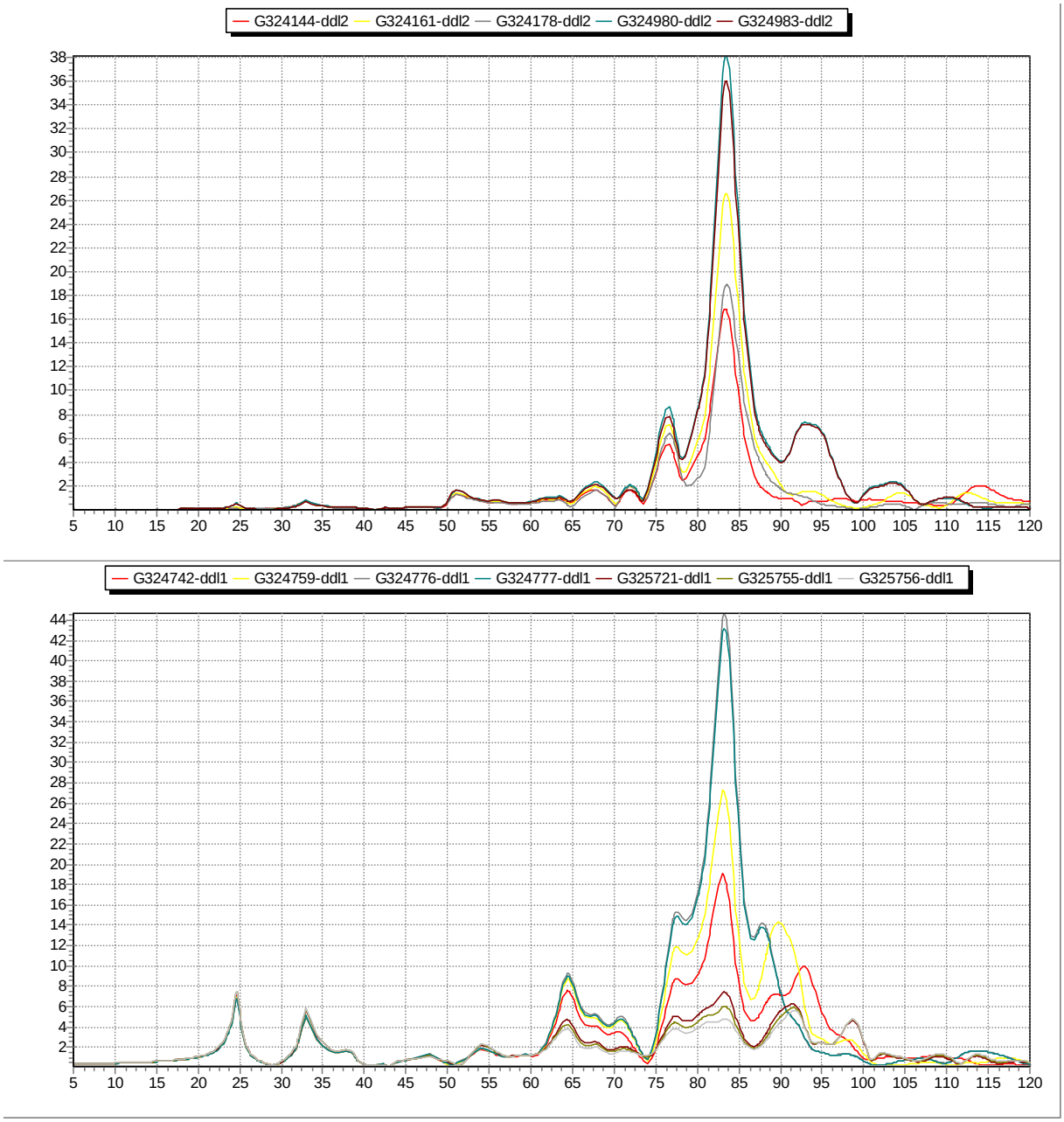

Figure 68: Accelerations of representative points (Y drive)

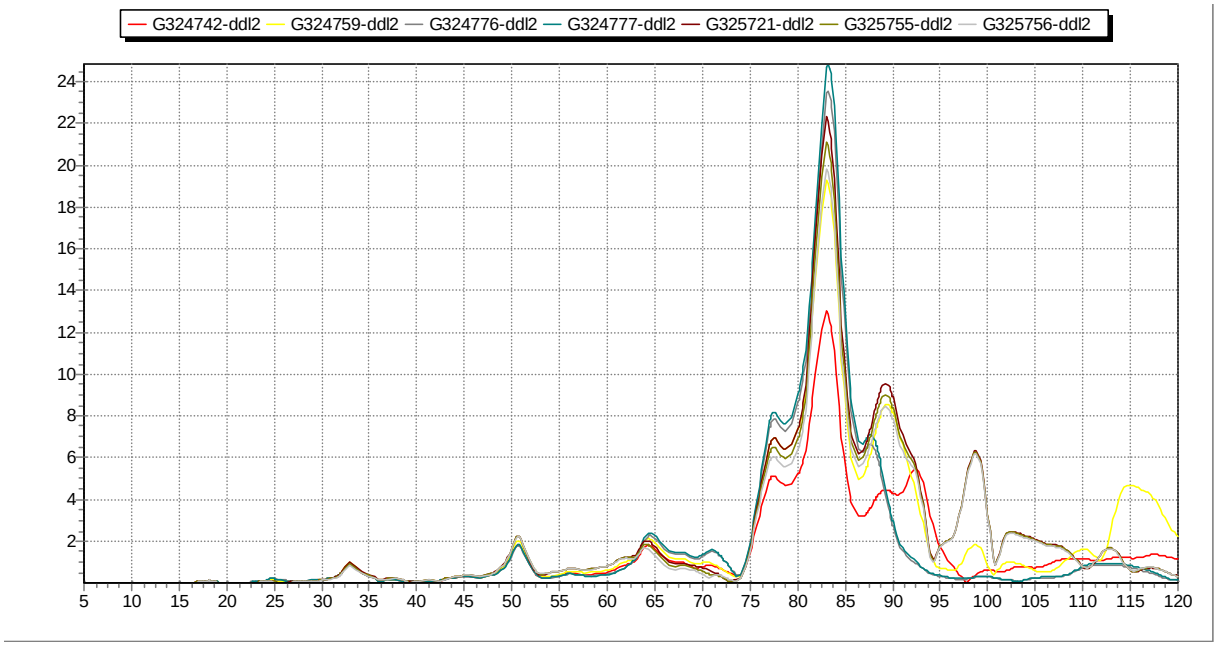

Figure 69: Accelerations of representative points (Z drive)

Comments :

An X-Z coupling occurs at 77Hz between sub-platform out of plane mode and lower structure Z mode, which must be assessed by sensitivity analyses (see § 9.2.4.5). Indeed, the sizing of the subplatform / lower structure I/F depends on the loads seen on this mode.

Also, since wave guide modes have very low effective masses and may differ slightly from LABEN IDEAS FEM wave guides modes, it has been decided to perform sensitivities on these wave guides modes in order to assess their tendency to couple with satellite high frequency modes (see §9.2.4.6).

The last sensitivity performed concerns upper structure I/F loads (see § 9.2.4.7) : even if no strong coupling is identified after this sine analysis, PR panel inserts have limited capability and worst case should be identified in order to verify the inserts integrity and non slippage under sine environment.

9.2.4.5 Sensitivity on RAA lower structure

Sensitivity on RAA lower structure has been performed in order to maximise the dynamic sine response on lower structure bending Z mode, excited by subplatform out of plane mode at 75Hz. No notching criterion is taken into account for this analysis.

Young modulus of lower structure (platforms and tubes) and has been modified in order to increase or decrease its stiffness.

Configuration	Lower structure bending (Z) mode frequency on rigid interface (Hz)	Platforms young modulus (MPa) (PSHELL 2)	Tubes young modulus (MPa) (PSHELL 4)
Nominal	94.24	110000	230000
1	88.08	30000	70000
2	90.17	40000	100000
3	95.72	160000	320000
4	98.06	400000	700000

Table 50: Sensitivity on lower structure stiffness : description of 3 configurations

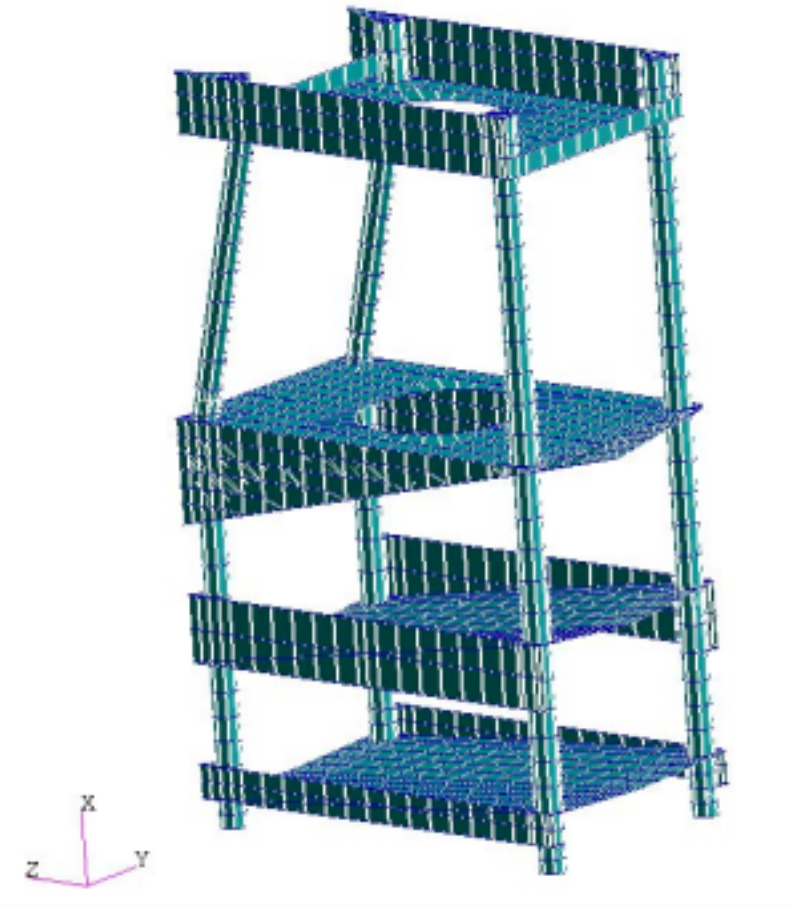

Figure 70: RAA lower structure view

Sine analyses on spacecraft are performed in order to compare every configuration.
The tensors of the 4 interfaces between RAA and sub platform are computed in order to compare the 3 configurations. A first comparison of every acceleration of points on RAA platforms has not permitted to identify a worst case.

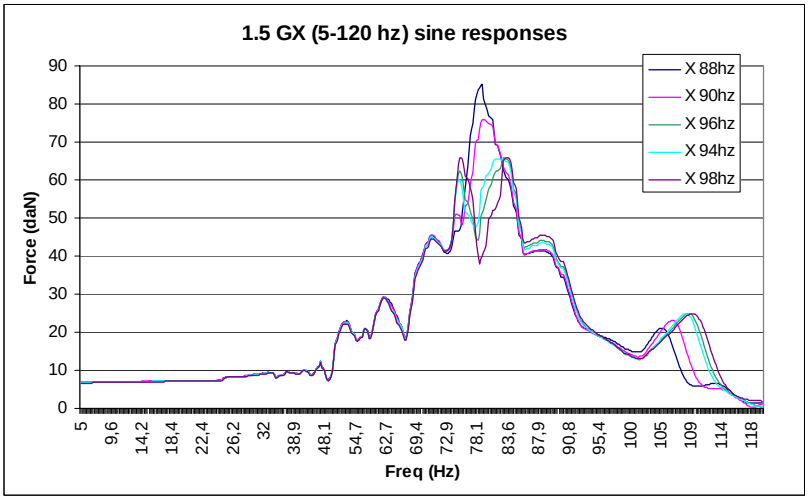

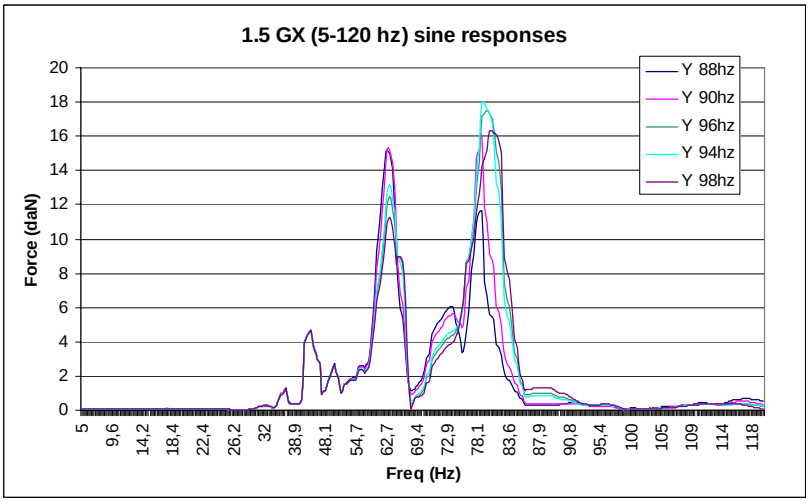

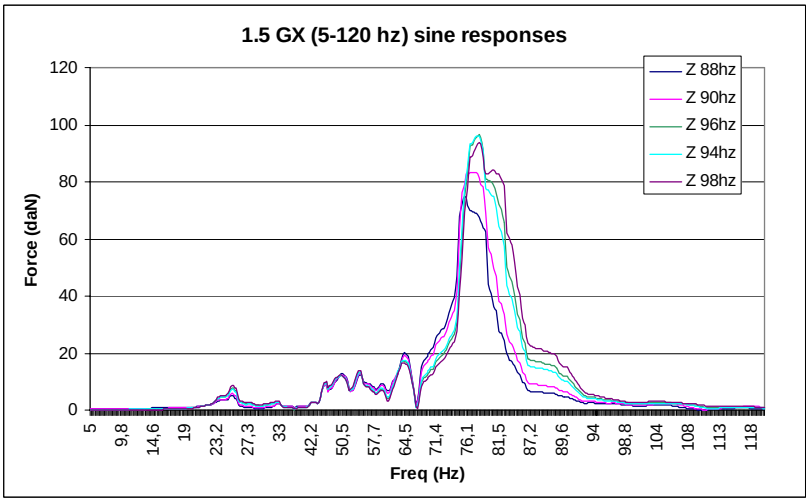

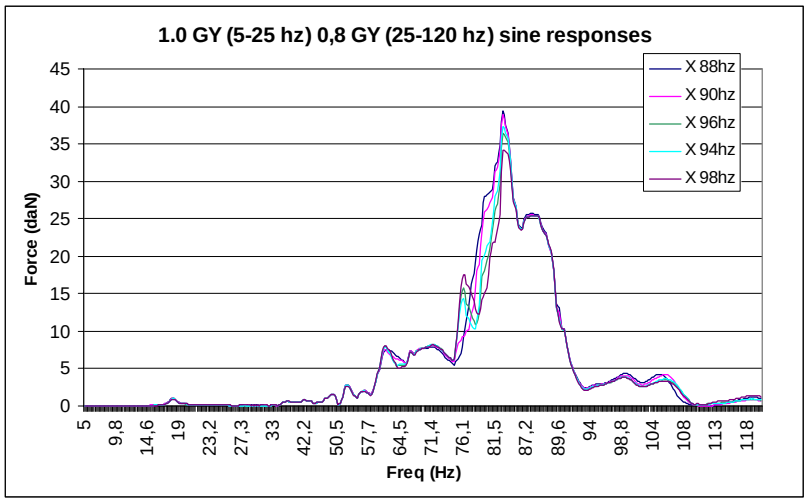

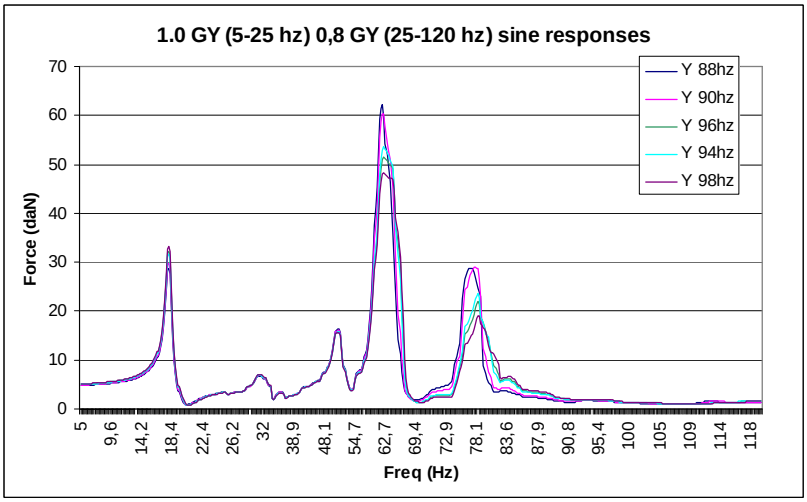

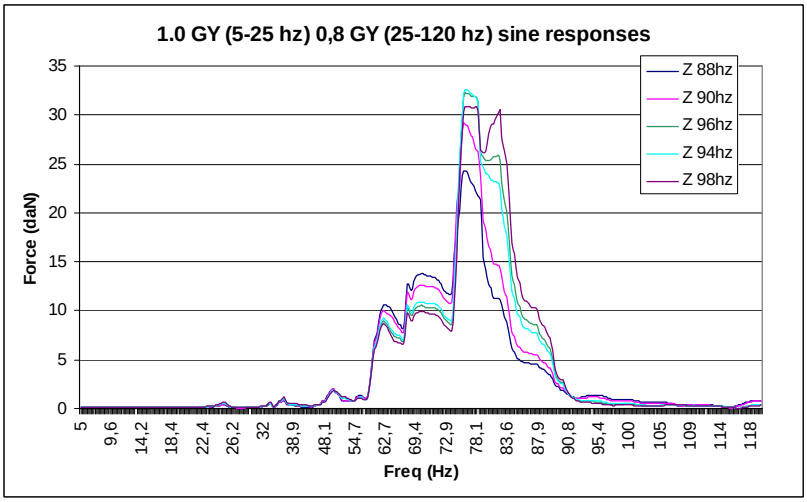

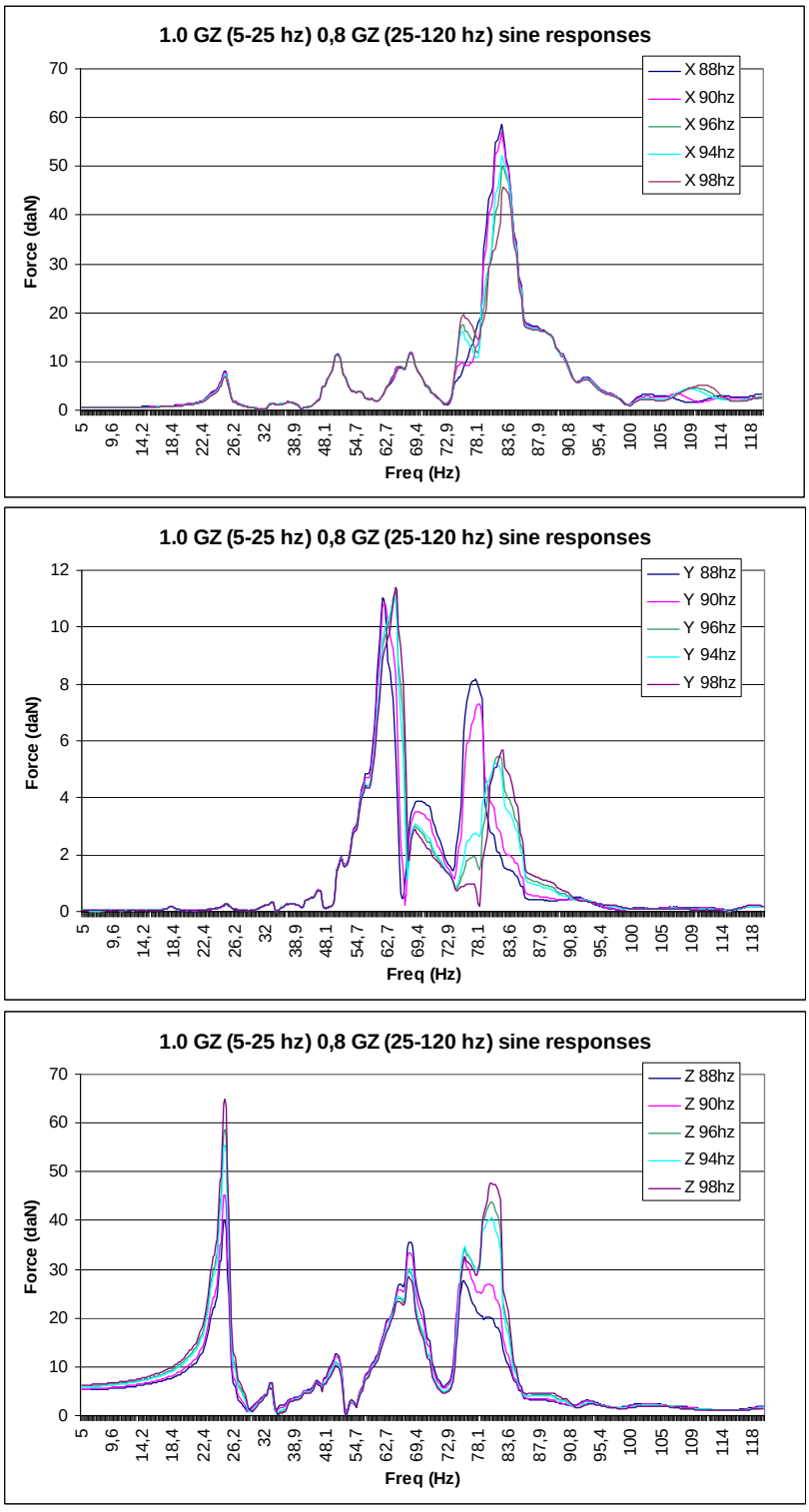

Figure 71: RAA lower structure / sub platform interfaces tensors

The maximum force is obtained for nominal configuration: 96.30 daN in direction Z at 77.59 Hz under 1.5 GX excitation.
Note that the resultant in X direction of the configurations 1 for X drive is greater than the resultants of the other configurations.

For this sensitivity, 2 worst cases (nominal configuration and configuration 1) have been identified.

In order to confirm these results, the loads of every lower structure interface are compared for both worst cases.

IF RAA - SUBPLATFORM

	FORCE GX 88 Hz (N;Nm)	freq (Hz)	FORCE GX nominal (N;Nm)	freq (Hz)
352061	223	78,4	186	81,0
352062	37	78,4	59	80,4
352063	177	75,2	228	77,6
352064	0	75,6	1	78,0
352065	41	75,6	53	78,0
352066	12	78,4	18	80,4
352071	235	79,1	230	81,5
352072	33	79,1	43	80,2
352073	179	75,2	232	78,0
352074	0	79,1	0	80,8
352075	42	75,6	54	78,0
352076	11	79,1	13	80,5
352081	187	78,4	123	75,8
352082	54	62,4	49	62,9
352083	187	75,2	240	77,6
352084	0	62,7	0	78,3
352085	43	75,6	54	78,0
352086	17	62,7	14	62,9
352091	198	79,1	140	83,1
352092	59	62,7	51	63,1
352093	192	75,2	245	77,6
352094	0	62,7	0	80,6
352095	44	75,2	56	78,0
352096	18	62,7	15	63,1
351000	526	42,3	528	42,3
351001	54	62,7	46	80,2
351002	406	75,2	452	77,4
351003	9	74,7	9	77,1
351004	90	78,0	75	78,5
351005	36	62,7	26	63,1

IF RAA - FRAME (global tensor)

	FORCE GX 88 Hz (N;Nm)	freq (Hz)	FORCE GX nominal (N;Nm)	freq (Hz)
352001	34	75,2	40	77,1
352002	371	77,6	445	77,6
352003	532	75,6	657	77,6
352004	8	75,6	9	77,6
352005	1	75,2	1	77,3
352006	0	75,2	0	77,5
352051	33	75,0	40	77,3
352052	359	75,2	422	77,5
352053	493	75,2	580	77,5
352054	0	62,7	0	63,4
352055	0	75,2	0	77,3
352056	0	75,2	0	77,3

Table 51: Comparison of RAA Lower structure interface loads for every configuration

In conclusion, the RAA lower structure interface sizing has to be verified with configurations 1 and nominal.

9.2.4.6 Sensitivity on wave guides stiffness

Sensitivities on wave guides stiffness have been performed in order to maximise the dynamic sine response (wave guides mode). No notching criterion is taken into account for this analysis.

Young modulus of wave guides has been modified in order to increase or decrease the stiffness.

Configuration	RAA 1st mode frequency on rigid interface (Hz)	Wave guides young modulus (MPa) (PSHELL 12)
Nominal	79.08	120000
1	73.63	90000
2	75.84	100000
3	82.23	150000

Table 52: Sensitivity on wave guides stiffness: description of 3 configurations

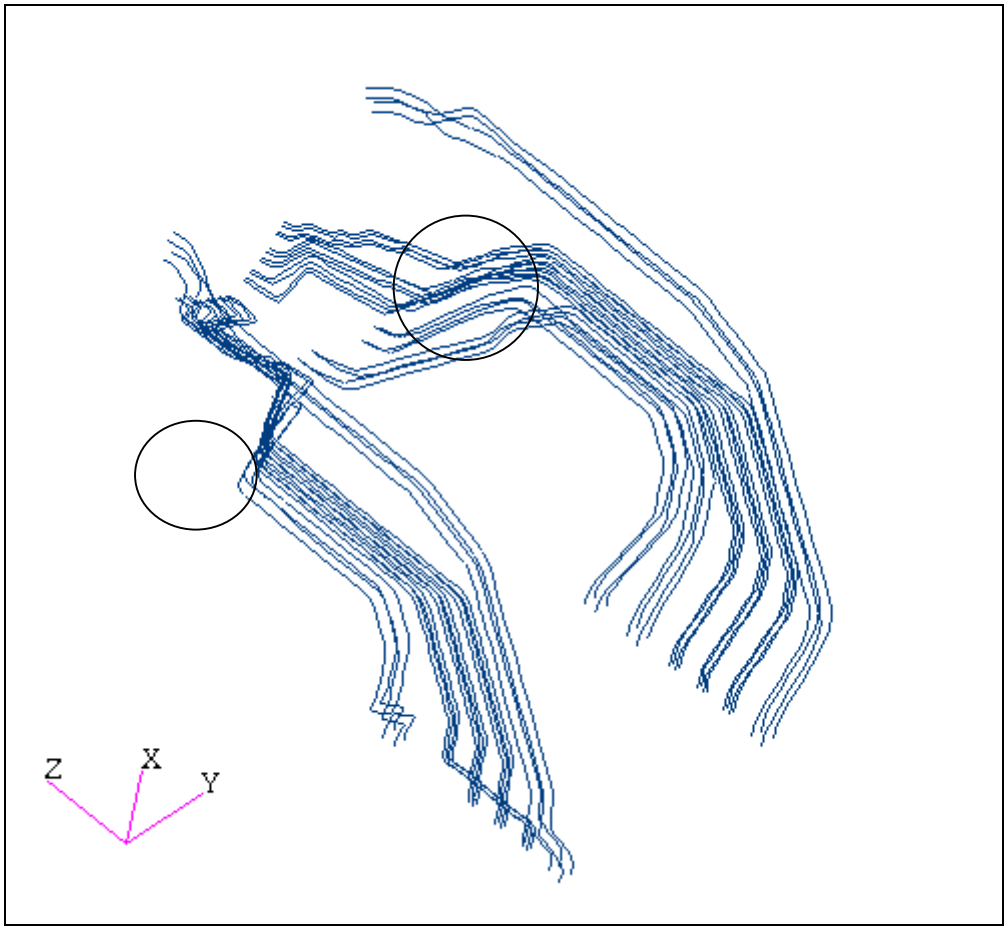

Figure 72: Wave guides

Sine analyses on spacecraft are performed in order to compare each configuration.
Accelerations of some points on wave guides are compared in order to determine the worst case. These points are the more representative regarding dynamic behaviour of wave guides. Only sine analysis under X drive excitation is performed, according to dynamic analysis, which shows that the maximum acceleration is obtained on this drive.

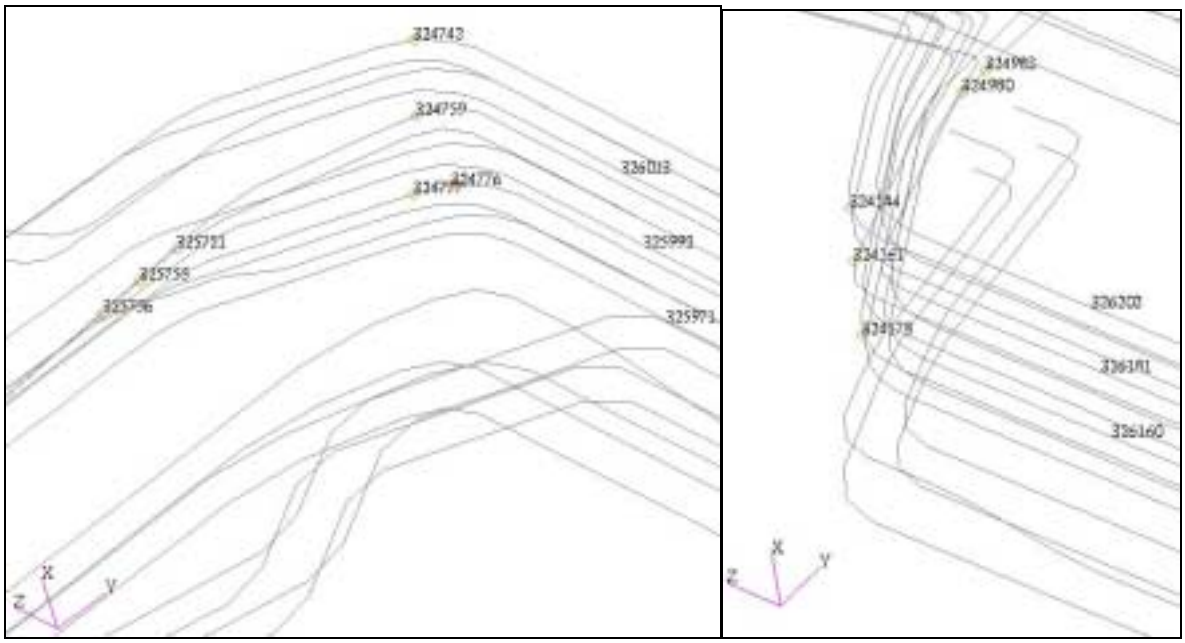

Figure 73: Wave guides representative points

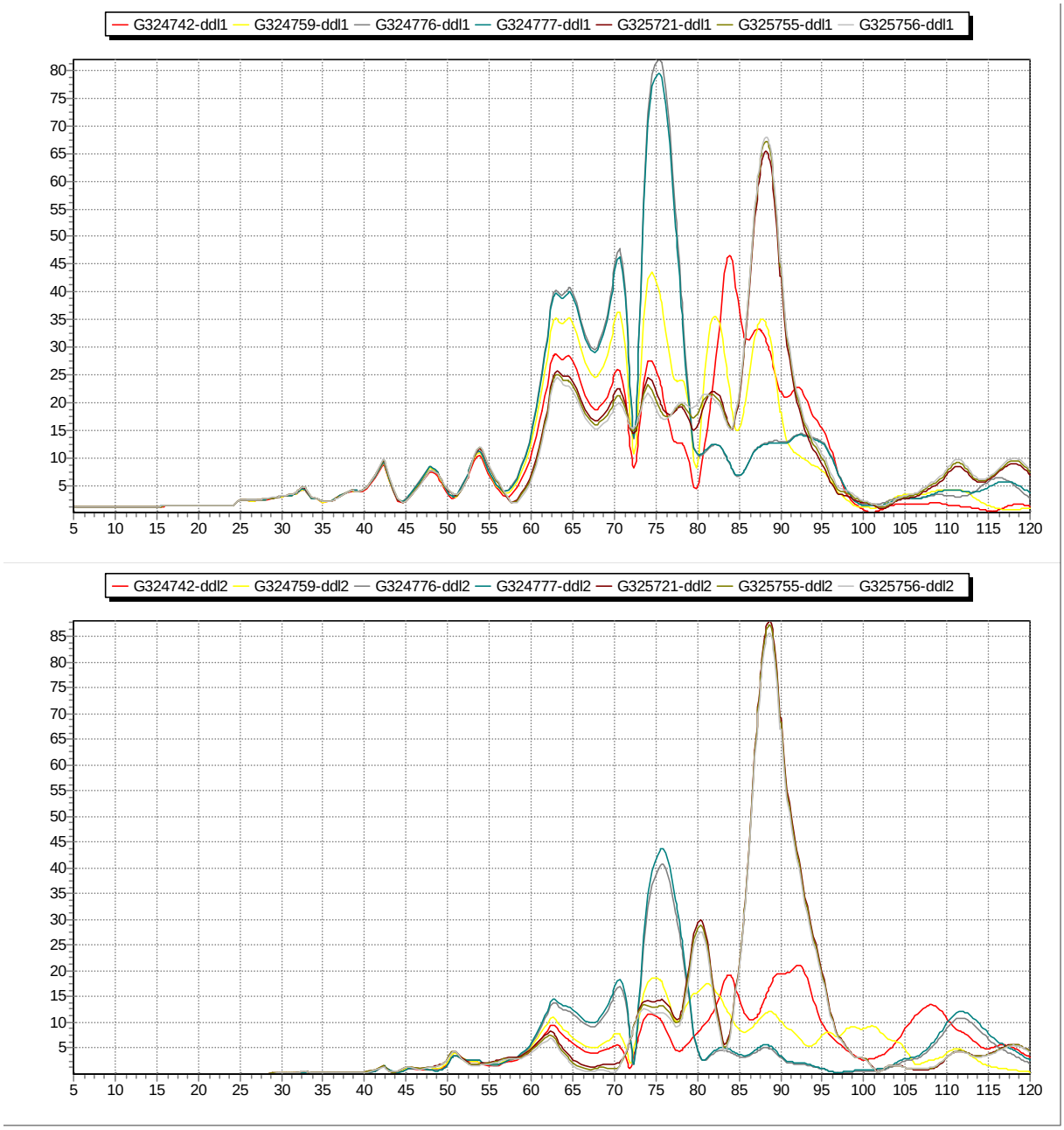

Figure 74: Configuration 1 accelerations sine response

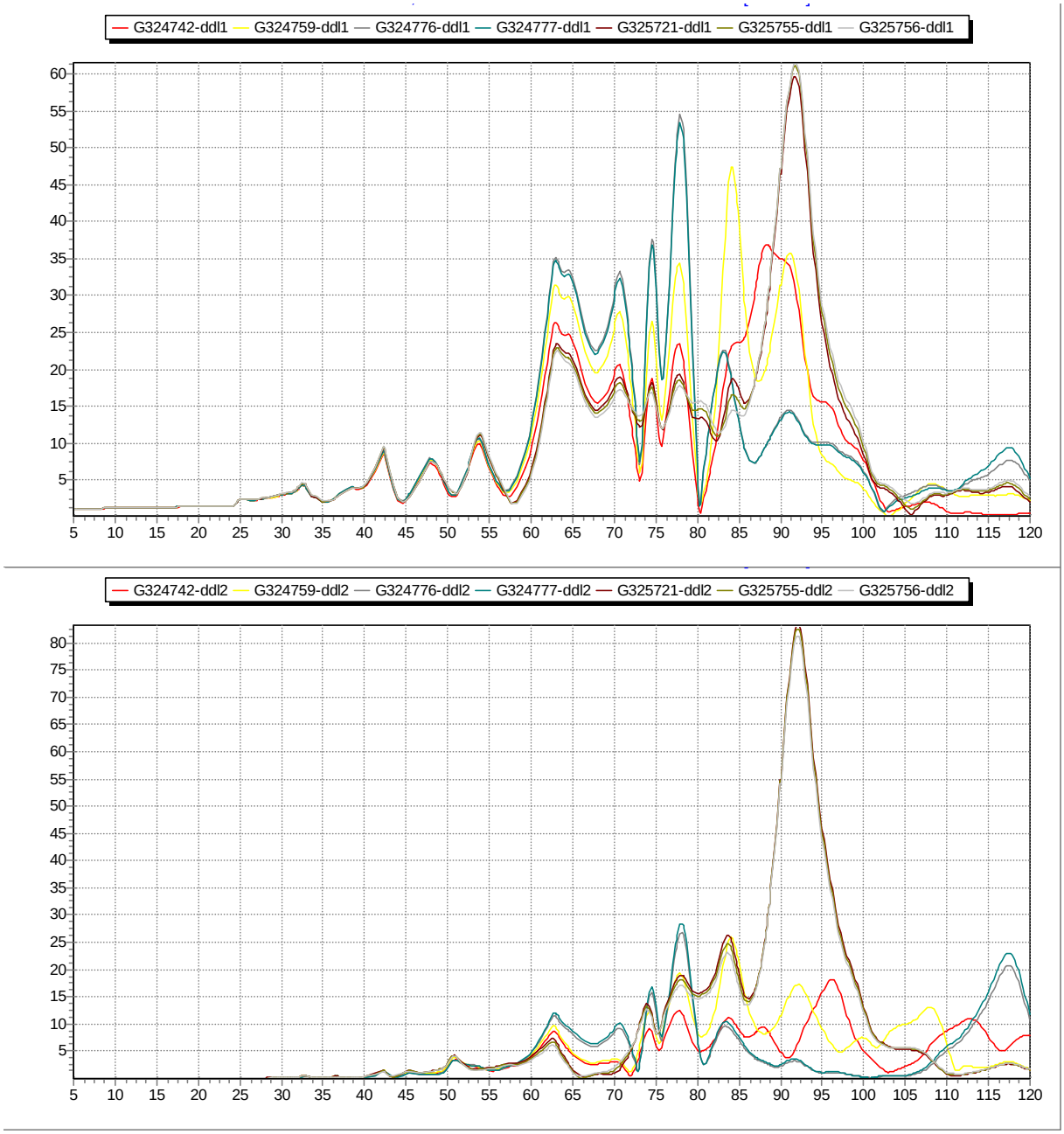

Figure 75: Configuration 2 accelerations sine response

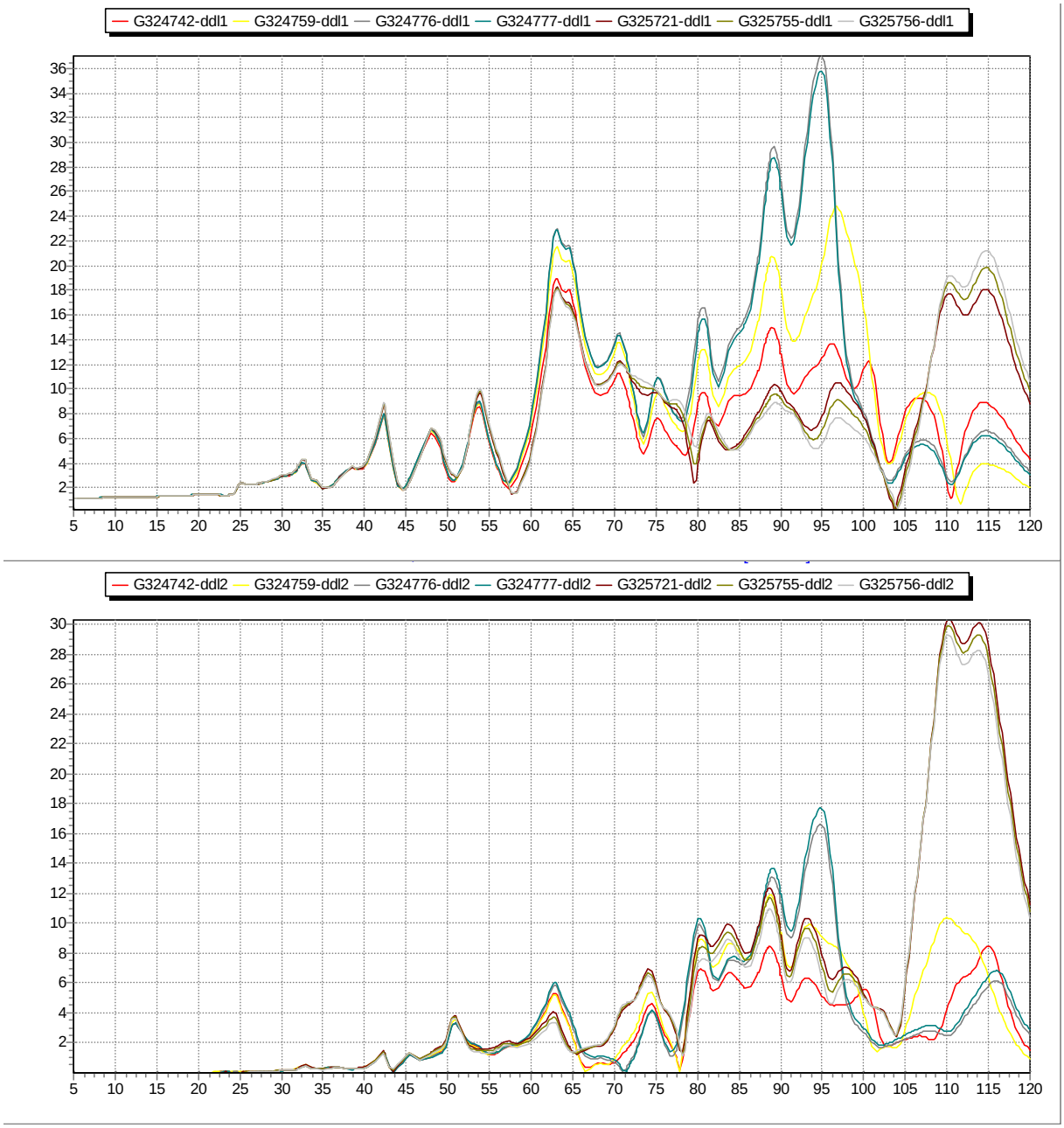

Figure 76: Configuration 3 accelerations sine response

Configuration	Max acceleration (g)	Frequency (Hz)	Node	DOF
Nominal	41.94	84.03	324178	1
1	88.07	88.62	325721	2
2	83.23	92.20	325721	2
3	36.99	94.8	324776	1

Table 53: Accelerations - sensitivity on wave guides stiffness

The worst case configuration for the wave guides accelerations is identified as being configuration 1.

In order to verify that the wave guides modes have low effects on upper structure I/F loads, the RAA upper structure / PR panel interface loads for nominal configuration and configuration 1 are compared.

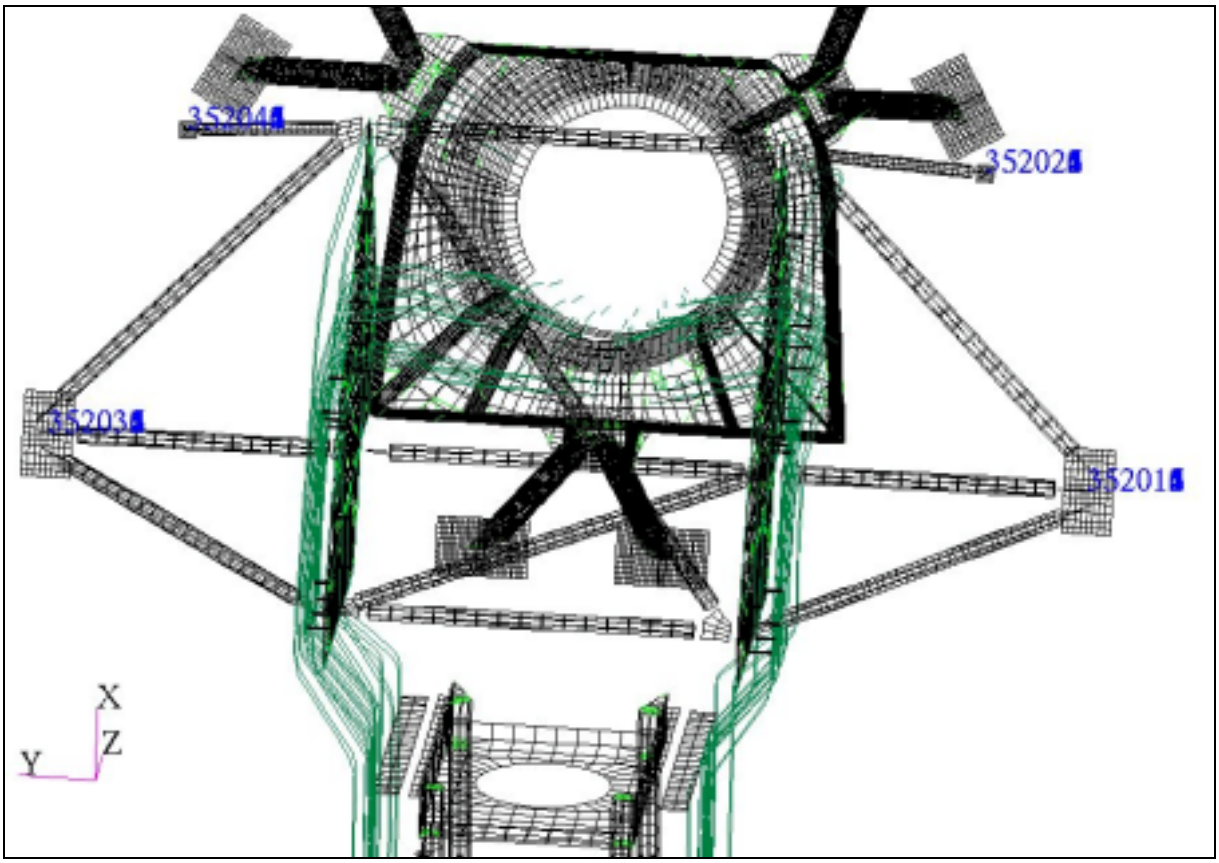

Figure 77: Interface RAA upper structure view

RAA - UPPER STRUCTURE (global tensor)

	FORCE GX 88 Hz (N;Nm)	freq (Hz)	FORCE GX nominal (N;Nm)	freq (Hz)	Diff 88hz/nominal (%)
352011	191	53,2	186	53,2	-2,68%
352012	646	64,6	642	64,6	-0,58%
352013	264	54,1	255	64,4	-3,78%
352014	11	64,7	11	64,7	-2,70%
352015	5	42,5	4	42,5	-15,00%
352016	5	53,5	5	53,5	0,00%
352031	197	53,2	192	53,2	-2,24%
352032	576	64,6	610	64,6	5,58%
352033	253	54,1	241	54,1	-5,01%
352034	10	42,4	10	42,4	4,72%
352035	5	76,3	5	76,0	0,00%
352036	5	53,5	5	53,5	0,00%
352021	8	80,3	8	78,5	-3,66%
352022	202	42,5	175	42,5	-15,25%
352023	132	42,5	114	78,0	-16,12%
352024	2	42,5	2	42,5	0,00%
352025	0	95,6	0	93,2	0,00%
352026	0	79,8	0	77,1	0,00%
352041	10	76,1	12	76,0	15,45%
352042	201	75,9	218	75,8	7,90%
352043	148	75,9	165	75,8	10,18%
352044	1	79,8	1	77,6	-16,67%
352045	0	95,2	0	83,6	0,00%
352046	0	79,5	0	77,1	0,00%

Table 54: RAA upper structure / PR panel interface comparison (X drive)

The wave guides modes have no significant effect on the RAA upper structure / PR panel interface loads (a difference lower than 15% for a maximum wave guides acceleration twice greater).

On the basis of the results shown above, the worst coupled case for the wave guides corresponds to the configuration 1.

9.2.4.7 Sensitivity on RAA upper structure

Sensitivity on RAA upper structure has been performed in order to maximize the dynamic sine response. The sensitivity parameter is upper structure stiffness. No notching criterion is taken into account for this analysis.

Young modulus, thickness and geometrical properties of upper structure (tubes) have been modified in order to increase or decrease its stiffness.

Configuration	Lower structure bending (Z) mode frequency on rigid interface (Hz)	Tubes young modulus (MPa) (PSHELL 18)	Tubes properties (MPa) (PSHELL 22)	
			T (m)	12I/T ^ 3
Nominal	79.08	110000	0.00135	1.
1	75.06	70000	0.0011	0.9
2	83.01	300000	0.0027	2.

Table 55: Sensitivity on upper structure stiffness: description of configurations

The mass difference between configurations 1 and 2 is 0.33 kg. It is negligible.

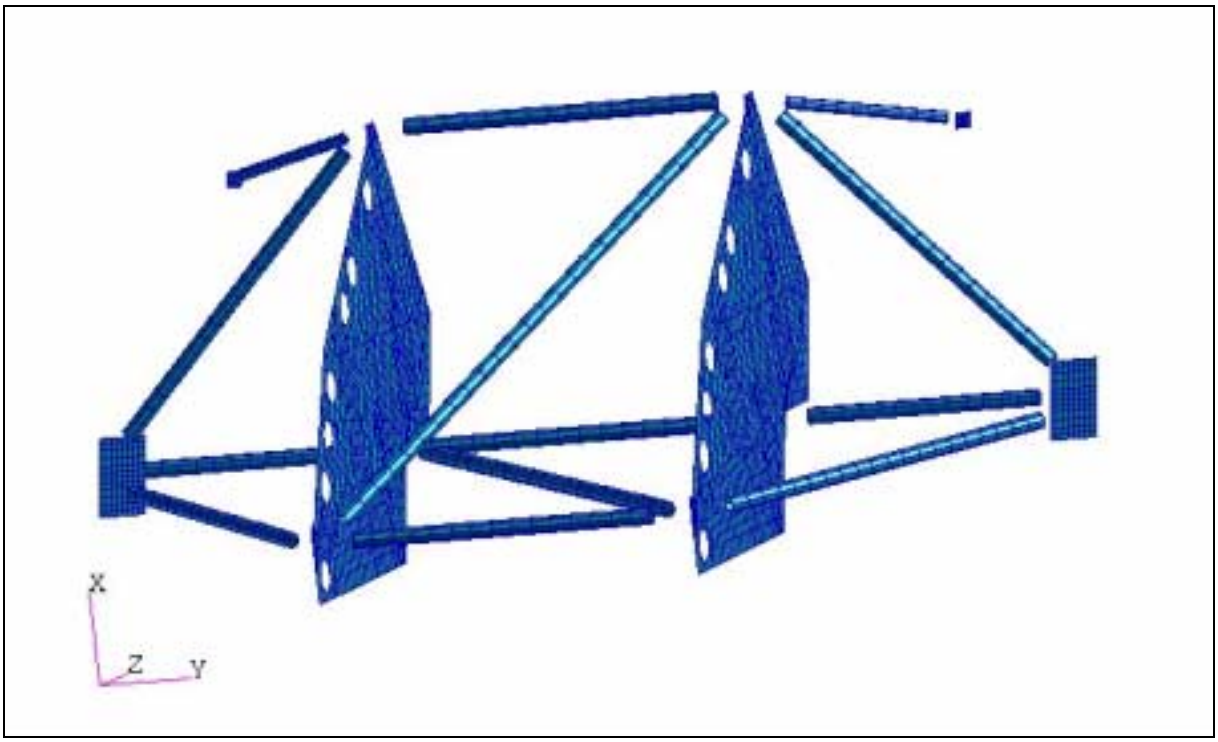

Figure 78: RAA upper structure view

Sine analyses on spacecraft are performed in order to compare every configuration.
The tensors of the 4 interfaces between RAA and PR panel are computed in order to compare every configuration.

RAA - UPPER STRUCTURE (global tensor)

	FORCE GX 75 Hz (N;Nm)	freq (Hz)	FORCE GX 83 Hz (N;Nm)	freq (Hz)	FORCE GX nominal (N;Nm)	freq (Hz)
352011	186	53,5	184	53,5	186	53,2
352012	631	64,7	804	64,7	642	64,6
352013	276	64,5	268	64,5	255	64,4
352014	11	42,3	14	42,3	11	64,7
352015	4	64,2	4	64,2	4	42,5
352016	5	53,5	5	53,5	5	53,5
352031	193	53,5	193	53,5	192	53,2
352032	599	64,7	770	64,7	610	64,6
352033	247	64,5	239	64,5	241	54,1
352034	10	42,3	14	42,3	10	42,4
352035	3	75,4	4	75,4	5	76,0
352036	5	53,5	5	53,5	5	53,5
352021	11	42,5	6	42,5	8	78,5
352022	244	42,5	169	42,5	175	42,5
352023	177	73,5	117	73,5	114	78,0
352024	2	42,5	2	42,5	2	42,5
352025	0	64,6	0	64,6	0	93,2
352026	0	64,7	0	64,7	0	77,1
352041	12	75,1	7	75,1	12	76,0
352042	202	75,1	207	75,1	218	75,8
352043	152	75,4	149	75,4	165	75,8
352044	2	74,0	1	74,0	1	77,6
352045	0	64,6	0	64,6	0	83,6
352046	0	64,7	0	64,7	0	77,1

RAA - UPPER STRUCTURE (global tensor)

	FORCE GY 75 Hz (N;Nm)	freq (Hz)	FORCE GY 83 Hz (N;Nm)	freq (Hz)	FORCE GY nominal (N;Nm)	freq (Hz)
352011	665	18,1	1014	18,1	792	18,1
352012	432	18,1	1025	18,1	614	18,2
352013	406	18,1	694	18,1	494	18,1
352014	7	18,1	15	18,1	10	18,1
352015	7	18,1	9	18,1	8	18,1
352016	13	18,1	21	18,1	16	18,1
352031	664	18,1	1023	18,1	792	18,1
352032	447	18,1	1023	18,1	621	18,1
352033	398	18,1	694	18,1	488	18,1
352034	7	18,1	14	18,1	10	18,1
352035	6	18,1	8	18,1	7	18,1
352036	13	18,1	22	18,1	16	18,1
352021	9	18,1	13	18,1	12	18,1
352022	1029	18,1	1627	18,1	1218	18,1
352023	628	18,1	1018	18,1	758	18,1
352024	11	18,1	13	18,1	11	18,1
352025	0	51,1	0	51,1	0	18,1
352026	1	18,1	2	18,1	1	18,1
352041	12	18,1	17	18,1	16	18,1
352042	1042	18,1	1665	18,1	1235	18,1
352043	626	18,1	1026	18,1	758	18,1
352044	11	18,1	14	18,1	12	18,1
352045	0	32,9	0	32,9	0	32,9
352046	1	18,1	2	18,1	1	18,1

RAA - UPPER STRUCTURE (global tensor)

	FORCE GZ 75 Hz (N;Nm)	freq (Hz)	FORCE GZ 83 Hz (N;Nm)	freq (Hz)	FORCE GZ nominal (N;Nm)	freq (Hz)
352011	98	82,7	76	82,7	108	82,5
352012	1293	24,7	1662	24,7	1463	24,7
352013	688	24,7	734	24,7	742	24,7
352014	20	24,7	25	24,7	22	24,7
352015	9	24,7	8	24,7	10	24,7
352016	3	24,7	3	24,7	2	82,5
352031	88	82,7	83	82,7	96	82,5
352032	1147	24,7	1528	24,7	1316	24,7
352033	646	24,7	695	24,7	700	24,7
352034	18	24,7	23	24,7	20	24,7
352035	8	24,7	8	24,7	9	24,7
352036	5	24,7	5	24,7	4	24,7
352021	7	24,7	9	24,7	9	24,7
352022	99	32,8	103	32,8	126	32,9
352023	66	32,8	68	32,8	85	32,9
352024	1	24,7	2	24,7	1	24,7
352025	0	24,7	0	24,7	0	24,7
352026	0	24,7	0	24,7	0	24,7
352041	4	24,6	5	24,6	5	33,0
352042	129	33,0	118	33,0	122	33,0
352043	82	33,0	79	33,0	83	33,0
352044	1	24,7	2	24,7	1	24,7
352045	0	24,7	0	24,7	0	24,7
352046	0	24,7	0	24,7	0	24,7

Table 56: IF RAA lower structure / sub platform tensors comparison

There is no obvious coupling with spacecraft for upper structure at high frequencies. The frequencies of maximum loads are identical and near 25 Hz, whereas RAA modes frequencies on rigid support are greater than 75 Hz. The loads increase at this frequency is due to artificial interface stiffness increase and not to coupling effects.

Also, wave guides accelerations are checked in order to verify the influence of upper structure stiffness on wave guides responses:

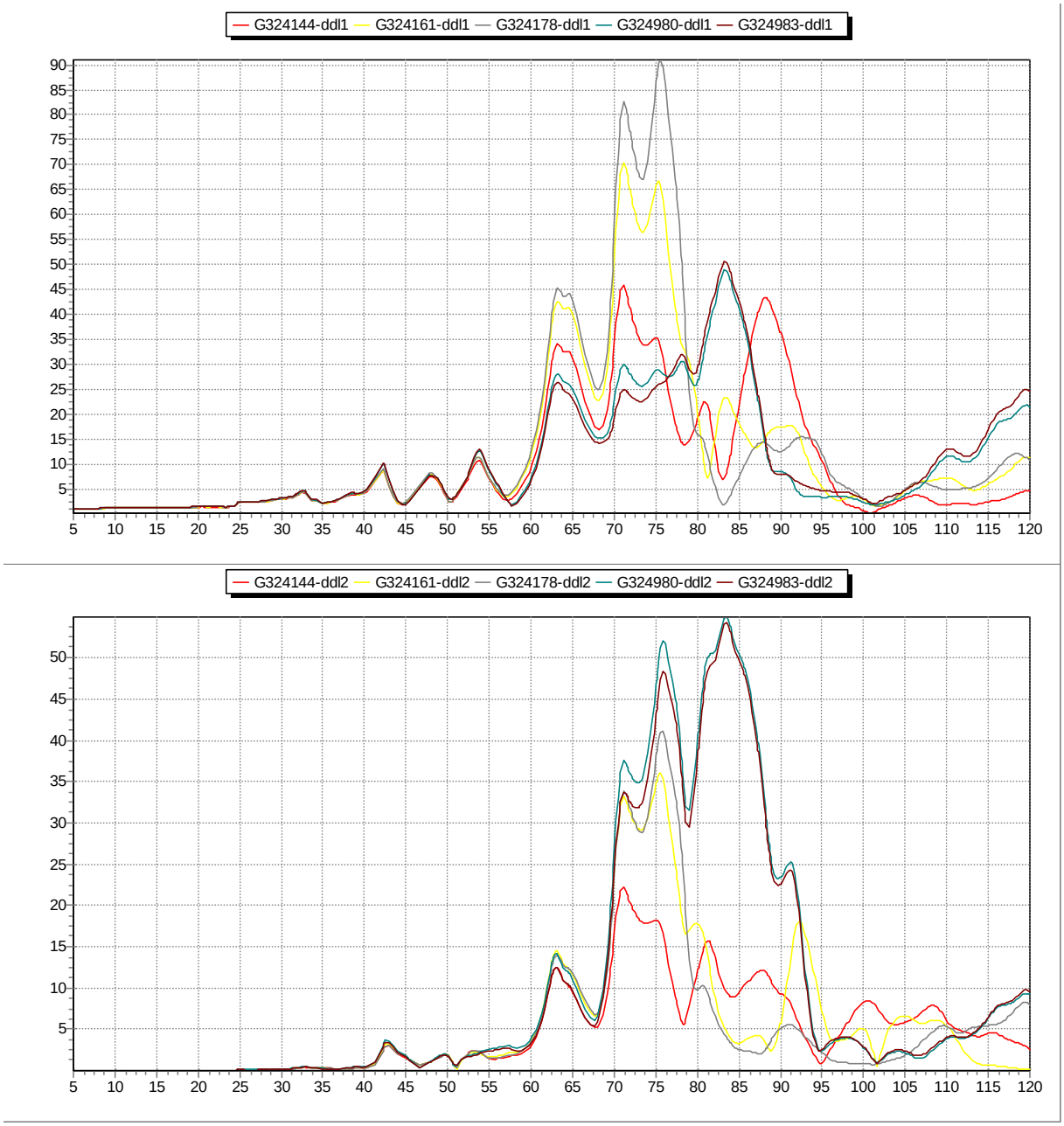

Figure 79: Wave guides representative points accelerations (X drive, configuration 1)

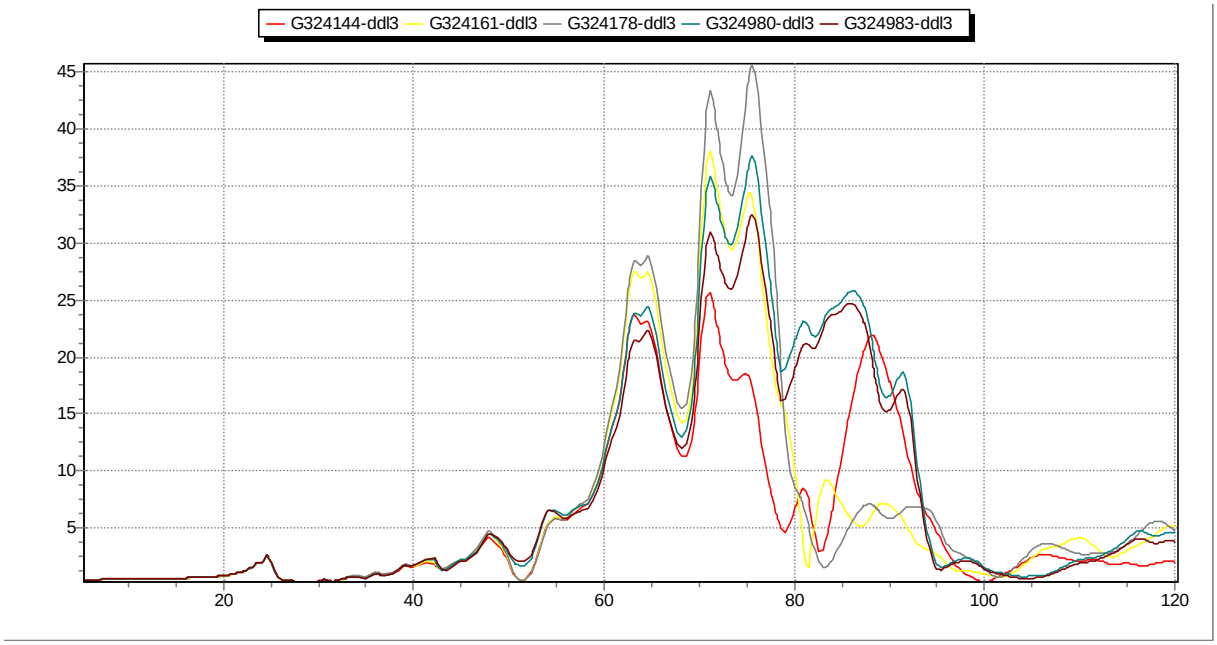

Figure 80: Wave guides representative points accelerations (X drive, configuration 1)

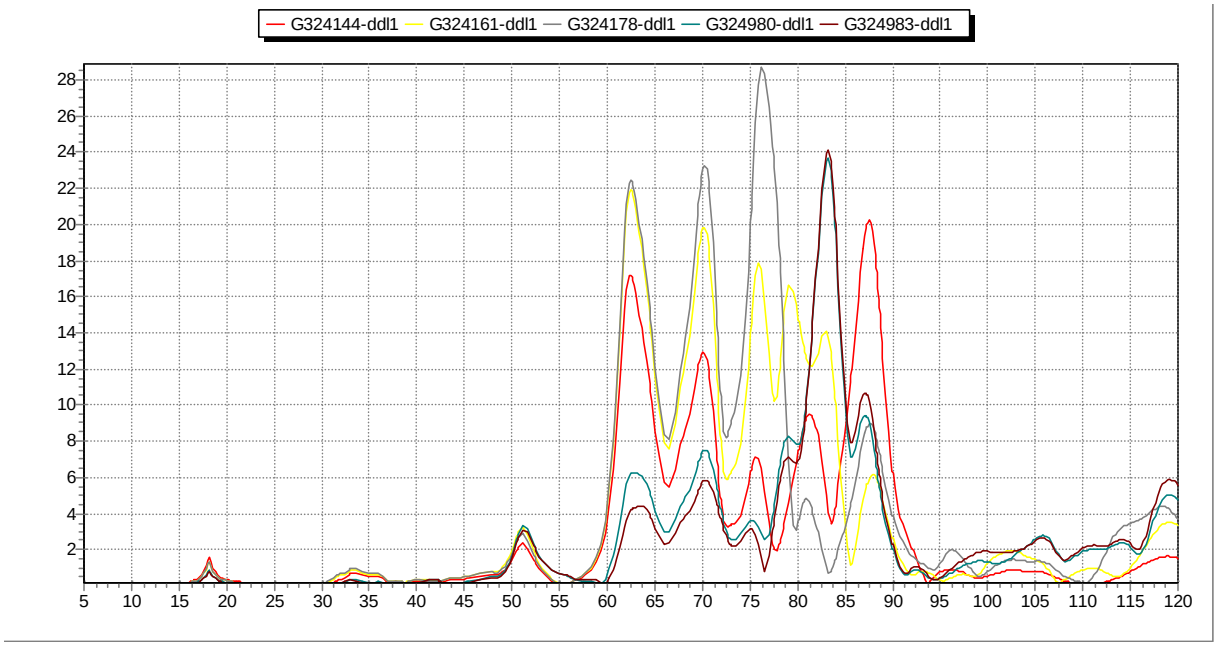

Figure 81: Wave guides representative points accelerations (Y drive, configuration 1)

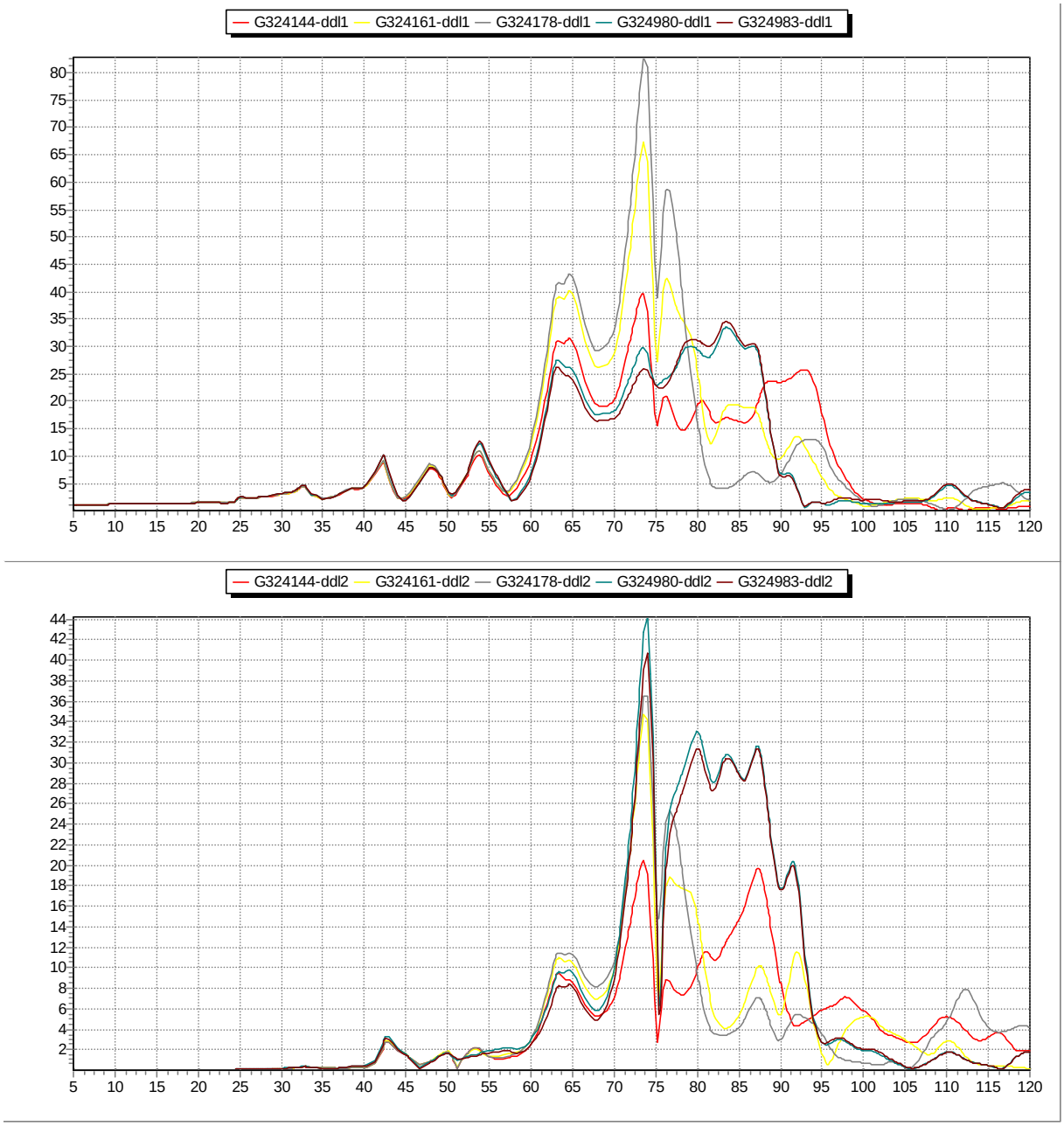

Figure 82: Wave guides representative points accelerations (X drive, configuration 2)

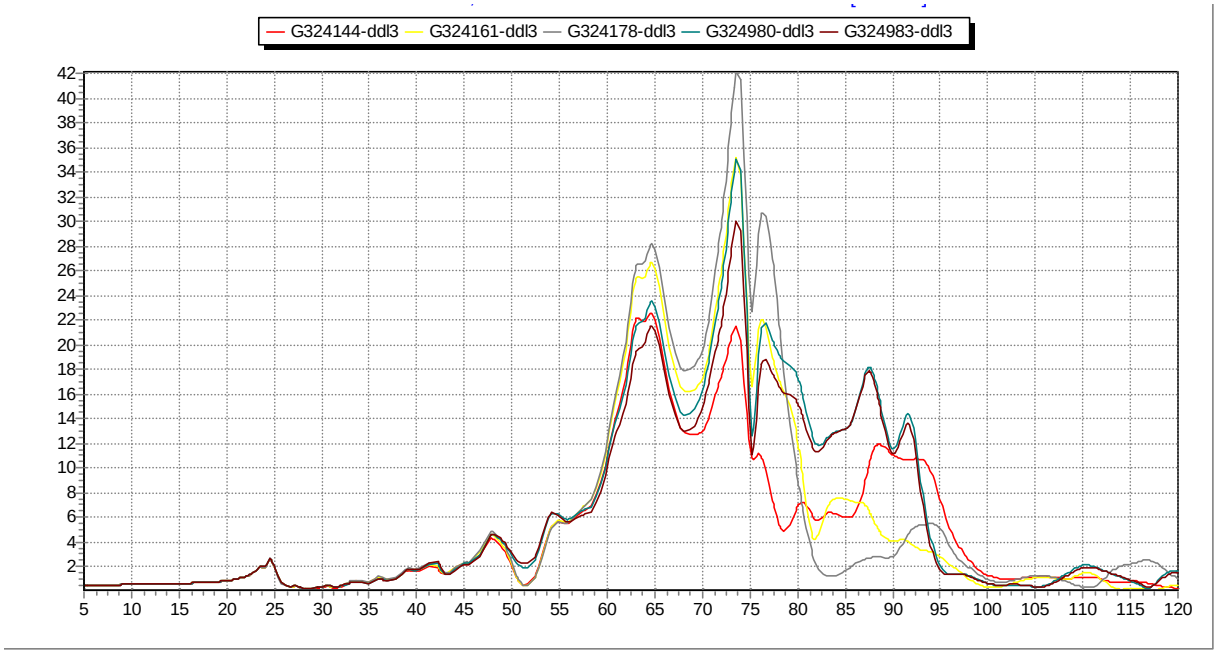

Figure 83: Wave guides representative points accelerations (X drive, configuration 2)

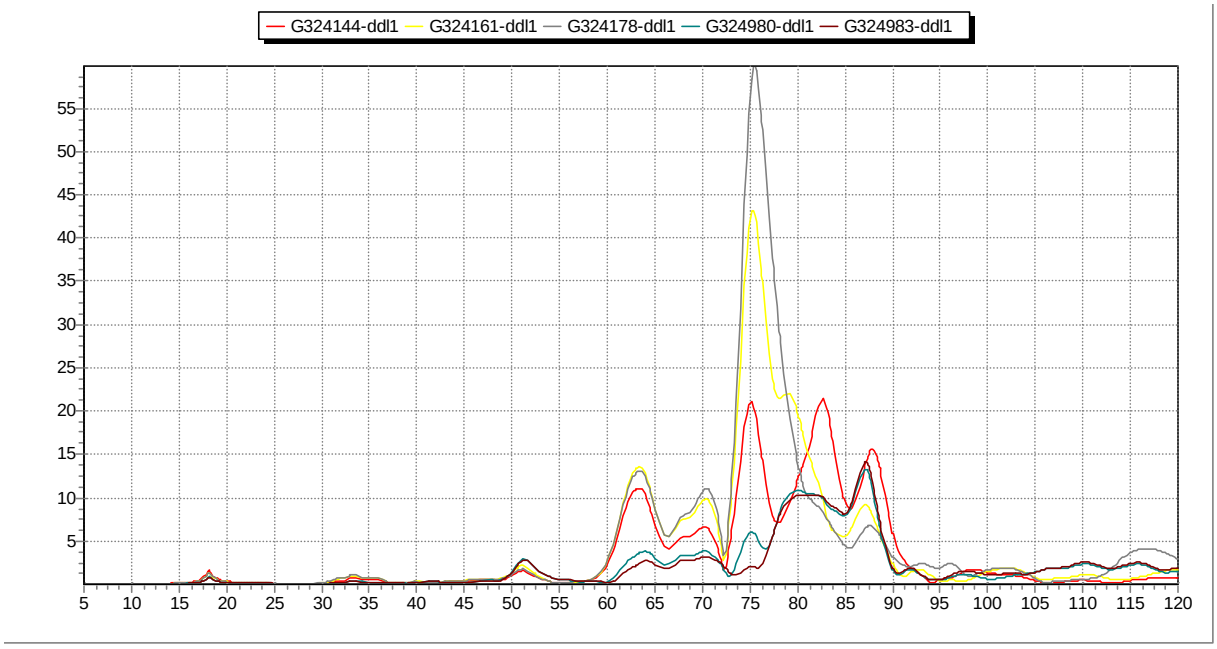

Figure 84: Wave guides representative points accelerations (Y drive, configuration 2)

The maximum acceleration is obtained for configuration 1: 91 g at 75.6 Hz.

So, coupling effects on wave guides due to slight upper structure stiffness changes can appear. As a consequence, both the wave guides and upper structure sensitivity analyses have to be taken into account for the wave guides sizing.

9.2.5 RAA / Planck link sizing

9.2.5.1 Introduction

Three kinds of interface have to be verified:

- interface between RAA upper structure and PR panel,
- interface between RAA lower structure and frame,
- interface between RAA lower structure and sub platform.

The maximum notched loads are extracted from the RAA finite element models issued from sensitivity analyses.

9.2.5.2 Notched inputs

Notched input at satellite base are determined as in §6.2.

9.2.5.3 RAA upper structure / PR panel interfaces

9.2.5.3.1 Description

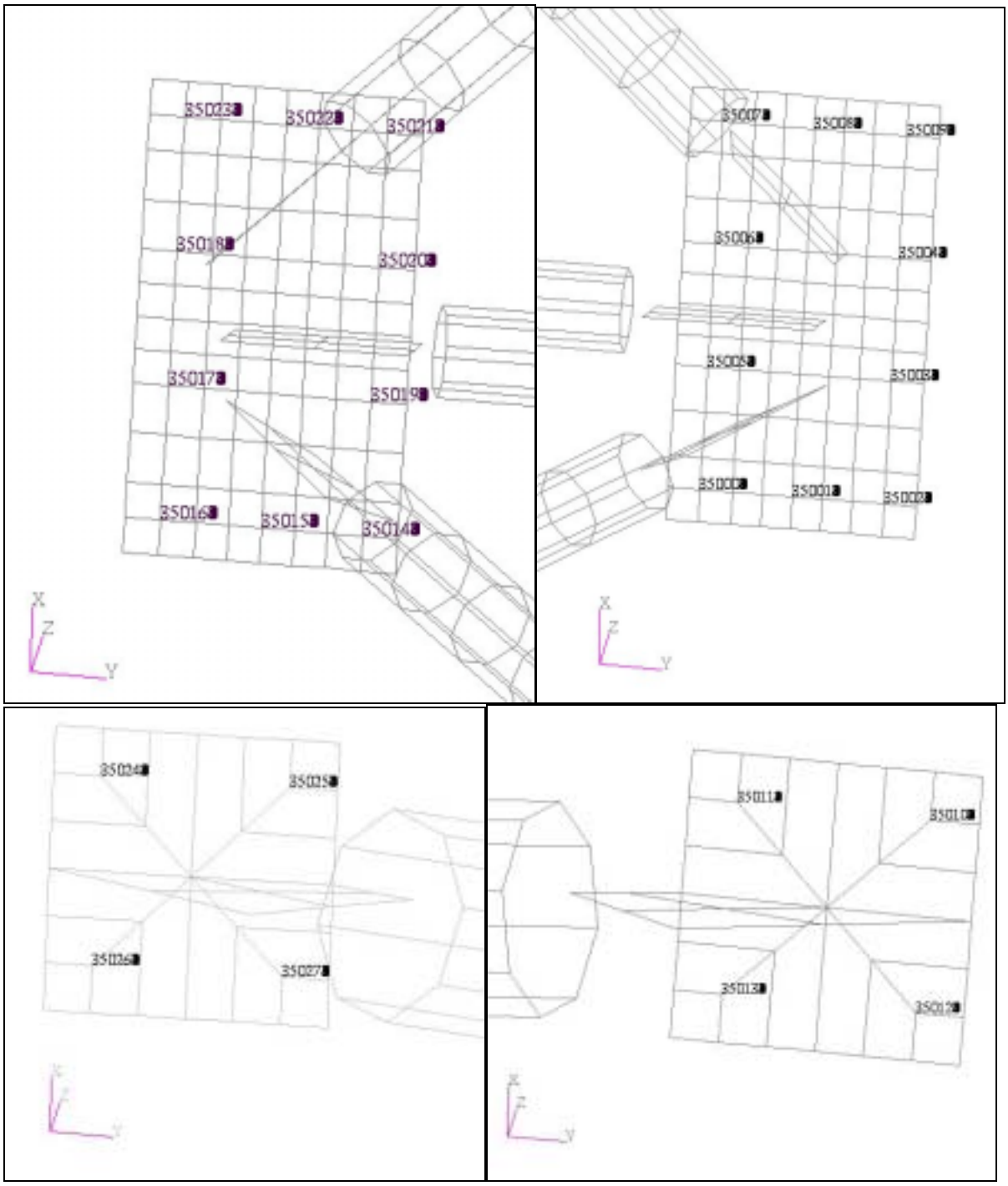

Figure 85: RAA upper structure / PR panel interfaces

	F_{in} plane	F_{perp}
Shur lok insert	10491 N	615 N

Table 57 : RAA upper structure / PR panel insert allowables

These allowables are issued from [RD 28].

The screws are M4 screws. The minimal guaranteed tension for these screws is 2690N [RD 28]. The friction coefficient tgϕ is taken equal to 0,26 for aluminium(insert) / titanium(RAA I/F plate) I/F.

Since maximum loads are reached on low frequency modes, nominal configuration is used for this sizing in order not to inject unrealistic loads due to artificial stiffness changes implemented only for high frequency couplings study.

9.2.5.3.2 Results

In the following tables the envelop results on all sensitivity analyses of the sizing analysis for inserts and screws at RAA upper structure / PR panel interfaces are presented:

	Fappl (N)	Element	Drive / Freq	F allow (N)	Coef	SM (%)
F lateral	434	35008-	GY 19 Hz	10491	2	1109%
F axial	301	35012-	GY 19 Hz	615	2	2%
F equiv sliding	1814	35015-	GY 19 Hz	2690	1,5	-1%

Table 58 : RAA upper structure / PR panel interfaces results

The negative MoS for sliding is not an issue, since :

- local meshing by LABEN of I/F plate with 10 screws seems unrealistic since almost al the global in plane load is taken by 2 screws only (artificial stiffness due to adding of RBE2 elements on the plate)
- for links with so many screws, load will be transferred to other screws before slippage

So, clearly, MoS are positive for sliding.

9.2.5.4 RAA lower structure / frame interfaces

9.2.5.4.1 Description

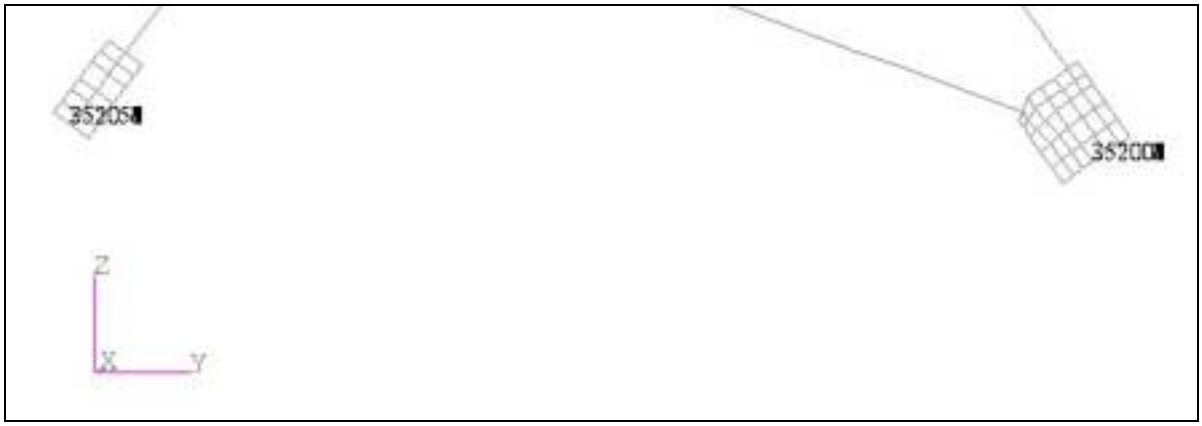

Figure 86: RAA / frame interfaces

Forces are computed in global coordinate system.
The link is composed of three screws fixed in a screwed titanium plate (on frame size).
The allowables are 3000N in the plane (YZ) and 300N out of plane (extrapolated from [RD 28], see [RD 27]).

The analyses are performed with nominal configuration, which is the dimensioning configuration for the frame I/F issued from sensitivity analyses.

9.2.5.4.2 Results

In the following tables the envelop results of the sizing analysis at RAA / PR panel interfaces are presented:

	Fappl (N)	Element	Drive / Freq	F allow (N)	Coef	SM (%)
F out of plane	15	35000-	GX 77.6Hz	300	2	900%
F in plane	793	35000-	GX 77.6Hz	3000	2	89%

Table 59 : RAA / frame interfaces results

9.2.5.5 RAA lower structure / sub platform interfaces

9.2.5.5.1 Description

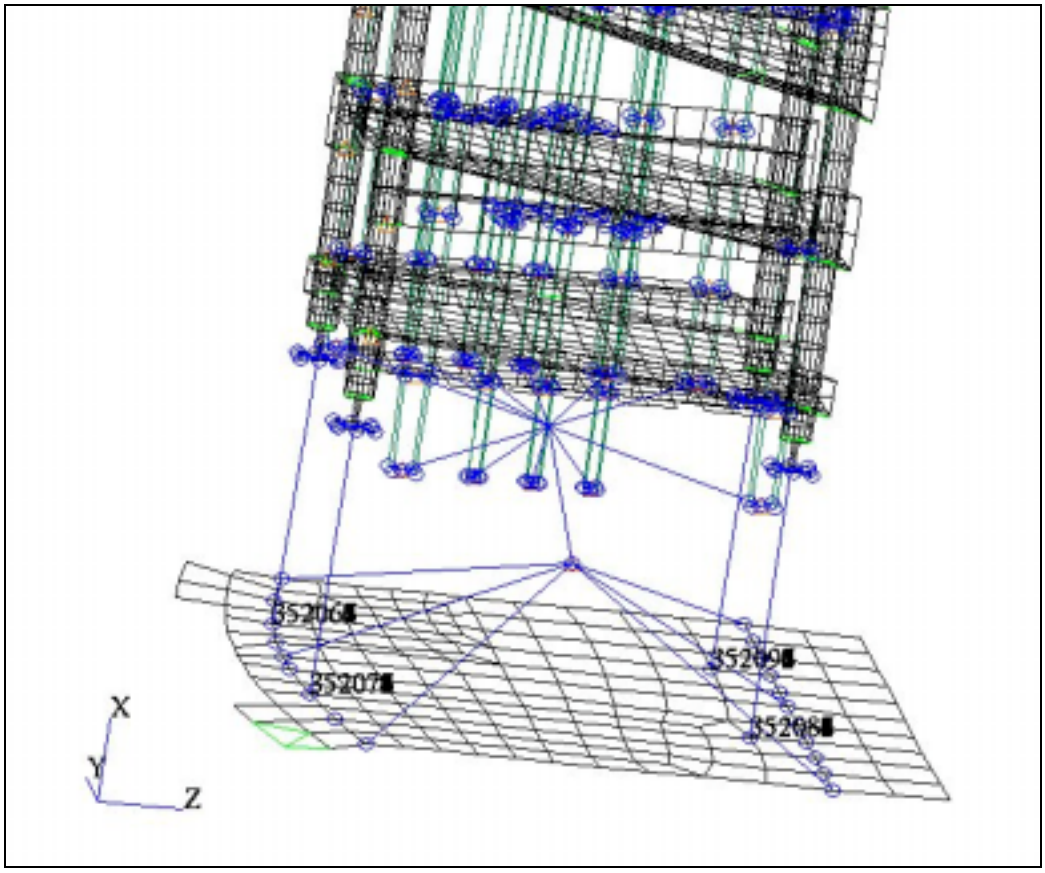

Figure 87: RAA lower structure / sub platform interfaces

For each foot, the following I/F load spec is the following (see [RD 42]). These loads have been specified to Alenia for the subplatform inserts sizing, without safety factor included. So, no safety factor must be applied for this I/F sizing.

	$F_{allowable}$ (N)
F X	800
F Y	610
F Z	610
M Y	110
M Z	110

Table 60 : RAA lower structure / sub platform allowables

Forces are computed in global coordinate system.

The analyses are performed with configuration 1 of sensitivity on lower structure and with nominal configuration which are the 2 dimensioning configurations for this interface.

9.2.5.5.2 Results

In the following tables the envelop results of the sizing analysis at RAA lower structure / sub platform interfaces are presented:

	Fappl (N,Nm)	Element	Configuration	Drive / Freq	F allow (N,Nm)	Coef	SM (%)
F X	235	352071	Nominal	GX 79.1Hz	800	1*	240%
F Y	178	352082	1	GY 63.6Hz	610	1*	242%
F Z	240	352083	1	GX 77.6Hz	610	1*	155%
M Y	56	352095	1	GX 78Hz	110	1*	98%
M Z	52	352096	1	GY 63.6Hz	110	1*	113%

Table 61 : RAA lower structure / sub platform interfaces results

* see § 9.2.5.5.1

9.2.6 Subsystem dynamic analysis

9.2.6.1 Description

A subsystem sine analysis (with nominal configuration) is performed in order to update the LABEN sine specification which covers system sine responses.

Several loads and acceleration are checked:

- Wave guides accelerations (as defined in dynamic analysis).
- RAA lower structure / sub platform interface.
- RAA upper structure / PR panel interface.
- RAA / frame interface.

Note that the loads correspond to the loads used for the link sizing.
The wave guides accelerations are extracted from a model issued from 2 sensitivities (upper structure and wave guides stiffness).

9.2.6.2 Subsystem sine analysis

The following graph shows input profile to be applied on the RAA alone mounted on a rigid support, which permits to cover the system loads and accelerations.

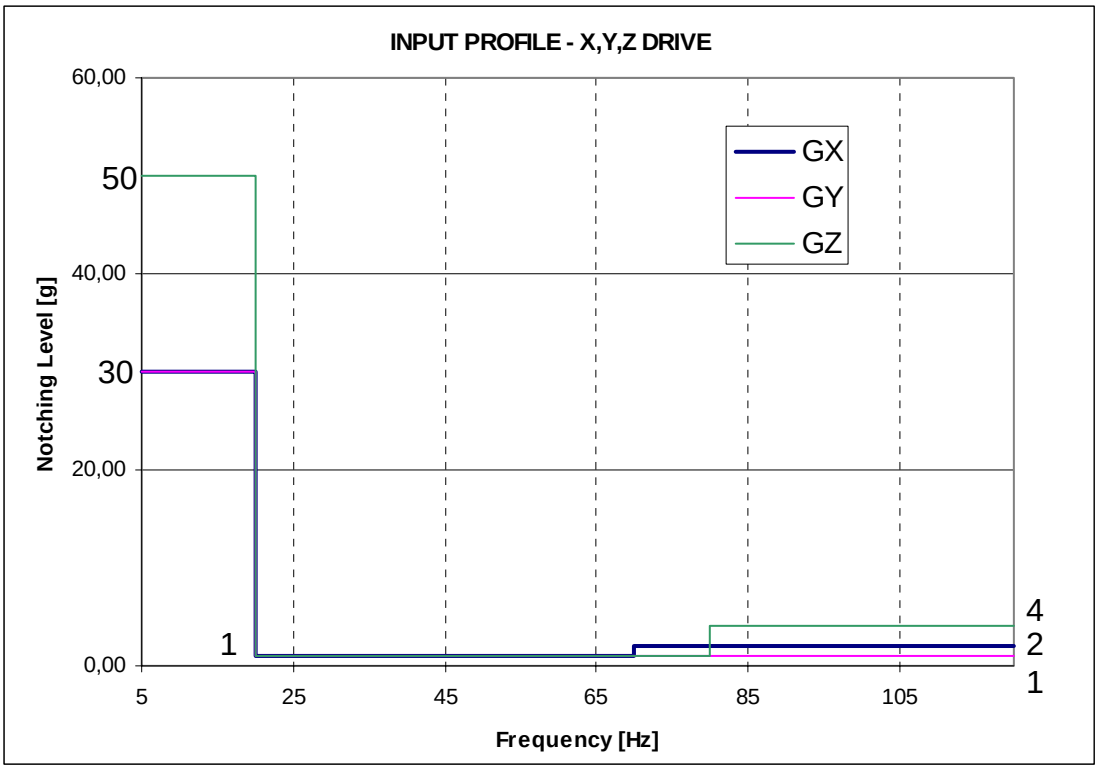

Figure 88: Input profile for subsystem sine analysis

Quasi static inputs (50g on axe Z, 30g on axes X,Y) have been applied in a low frequency range (5-20 Hz).
50 g on axe Z mainly permits to size interfaces between RAA and upper structure, frame, sub platform.
30 g on axe Y mainly permits to size interfaces between RAA and sub platform.
Inputs in frequency range upper than 70 Hz mainly permit to cover wave guides accelerations at system level.

The sine response of several points of RAA structure and wave guides are presented hereafter:

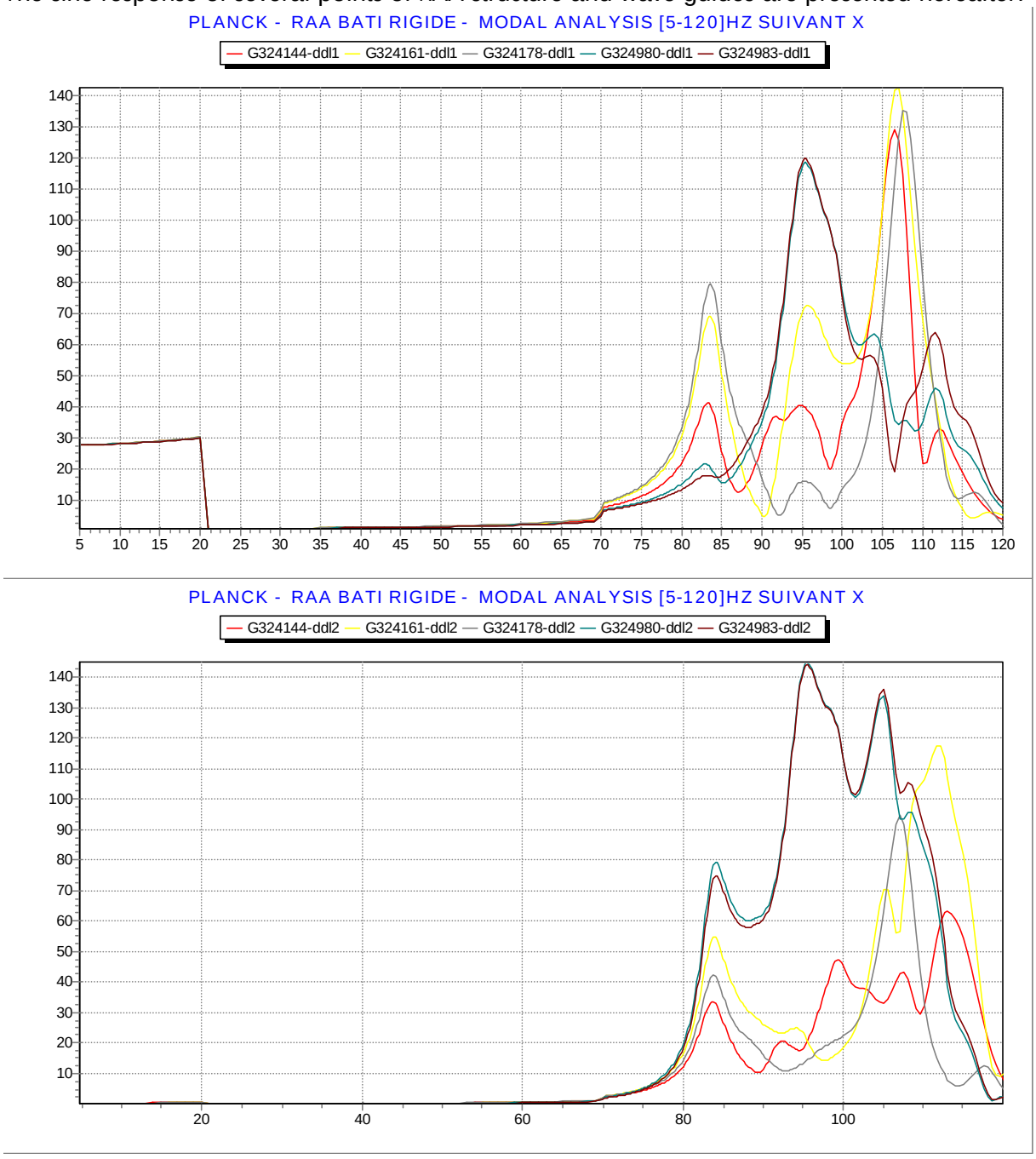

Figure 89: Accelerations of representative points (X drive)

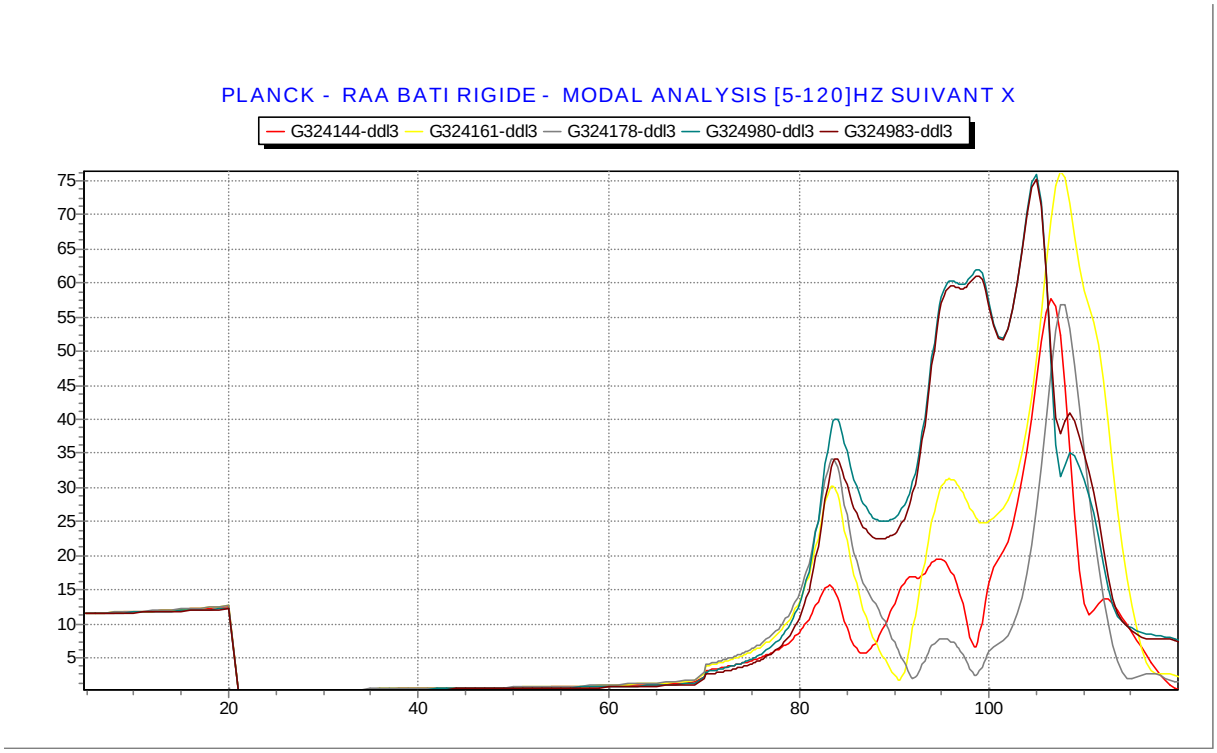

Figure 90: Accelerations of representative points (X drive)

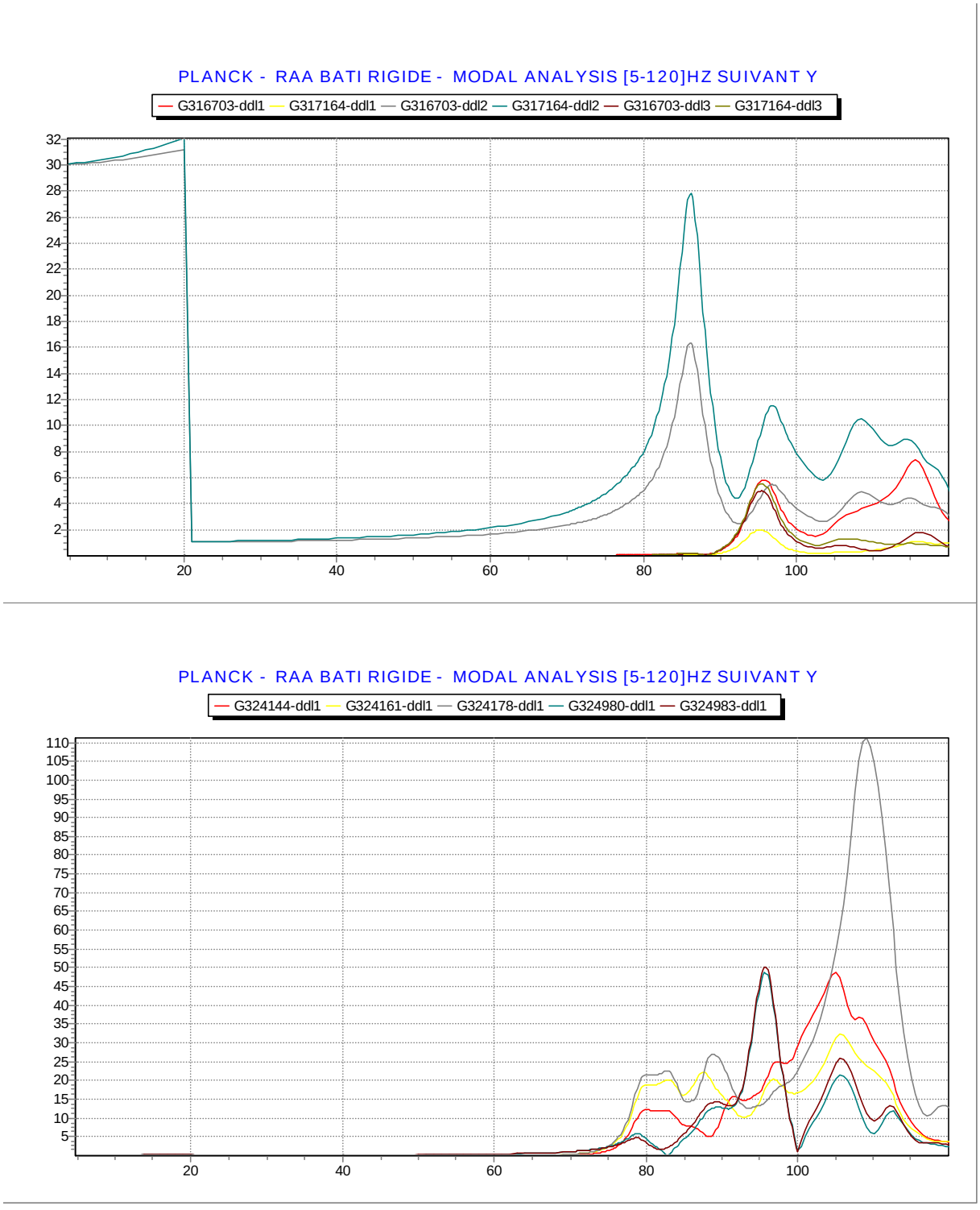

Figure 91: Accelerations of representative points (Y drive)

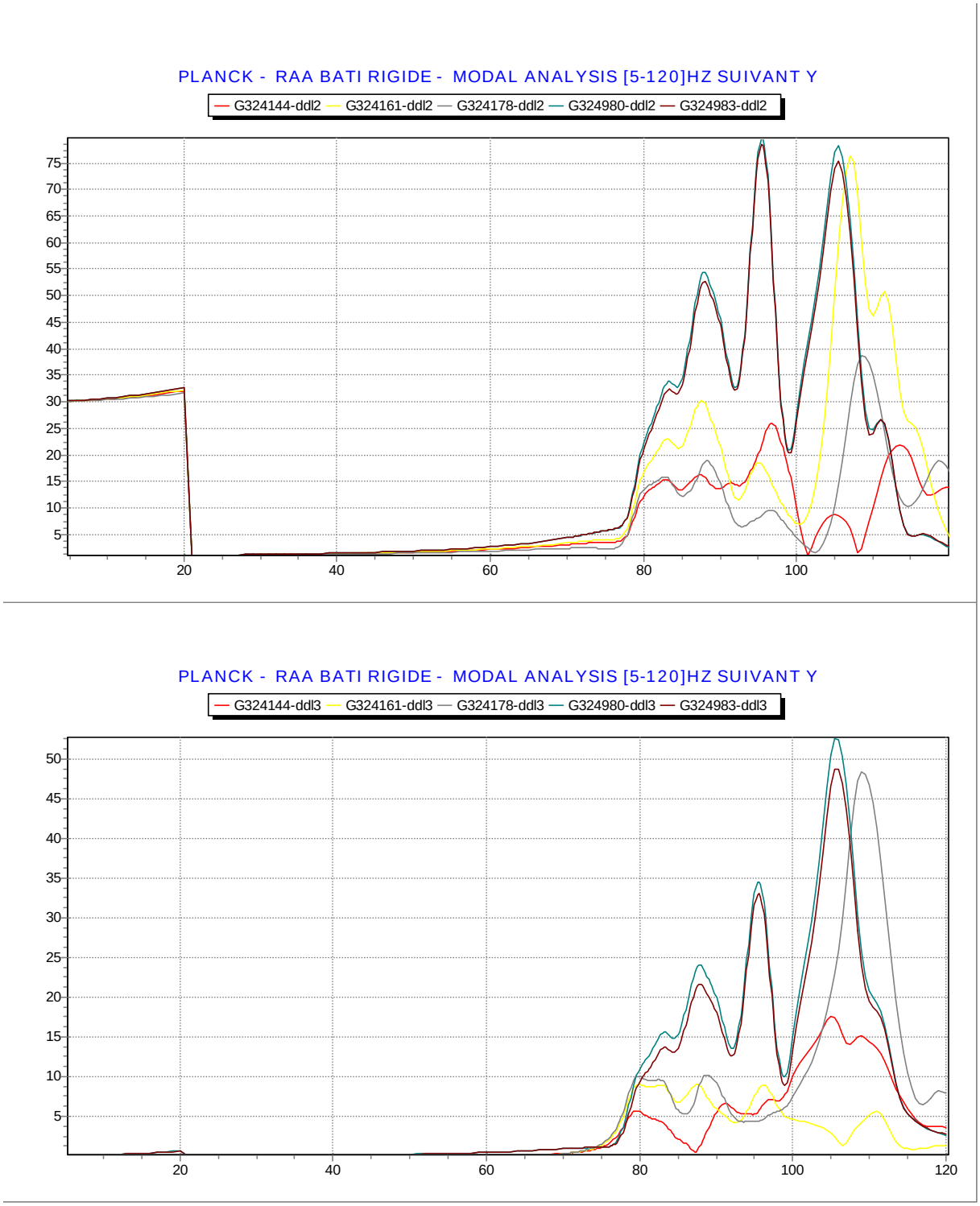

Figure 92: Accelerations of representative points (Y drive)

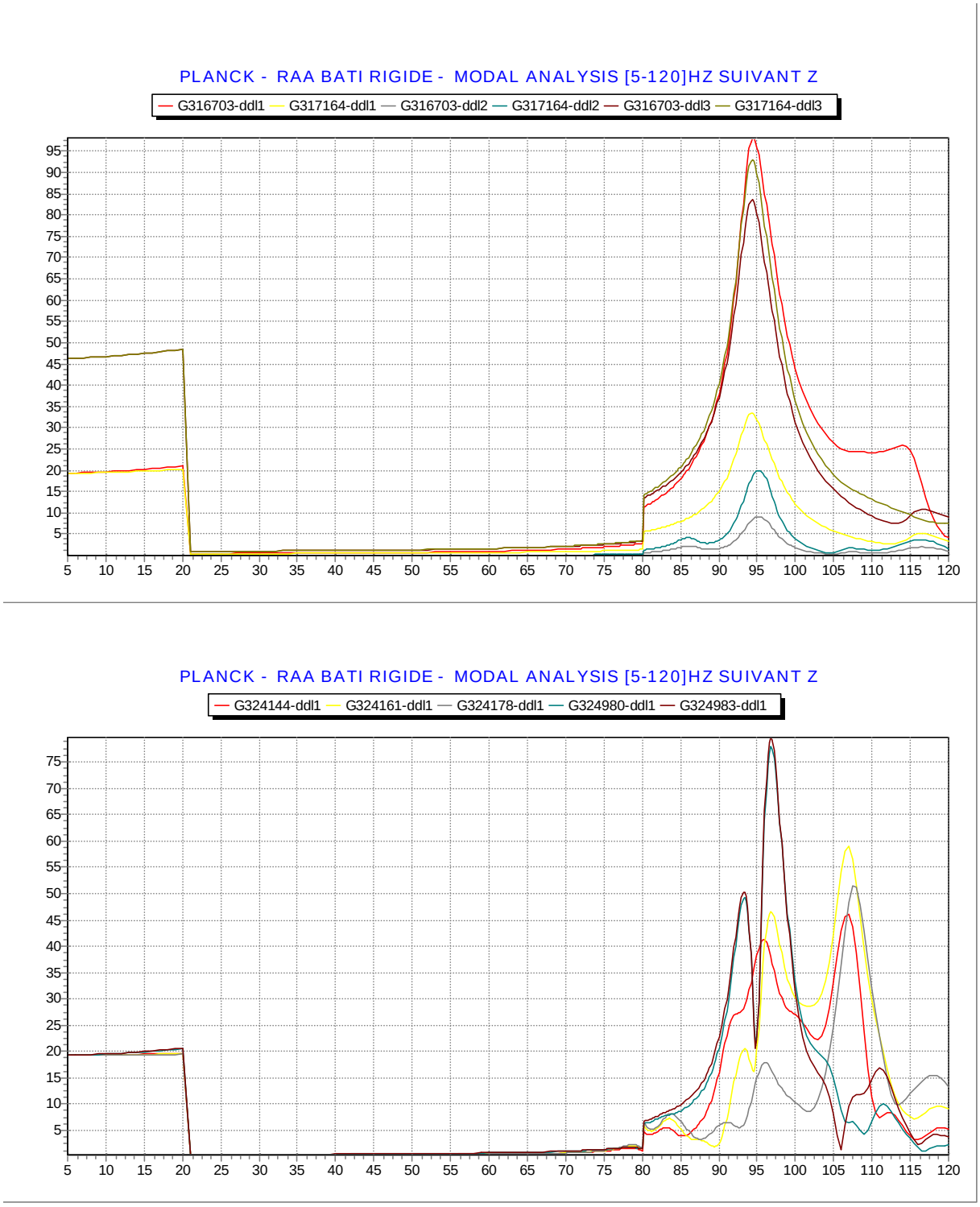

Figure 93: Accelerations of representative points (Z drive)

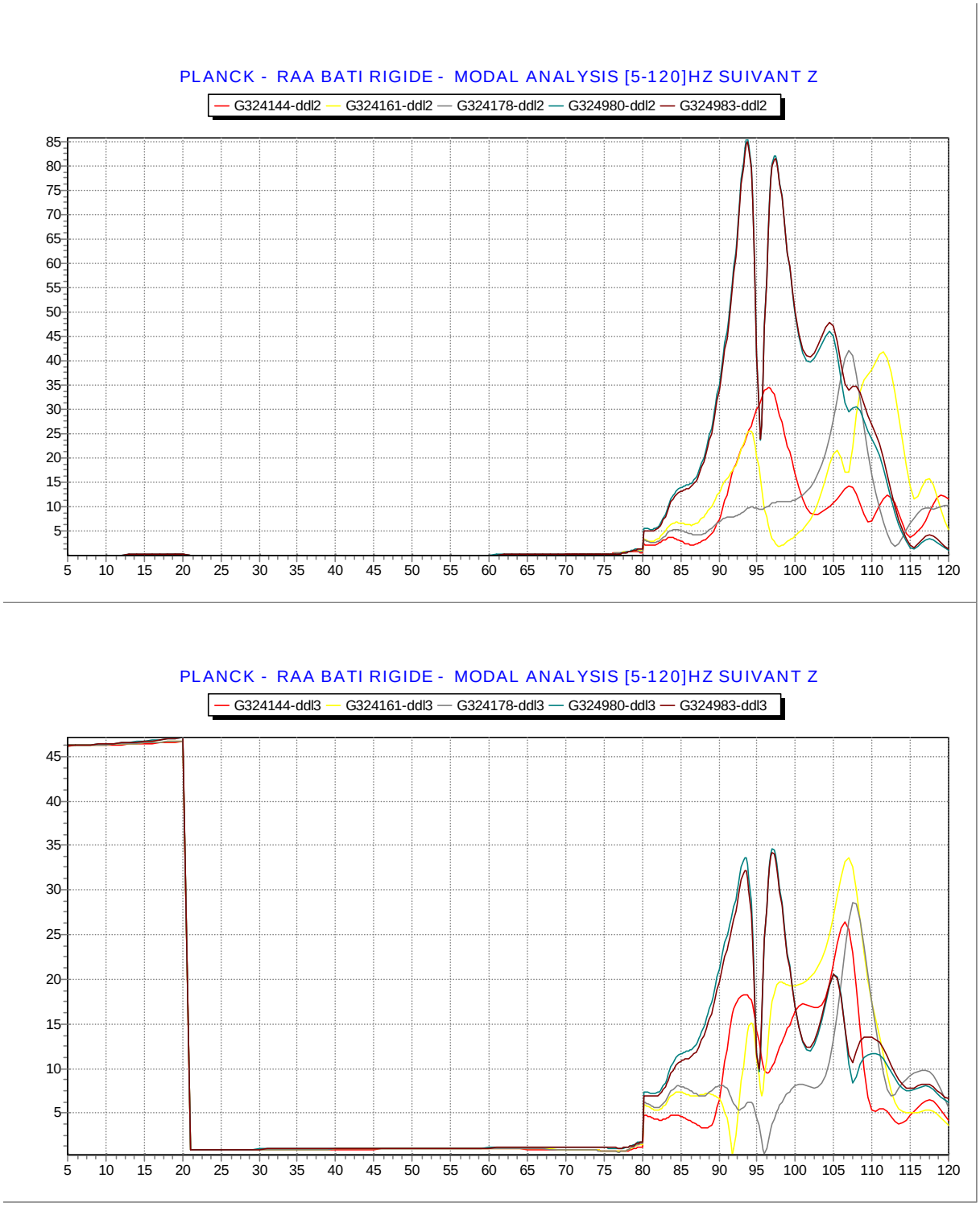

Figure 94: Accelerations of representative points (Z drive)

In the following tables the envelop results of the subsystem sine analysis at RAA structure / spacecraft interfaces are presented:

RAA - SUBPLATFORM interface (global tensor)

	FORCE GX (N;Nm)	freq (Hz)	FORCE GY (N;Nm)	freq (Hz)	FORCE GZ (N;Nm)	freq (Hz)	MAX (N)
352061	409	20,0	52	20,0	138	96,2	409
352062	56	115,5	334	20,0	95	94,4	334
352063	2	106,0	15	95,6	514	20,0	514
352064	0	115,5	1	20,0	2	20,0	2
352065	1	20,0	4	95,6	76	20,0	76
352066	16	115,5	63	20,0	29	94,4	63
352071	413	20,0	54	20,0	236	94,4	413
352072	67	115,5	334	20,0	55	95,6	334
352073	2	106,0	14	95,2	514	20,0	514
352074	0	115,5	1	20,0	0	96,0	1
352075	1	20,0	3	95,2	76	20,0	76
352076	20	115,5	63	20,0	18	95,4	63
352081	409	20,0	45	20,0	234	94,4	409
352082	84	115,5	373	20,0	94	94,6	373
352083	4	20,0	16	95,4	523	20,0	523
352084	0	115,5	0	20,0	0	20,0	0
352085	1	20,0	4	95,4	78	20,0	78
352086	23	115,5	75	20,0	28	94,6	75
352091	409	20,0	49	96,2	151	96,4	409
352092	91	115,5	372	20,0	63	96,2	372
352093	4	20,0	15	95,4	523	20,0	523
352094	0	115,5	1	20,0	0	20,0	1
352095	2	20,0	3	95,4	78	20,0	78
352096	25	115,5	75	20,0	20	96,2	75

RAA - UPPER STRUCTURE interface (global tensor)

	FORCE GX (N;Nm)	freq (Hz)	FORCE GY (N;Nm)	freq (Hz)	FORCE GZ (N;Nm)	freq (Hz)	MAX (N)
352011	903	20,0	88	115,0	698	5,0	903
352012	1101	20,0	1094	20,0	1101	20,0	1101
352013	501	20,0	220	20,0	1191	20,0	1191
352014	18	20,0	21	20,0	8	20,0	21
352015	12	20,0	4	20,0	12	20,0	12
352016	20	20,0	2	104,5	22	5,0	22
352031	861	20,0	108	111,0	778	5,0	861
352032	1003	20,0	1018	20,0	989	20,0	1018
352033	461	20,0	214	20,0	1177	20,0	1177
352034	16	20,0	19	20,0	5	20,0	19
352035	11	20,0	4	20,0	11	20,0	11
352036	19	20,0	3	106,5	24	20,0	24
352021	7	20,0	14	20,0	10	5,0	14
352022	283	5,0	148	104,5	594	5,0	594
352023	201	20,0	116	104,5	411	5,0	411
352024	1	83,8	5	20,0	2	20,0	5
352025	0	94,6	0	20,0	0	20,0	0
352026	0	95,0	1	20,0	0	20,0	1
352041	8	106,5	18	20,0	14	20,0	18
352042	217	106,0	191	105,5	713	5,0	713
352043	172	106,5	141	105,0	494	5,0	494
352044	1	107,5	5	20,0	2	5,0	5
352045	0	94,2	0	20,0	0	20,0	0
352046	0	107,0	1	20,0	0	5,0	1

RAA - FRAME interface (global tensor)

	FORCE GX (N;Nm)	freq (Hz)	FORCE GY (N;Nm)	freq (Hz)	FORCE GZ (N;Nm)	freq (Hz)	MAX (N)
352001	2	5,0	6	86,4	12	96,2	12
352002	48	106,5	424	20,0	545	20,0	545
352003	46	94,6	580	20,0	1046	94,2	1046
352004	1	106,5	6	20,0	5	20,0	6
352005	0	5,0	0	86,4	0	96,2	0
352006	0	20,0	0	96,2	0	94,6	0
352051	1	20,0	6	86,4	15	94,4	15
352052	30	95,8	426	20,0	559	20,0	559
352053	43	107,0	586	20,0	774	20,0	774
352054	0	106,5	0	96,4	0	95,6	0
352055	0	94,8	0	86,4	0	94,4	0
352056	0	20,0	0	86,6	0	94,4	0

Table 62: RAA structure / spacecraft interfaces max loads

In the following tables the envelop wave guides accelerations issued of the subsystem sine analysis are presented:

WAVE GUIDES

		ACCE GX (g)	freq (Hz)	ACCE GY (g)	freq (Hz)	ACCE GZ (g)	freq (Hz)	MAX (g)
324742	ddl1	77,7	108,0	111,5	107,5	137,7	94,4	138
324742	ddl2	76	107,5	46	106,0	65	94,6	76
324742	ddl3	31	108,0	45	107,5	60	94,6	60
324759	ddl1	81,4	101,5	68,2	89,8	67,5	93,0	81
324759	ddl2	147	110,5	66	112,0	52	116,5	147
324759	ddl3	42	107,0	31	89,8	47	20,0	47
324776	ddl1	89,1	83,6	130,9	109,5	26,9	94,0	131
324776	ddl2	48	107,0	41	87,8	21	95,4	48
324776	ddl3	41	83,6	61	109,5	47	20,0	61
324777	ddl1	86,3	83,6	129,1	109,5	26,1	94,0	129
324777	ddl2	53	107,5	44	87,8	22	95,4	53
324777	ddl3	43	83,6	56	109,5	47	20,0	56
325721	ddl1	136,5	100,5	127,3	107,0	51,7	109,0	136
325721	ddl2	204	100,5	219	107,0	71	95,8	219
325721	ddl3	83	111,0	104	107,0	47	20,0	104
325755	ddl1	151,7	110,0	140,7	107,0	60,7	109,0	152
325755	ddl2	204	101,0	213	107,0	69	95,8	213
325755	ddl3	80	111,0	97	107,0	47	20,0	97
325756	ddl1	166,5	110,0	151,2	107,0	68,8	109,0	166
325756	ddl2	202	101,0	204	107,0	66	95,8	204
325756	ddl3	74	111,0	85	107,0	47	20,0	85
324144	ddl1	129,1	106,5	48,8	105,0	46,1	107,0	129
324144	ddl2	63	113,0	32	20,0	35	96,6	63
324144	ddl3	58	106,5	18	105,0	47	20,0	58
324161	ddl1	142,4	107,0	32,4	105,5	59,0	107,0	142
324161	ddl2	118	111,5	76	107,0	42	111,5	118
324161	ddl3	76	107,5	9	79,8	47	20,0	76
324178	ddl1	135,1	107,5	111,2	109,0	51,4	107,5	135
324178	ddl2	95	107,0	39	108,5	42	107,0	95
324178	ddl3	57	107,5	48	109,0	47	20,0	57
324980	ddl1	118,5	95,4	48,6	95,6	77,8	96,8	118
324980	ddl2	145	95,4	80	95,4	86	93,8	145
324980	ddl3	76	105,0	53	105,5	47	20,0	76
324983	ddl1	119,8	95,4	50,2	95,6	79,7	96,8	120
324983	ddl2	144	95,4	79	95,4	85	93,8	144
324983	ddl3	75	105,0	49	105,5	47	20,0	75

Table 9.2.6 : Wave guides max accelerations

9.2.7 System / subsystem results comparison

9.2.7.1.1 RAA lower structure / sub platform interface

The ratio K used in the following tables is defined as:
K = MAX(subsystem analysis) / MAX(system analysis)

RAA - SUBPLATFORM interface									
								SUBSYSTEM	
	FORCE GX (N;Nm)	freq (Hz)	FORCE GY (N;Nm)	freq (Hz)	FORCE GZ (N;Nm)	freq (Hz)	MAX (N)	MAX (N)	K
352061	223	78,4	135	62,7	132	82,4	223	409	1,83
352062	37	78,4	86	77,4	27	77,5	86	334	3,89
352063	177	75,2	58	76,6	83	67,7	177	514	2,91
352064	0	75,6	0	76,9	0	68,0	0	2	4,80
352065	41	75,6	14	76,8	16	68,0	41	76	1,85
352066	12	78,4	26	77,4	8	77,6	26	63	2,41
352071	235	79,1	118	63,4	139	81,9	235	413	1,76
352072	33	79,1	80	77,4	27	78,0	80	334	4,19
352073	179	75,2	58	76,6	88	67,7	179	514	2,87
352074	0	79,1	0	77,4	0	78,1	0	1	9,00
352075	42	75,6	14	76,8	17	68,0	42	76	1,81
352076	11	79,1	24	77,4	8	78,1	24	63	2,62
352081	187	78,4	101	82,9	153	82,4	187	409	2,19
352082	54	62,4	159	62,1	38	61,9	159	373	2,34
352083	187	75,2	60	76,6	90	67,7	187	523	2,79
352084	0	62,7	0	62,4	0	61,7	0	0	4,00
352085	43	75,6	14	76,8	17	68,0	43	78	1,82
352086	17	62,7	48	62,4	11	62,1	48	75	1,58
352091	198	79,1	100	82,9	153	82,4	198	409	2,07
352092	59	62,7	159	62,1	38	61,9	159	372	2,34
352093	192	75,2	63	76,6	88	67,7	192	523	2,72
352094	0	62,7	0	62,4	0	62,4	0	1	2,67
352095	44	75,2	15	76,6	17	68,0	44	78	1,79
352096	18	62,7	48	62,4	11	61,9	48	75	1,57

Table 63 : RAA lower structure / sub platform interface loads comparison (configuration 1 of sensitivity)

RAA - SUBPLATFORM interface									
								SUBSYSTEM	
	FORCE GX (N;Nm)	freq (Hz)	FORCE GY (N;Nm)	freq (Hz)	FORCE GZ (N;Nm)	freq (Hz)	MAX (N)	MAX (N)	K
352061	186	81,0	186	63,9	145	25,7	186	409	2,20
352062	59	80,4	65	78,7	19	63,6	65	334	5,12
352063	228	77,6	78	77,1	97	80,8	228	514	2,25
352064	1	78,0	0	78,5	0	80,8	1	2	3,43
352065	53	78,0	18	78,3	24	80,8	53	76	1,44
352066	18	80,4	18	78,7	6	63,9	18	63	3,40
352071	230	81,5	157	63,9	147	81,9	230	413	1,80
352072	43	80,2	64	78,7	19	81,0	64	334	5,23
352073	232	78,0	78	77,1	97	80,8	232	514	2,22
352074	0	80,8	0	63,6	0	81,0	0	1	9,00
352075	54	78,0	19	78,5	25	80,8	54	76	1,42
352076	13	80,5	18	78,7	5	81,3	18	63	3,53
352081	123	75,8	95	63,9	135	25,7	135	409	3,03
352082	49	62,9	178	63,6	41	63,6	178	373	2,09
352083	240	77,6	81	77,1	100	80,8	240	523	2,18
352084	0	78,3	0	63,6	0	63,4	0	0	2,00
352085	54	78,0	19	78,3	25	80,8	54	78	1,44
352086	14	62,9	52	63,6	13	63,9	52	75	1,46
352091	140	83,1	84	83,3	136	25,7	140	409	2,93
352092	51	63,1	178	63,6	39	63,6	178	372	2,09
352093	245	77,6	84	77,1	103	80,8	245	523	2,13
352094	0	80,6	0	63,6	0	63,9	0	1	2,67
352095	56	78,0	19	78,3	25	80,8	56	78	1,40
352096	15	63,1	52	63,6	12	63,9	52	75	1,46

Table 64 : RAA lower structure / sub platform interface loads comparison (nominal configuration)

All the RAA lower structure / sub platform interface loads are covered by subsystem sine analyses.

9.2.7.1.2 RAA / frame

RAA - FRAME interface (global tensor)								SUBSYSTEM	
	FORCE GX (N;Nm)	freq (Hz)	FORCE GY (N;Nm)	freq (Hz)	FORCE GZ (N;Nm)	freq (Hz)	MAX (N)	MAX (N)	K
352001	40	77,1	18	63,9	19	80,6	40	12	0,30
352002	445	77,6	231	63,9	205	80,8	445	545	1,23
352003	657	77,6	370	63,9	281	80,6	657	1046	1,59
352051	40	77,3	23	63,6	17	80,5	40	15	0,39
352052	422	77,5	317	63,9	209	80,6	422	559	1,33
352053	580	77,5	430	63,9	288	80,6	580	774	1,34

Table 65 : RAA / frame interface loads comparison (nominal configuration)

Some values are not covered by subsystem analyses. These maximum values are obtained for sub platform out of plane mode. A displacement specification representing satellite main modes deformation, and especially sublatform out of plane mode, has been specified to LABEN, which covers these loads. Indeed, the maximum out of plane load computed by LABEN with the displacement spec is 53.3 N (X direction, > 40 N).

So, the RAA / frame interface loads are covered.

9.2.7.1.3 RAA upper structure / PR panel interface

RAA - UPPER STRUCTURE interface (global tensor)								SUBSYSTEM	
	FORCE GX (N;Nm)	freq (Hz)	FORCE GY (N;Nm)	freq (Hz)	FORCE GZ (N;Nm)	freq (Hz)	MAX (N)	MAX (N)	K
352011	184	53,5	414	19,0	76	82,7	414	903	2,18
352012	804	64,7	554	33,0	461	64,5	804	1101	1,37
352013	268	64,5	295	19,0	201	33,0	295	1191	4,04
352014	12	64,7	6	19,0	9	32,9	12	21	1,68
352015	4	64,2	4	19,0	4	33,0	4	12	3,03
352016	5	53,5	9	19,0	2	82,2	9	22	2,57
352031	193	53,5	418	19,0	83	82,7	418	861	2,06
352032	770	64,7	542	33,0	394	25,7	770	1018	1,32
352033	239	64,5	294	19,0	206	33,0	294	1177	4,00
352034	11	64,7	6	19,0	8	32,9	11	19	1,67
352035	4	75,4	3	19,0	4	33,0	4	11	2,85
352036	5	53,5	9	19,0	1	82,2	9	24	2,66
352021	4	74,0	6	33,0	5	33,0	6	14	2,09
352022	160	73,5	667	19,0	103	32,8	667	594	0,89
352023	117	73,5	419	19,0	68	32,8	419	411	0,98
352024	1	70,8	5	19,0	1	32,8	5	5	0,98
352025	0	64,6	0	51,1	0	25,7	0	0	3,00
352026	0	64,7	1	19,0	0	25,7	1	1	0,75
352041	7	75,1	9	33,0	4	33,0	9	18	2,02
352042	207	75,1	684	19,0	118	33,0	684	713	1,04
352043	149	75,4	422	19,0	79	33,0	422	494	1,17
352044	1	74,0	6	19,0	1	33,0	6	5	0,90
352045	0	64,6	0	33,0	0	25,7	0	0	4,00
352046	0	64,7	1	19,0	0	25,7	1	1	0,88

Table 66 : RAA upper structure / PR panel interface loads comparison (worst configuration of sensitivity)

Some values are not covered by subsystem analyses. These maximum values are obtained for spacecraft lateral Y mode. As explained before, for lateral Y mode, the loads are artificially increased by the stiffness of the RAA upper structure issued from sensitivity analyses. In this case we can take into account the results extracted from nominal model.

RAA - UPPER STRUCTURE interface (global tensor)

								SUBSYSTEM	
	FORCE GX (N;Nm)	freq (Hz)	FORCE GY (N;Nm)	freq (Hz)	FORCE GZ (N;Nm)	freq (Hz)	MAX (N)	MAX (N)	K
352011	187	53,2	321	19,0	108	82,5	321	903	2,81
352012	642	64,6	429	33,0	391	64,4	642	1101	1,72
352013	254	64,4	212	19,0	222	33,0	254	1191	4,68
352014	11	64,7	6	33,0	7	64,4	11	21	1,89
352015	4	64,3	4	19,0	4	33,0	4	12	2,88
352016	5	53,5	7	19,0	2	82,5	7	22	3,32
352031	193	53,2	322	19,0	96	82,5	322	861	2,68
352032	610	64,6	416	33,0	332	25,7	610	1018	1,67
352033	241	54,1	208	19,0	219	33,0	241	1177	4,89
352034	10	64,7	5	33,0	5	25,7	10	19	1,90
352035	5	76,0	3	19,0	4	33,0	5	11	2,29
352036	5	53,5	7	19,0	2	81,9	7	24	3,60
352021	8	78,5	6	77,1	5	33,0	8	14	1,68
352022	153	77,6	498	19,0	126	32,9	498	594	1,19
352023	114	78,0	310	19,0	85	32,9	310	411	1,32
352024	1	76,0	5	19,0	1	32,8	5	5	1,15
352025	0	93,2	0	79,4	0	83,1	0	0	3,00
352026	0	77,1	1	19,0	0	77,3	1	1	1,00
352041	12	76,0	8	77,1	5	33,0	12	18	1,46
352042	219	75,8	505	19,0	122	33,0	505	713	1,41
352043	165	75,8	310	19,0	83	33,0	310	494	1,59
352044	1	77,6	5	19,0	1	77,1	5	5	1,06
352045	0	83,6	0	33,0	0	83,3	0	0	4,00
352046	0	77,1	1	19,0	0	77,1	1	1	1,17

Table 67 : RAA upper structure / PR panel interface loads comparison (nominal configuration)

All the RAA upper structure / PR panel interface loads are covered by subsystem sine analysis.

9.2.7.1.4 Wave guides acceleration

WAVE GUIDES									SUBSYSTEM	
		ACCE GX (g)	freq (Hz)	ACCE GY (g)	freq (Hz)	ACCE GZ (g)	freq (Hz)	MAX (g)	MAX (g)	K
324742	ddl1	51,8	83,8	24,8	84,0	43,8	83,6	52	138	2,66
324742	ddl2	22	91,8	15	84,0	20	83,6	22	76	3,48
324742	ddl3	24	83,8	11	83,9	20	83,5	24	60	2,50
324759	ddl1	46,8	87,1	24,9	79,1	35,1	81,9	47	81	1,74
324759	ddl2	23	80,9	23	79,1	23	81,9	23	147	6,32
324759	ddl3	25	64,6	12	79,6	15	81,9	25	47	1,87
324776	ddl1	62,3	74,8	25,3	78,6	20,9	75,9	62	131	2,10
324776	ddl2	30	75,4	15	78,4	11	75,9	30	48	1,61
324776	ddl3	32	75,2	13	78,6	11	75,9	32	61	1,92
324777	ddl1	60,5	74,8	24,3	78,6	20,1	75,9	61	129	2,13
324777	ddl2	32	75,4	16	78,4	12	76,2	32	53	1,68
324777	ddl3	34	75,2	14	78,6	11	75,9	34	56	1,66
325721	ddl1	80,8	87,7	17,4	88,3	22,4	88,2	81	136	1,69
325721	ddl2	111	88,2	31	79,1	33	88,6	111	219	1,97
325721	ddl3	39	88,6	14	79,1	14	82,1	39	104	2,66
325755	ddl1	82,8	87,7	18,5	88,3	23,2	88,2	83	152	1,83
325755	ddl2	110	88,2	30	79,1	32	88,6	110	213	1,93
325755	ddl3	38	88,5	13	79,1	12	82,1	38	97	2,55
325756	ddl1	83,3	87,9	19,1	88,3	23,7	88,2	83	166	2,00
325756	ddl2	108	88,1	28	79,1	31	88,6	108	204	1,88
325756	ddl3	34	88,5	11	79,1	10	88,9	34	85	2,46
324144	ddl1	45,8	71,1	20,2	87,5	17,8	81,6	46	129	2,82
324144	ddl2	22	71,1	8	62,3	12	81,8	22	63	2,86
324144	ddl3	26	71,1	10	87,5	7	81,5	26	58	2,24
324161	ddl1	70,5	71,1	19,9	70,1	18,6	76,2	71	142	2,02
324161	ddl2	36	75,6	11	75,6	13	76,2	36	118	3,26
324161	ddl3	38	71,1	11	70,1	10	75,9	38	76	2,01
324178	ddl1	91,0	75,6	28,7	76,2	25,3	76,2	91	135	1,48
324178	ddl2	41	75,9	12	76,2	12	76,2	41	95	2,31
324178	ddl3	46	75,6	14	76,2	13	76,2	46	57	1,25
324980	ddl1	48,9	83,3	23,7	83,3	16,1	82,6	49	118	2,42
324980	ddl2	55	83,5	27	83,5	22	80,4	55	145	2,64
324980	ddl3	38	75,6	12	75,9	14	76,2	38	76	2,02
324983	ddl1	50,5	83,3	24,1	83,3	16,6	82,6	51	120	2,37
324983	ddl2	54	83,5	26	83,5	20	80,4	54	144	2,66
324983	ddl3	33	75,6	11	83,6	12	76,2	33	75	2,31

Table 68 : Wave guides accelerations comparison (worst configurations of sensitivities)

All the wave guides accelerations are covered by subsystem sine analysis.

9.2.8 conclusion

The link sizing under dynamic loads demonstrates that the design proposed for RAA interfaces is compliant with the strength requirements. All Margin of Safety are positive.

The results of subsystem sine analyses cover RAA loads and wave guides accelerations extracted from system sine analyses. The proposed inputs for LABEN sine analyses are so acceptable.

The RAA finite element model integration has no effect on spacecraft global behaviour with respect to CDR configuration.

9.3 Micro-vibrations analyses

Microvibration analyses are conducted at system level. They cover both in flight and ground testing aspects.

In Flight analyses will be available within the system CDR datapackage.
There is an on going analyses with CSL regarding ground testing microvibration analysis. Preliminary results are available in [RD 52].

10. STATUS ON SUB-CONTRACTORS ANALYSES

Analyses performed on sub-systems that are part of, or interfaced with, PPLM structure are presented hereafter.
Concerning PR and SR, Alcatel has not been directly involved in the corresponding analyses, so results are not presented.

10.1 CSAG analyses

CSAG mechanical analyses on cryo-structure and telescope are completed and presented in their 2 CDR documents [RD 22] and [RD 28].
No blocking point has been identified at CSAG CDR for our CDR.
However, there is still an open point concerning the out of plane strength of the 0.1K and 4K interfaces on the lower beam, which appeared to be very low (only 40N). Analyses are being conducted at Alcatel in order to check this strength, and in the meantime, analyses are being performed by Air Liquide and RAL in order to check the pipes interface loads. Work is in progress on this topic.

Note : I/F loads specification [RD 27] are issued from CSAG allowables for the different I/F presented in [RD 28].

10.2 LFI analyses

10.2.1 LABEN analyses

A series of drafts for all mechanical environments specified in [RD 27] have been delivered by LABEN and corresponding analyses results are summarised in presentation “Instrument mechanical design” of LFI IHDR held on 24th-25th March 2004.

LABEN still have to deliver referenced official analyses documents.

Remaining open points are :

- Negative MoS on Cu wave guides between upper structure and FPU under sine environment
  -> Release of sine spec presented in § 9.2 and updated in [RD 27] may help to solve the problem

- Out of plane interface loads between upper structure and PR panel exceed specified loads for thermo-elastic and random
  -> For thermo-elastic, slippage could be assessed with a conservative approach in order to release out of plane loads. For random, interface plate could be meshed more realistically in order to have a more realistic distribution of the loads between the 10 inserts under I/F plate.

10.2.2 JPL analyses

Analyses performed on the PACE at PPLM level are the following :

- Dynamic displacements analyses [RD 46], showing positive MoS.
- Frequency analyses [RD 51], showing a minimum frequency at 111Hz instead of 130Hz specified (all other frequencies > 130Hz). Alcatel has checked this out of spec is not a concern. However, since this analysis, it seems that with the final design some modes are closer to 100 Hz (see RFD PL-LFI-JPL-RFD-001). This topic shall be discussed with JPL by end of April.

JPL refuses to use the pipe random specification defined by Alcatel in [RD 27] for the PACE sizing, despite Alcatel demonstration that amplification of pipe once mounted on V-grooves can be important on pipe modes (see [RD 35]), and despite the agreement from Alcatel to define notching criteria on pipe responses, and to use increased damping on certain pipe modes if properly demonstrated by JPL.

In order to solve this issue, and also to obtain data from characterisation tests, the following approach has been agreed :
- JPL perform sine tests on pipe samples in order to demonstrate they can sustain qualification sine loads, and in order to characterise low frequency damping due to inner/outer pipe interaction.
- JPL perform acoustic test on a V-groove simulator, on which pipe samples are mounted, with the Ariane 5 qualification acoustic input.
- Results (response amplitudes, modes frequencies for correlation) of the acoustic test are used as input data for a final verification by acoustic analyses, using cryo-structure FEM delivered by Alcatel, on which JPL pipe FEM is mounted.

Sine and acoustic tests are finished and presented in [RD 36]. Acoustic tests results show that pipe amplification can be high on certain pipe modes (Q>7), as expected by Alcatel, and levels seen at the pipe base, and on pipes, are in line with Alcatel analyses.

Last step of verification consisting of acoustic coupled analyses (pipe mounted on V-grooves) is currently being performed by JPL (see [RD 36] conclusion). Sizing of the PACE mounted on PPLM will be verified within this analysis.

Updated JPL analyses document IM 352G:0404:CFS has just been received on 07/04/2004 and has not been reviewed yet. It presents positive MoS for displacements, thermo-elastic and JPL internal QS criterion. It presents 2 modes below 130Hz (minimum at 106Hz), which shall be checked at system level. However, acoustic coupled analyses are not presented in this document.

10.3 HFI analyses

10.3.1 IAS analyses

Analyses performed on HFI instrument are not directly under Alcatel responsibility since the instrument is not interfaced with the PPLM structure, but with LFI FPU.
However, following analyses concerning HFI have been presented to Alcatel for information so that Alcatel can make comments on HFI random tests approach :

- LFI/HFI coupled loads analyses and test predictions analyses [RD 47] And [RD 48] before HFI second random test campaign, from which proposition of test strategy based on notching on HFI I/F loads issued from coupled analyses has been discussed between Alcatel and IAS. Damage occurred for lateral excitation, which apparently was due to extrapolation and CoG response piloting problems. QS RMS loads passed at the based seemed much higher than those issued from coupled analyses (to be confirmed by test report, still not received).

Other analyses involving Alcatel are the following :

- Bellow analyses have been presented through [RD 49]. This document, issued after characterisation tests on Bellow is mainly aimed at providing modes frequency and associated damping for different lengths of Bellow between 2 attachment points. It evidences high damping as expected. This document has been used to determine realistic I/F loads to be applied by CSAG on cryo-strut / Bellow I/F (see [RD 28], appendix A.1).

Final document concerning Bellow tests and analyses is currently being finalised by IAS.
Micro-vibrations analyses are currently being performed by IAS.

10.3.2 Galileo analyses on JFET

Analyses corresponding to current design are presented in [RD 45], dated 24/11/2003. They concern modal, static and random analyses.

Design is compliant with mechanical spec [RD 27], except for first frequency mode located at 125Hz instead of 140Hz.

This is not expected to be a problem since JFET mass participates in low frequency panel modes, and since 125Hz remains comfortably above sine frequency range. It shall be checked at system level by end of April 2004.

10.3.3 Air liquide analyses on 0.1K pipe

Analyses results are presented in [RD 43].

Open points are the following :

- MoS < 0 (min = -25%) for pipe stresses generated by V-grooves relative displacements -> spec has been released (see [RD 50]) in order to help solving the problem
- I/F loads on lower beam exceed specification [RD 27] for QS spec -> spec has been released (see [RD 50]) in order to help solving the problem
- MoS < 0 for pipe stress under random environment -> should be solved by local spec release (see [RD 50])
- Recently identified problem for pipe sizing under thermo-elastic displacements between V-groove 3 and telescope frame

New run of analyses is being performed currently by Air Liquide taking into account spec updates [RD 50].

10.3.4 RAL analyses on 4K pipe

Only known available analyses document is [RD 44] which only concerns SVM part. Analyses for PPLM are currently in progress.